In Vitro Direct Conversion of Somatic Cells from the Adult Human Brain into Functional Neurons by Defined Factors

Dissertation

der Fakultät der Biologie

der Ludwig-Maximilians-Universität München

submitted by

Rodrigo Sánchez del Valle

September 2012

GUTACHTER

Erstgutachter**:** Prof. Dr. Benedikt Grothe

Zweitgutachter**:** Prof. Dr. George Boyan

Tag der Einreichung: 3. September 2012

Tag der mündlichen Prüfung: 28. Januar 2013

In Vitro Direct Conversion of Somatic Cells from the Adult Human Brain into Functional Neurons by Defined Factors

Dissertation

der Fakultät der Biologie

der Ludwig-Maximilians-Universität München

prepared at the Institute of Physiology, LMU München

submitted by

Rodrigo Sánchez del Valle

September 2012

A mi familia

Table of contents

Abbreviations

Acta2	αSMA
ALS	Amyotrophic lateral sclerosis
AMPA	α-amino-3-hydroxy-5-methyl-4-isoxazole-propionic acid
aNSCs	Adult neural stem cells
APC	Allophycocyanin
Atoh1	Atonal homolog 1
Axl	AXL receptor tyrosine kinase
BBB	Blood-brain barrier
bHLH	Basic helix loop helix
BLBP	Brain lipid binding protein
BM	Bone marrow
Brn2	POU3F2 (POU class 3 homeobox 2)
C/EBP	Basic leucine zipper transcription factor CCAAT/enhancer binding protein
CAG	Cytomegalovirus early enhancer element plus chicken beta-actin promoter
cAMP	Cyclic adenosine monophosphate
CBP	CREB-binding protein
CD13	Alanyl aminopeptidase
CD146	MCAM (melanoma cell adhesion molecule)
CD31	PECAM-1 (Platelet endothelial cell adhesion molecule)
CD34	Cluster of differentiation 34
cDNA	Complementary DNA
CFU-Fs	Colony-forming unit fibroblasts
CMV	Cytomegalovirus
CNQX	6-cyano-7-nitroquinoxaline-2,3-dione
CNS	Central nervous system
Cre	Cre recombinase
CREB	cAMP response element-binding
DAPI	4',6-diamidino-2-phenylindole
DG	Dentate gyrus
DIV	Days *in vitro*
Dlx	Distal-less homeobox

DNA	Deoxyribonucleic acid
DPI	Days post infection
DsRed	Red fluorescent protein
E	Embryonic day
E47	E-box binding protein
EGF	Epidermal growth factor
EGFP	Enhanced green fluoresce protein
ER	Estrogen receptor
ERT2	Estrogen receptor 2
ES	Embryonic stem
EYFP	Enhanced yellow fluorescent protein
FACS	Fluorescence activated cell sorting
FGF2	Basic fibroblast growth factor
FoxA2	forkhead box A2
GABA	Gamma aminobutyric acid
GFAP	Glial acidic fibrillary protein
GFP	Green fluoresce protein
GLAST	Glutamate Aspartate Transporter
Gli2	GLI family zinc finger 2
GLT-1	Glutamate transporter 1
GS	Glutamine synthetase
Hes	Hairy and enhancer of split
hESCs	Human embryonic stem cells
HMG	High mobility group
HSCs	Hematopoietic stem cells
HuCD	Neuronal RNA-binding protein 21
iPS	Induced pluripotency
iPSCs	Induced pluripotent stem cells
IRES	Internal ribosomal entry site
Klf4	Krüppel-like factor 4
lacZ	ß-galactosidase
Lmx1a	LIM homeobox transcription factor 1 alpha
LTR	Long terminal repeat
Mac1	Macrophage-1 antigen

MafA	Musculoaponeurotic fibrosarcoma oncogene family, protein A
MAP2	Microtubule-associated protein 2
Mash1	Mammalian homologue of achaete-scute 1
miR	MicroRNA
MMLV	Moloney Murine Leukemia Virus
mRNA	Messenger RNA
MSCs	Mesenchymal stem cells
Myc	Myelocytomatosis oncogene
MyoD	Myogenic differentiation
Myt1l	Myelin transcription factor 1-like
NeuN	Neuronal nuclear antigen
NeuroD	Neuronal differentiation
NG2	Chondroitin sulfate proteoglycan
Ngn	Neurogenin
NICD	Notch´s intracellular C-terminal domain
NPCs	Neural precursors cells
NRSF	Neuron-restrictive silencer factor
NSCs	Neural stem cells
NTR	Neurotrophin receptor
Nurr1	Nur related protein 1
NZG	Nuclear ß-galactosidase
Oct4	Octamer-binding protein 4
OLIG2	Oligodendrocyte transcription factor 2
OPC	Oligodendrocyte progenitor cell
p300	E1A binding protein p300
Pax	Paired box protein
PCAF	P300/CBP-associated factor
PcG	Polycomb group complex
PD	Parkinson´s disease
PDGF	Platelet-derived growth factor
PDGFR	Platelet-derived growth factor receptor
Pdx1	Pancreatic and duodenal homeobox 1
PE	Phycoerythrin

POU	Acronym derived from the names of three transcription factors, the pituitary-specific Pit-1, the octamer-binding proteins Oct-1 and Oct-2, and the neural Unc-86 from *Caenorhabditis elegans*
PPT1	Palmitoyl protein thioesterase-1
PRC1	Polycomb Repressor Complex 1
qRT-PCR	Quantitative reverse transcription polymerase chain reaction
REST	Repressor element 1 (RE1)-silencing transcription factor
RGCs	Radial glial cells
Rgs5	Regulator of G protein signaling 5
Ring1B	Ring finger protein 1
RNA	Ribonucleic acid
RT-PCR	Reverse transcription polymerase chain reaction
S100ß	S100 calcium binding protein B
SCNT	Somatic cell nuclear transfer
SEM	Standard error of the mean
SEZ	Subependymal zone
Shh	Sonic hedgehog
SMA	Spinal muscular atrophy
Smad	Homolog of protein SMA and mothers against decapentaplegic
SNc	Substantia nigra pars compacta
Sox	Sex determining region Y-related High Mobility Group-box
SRY	Sex determining region of chromosome Y
ß-Gal	ß-galactosidase
Stat3	Signal transducer and activator of transcription 3
SVZ	Subventricular zone
SWI/SNF	SWItch/Sucrose NonFermentable
Tbr	T-box brain 1
TN-AP	Tissue non-specific alkaline phosphatase
TTX	Tetrodotoxin
vGluT1	Vesicular glutamate transporter 1
VP16	Transcriptional activation domain of the herpes virus protein
vSMCs	Vascular smooth muscle cells
Z/EG	lacZ/EGFP
αSMA	Alpha-smooth muscle actin

Figures

Tables

Abstract

Reprogramming of somatic cells into neurons provides a new approach toward cell-based therapy of neurodegenerative diseases. Conversion of postnatal astroglia from the cerebral cortex of mice into functional neurons *in vitro* can be achieved by forced expression of a single transcription factor. Also skin fibroblasts have been successfully reprogrammed into functional neurons yet through the synergistic action of several transcription factors. A major challenge for the translation of neuronal reprogramming into therapy concerns the feasibility of this approach in adult human tissues. This work demonstrates the potential of perivascular cells isolated from the adult human brain to serve as a substrate prompted to neuronal reprogramming by forced co-expression of neurogenic transcription factors, namely the SRY-related HMG box protein Sox2 and the basic helix loop helix (bHLH) mammalian homologue of achaete-schute-1 Mash1 (also known as Ascl1). The cells used in this study display characteristics of pericytes assessed by immunocytochemistry, fluorescence-activated cell sorting (FACS) and real time RT-PCR. The presence of neural progenitor cells was excluded by real time RT-PCR analysis of mRNAs typically expressed by these cell lineages. Upon expression of Sox2 and Mash1, these cells adopt a neuronal phenotype characterized by the expression of neuronal markers such us ßIII-Tubulin, MAP2, NeuN, GABA and calretinin. Electrophysiological recordings reveal the ability of these cells to fire repetitive action potentials and to integrate into neuronal networks when co-cultured with mouse embryonic neurons. The pericytic nature of the reprogrammed cells was further demonstrated by isolation of PDGFRß-positive cells from adult human brain cultures by FACS and monitoring the Mash1/Sox2-induced neuronal conversion by time-lapse video microscopy. Genetic fate-mapping in mice expressing an inducible Cre recombinase under the tissue non-specific alkaline phosphatase promoter corroborated that pericytes from the adult cerebral cortex can be expanded and reprogrammed *in vitro* into neurons by co-expression of Sox2 and Mash1. These results demonstrate the feasibility of an *in vitro* neuronal reprogramming approach on somatic cells isolated from the adult human cerebral cortex which could have important implications in the development of *in vivo* direct repair strategies in neurodegenerative diseases and brain injury.

Introduction

The central nervous system lacks the ability for self repair, resulting in irreversible loss of functional neuronal activity upon injury or disease. However, it has been found that two areas of the adult mammalian brain retain neurogenic potential, namely the sub-ependymal zone of the lateral ventricle and the subgranular zone of the hippocampal dentate gyrus; interestingly, new neurons generated throughout lifespan have been shown to be of glial origin [1-4]. Analysis of the reaction of glial cells upon pathological conditions has led to the idea that glial cells residing in non-neurogenic regions may de-dedifferentiate, re-acquiring stem cell properties [5]. Different approaches for development of cell-based replacement therapies have been explored. One approach aims at transplanting stem cells which have been previously expanded *in vitro* and specified to differentiate into a target cell type. This strategy relies on an expandable source of cells, exemplified by embryonic stem cells which have been differentiated in distinct neuronal populations such as midbrain dopaminergic and spinal motoneurons [6,7]. Another method involving the generation of stem cells by means of transcription factor-based reprogramming of somatic cells from the skin (e.g. induced pluripotency) overcomes the use of embryos as a source of embryonic stem cells [8].

Adult neural stem cells represent an alternative source of cells for transplantation. However, its restricted neurogenic differentiation potential represents a limitation that can be overcome by forced expression of fate determinants, i.e. neurogenic transcription factors, leading to directed neuronal subtype specification both *in vivo* and *in vitro* [9-13]. An alternative approach aims at exploring the potential of endogenous sources within the CNS to achieve cell replacement. Along this line, two categories can be considered: 1, cell recruitment from adult neurogenic regions to pathological areas and growth factor treatment [14,15] and 2, recruitment of glial cells which are found widespread throughout the brain. If the latter approach is taken into account, a transcription factor-based reprogramming strategy for direct conversion of (astro-)glial to neuronal cells might be feasible. In the following section, I will discuss examples of cell-based strategies for neuronal replacement purposes at phase I/II clinical trials [16] which provide academic researchers with useful information regarding the design of direct conversion strategies to treat neurodegenerative human diseases.

1.1. New therapeutic strategies in CNS diseases

In order to treat human neurodegenerative diseases, one approach involving transplantation of stem cells to restore functionality or to ameliorate the symptoms has been proposed. At present, different sources of stem cells for clinical trials are been taken into consideration, namely human embryonic stem cells (hESCs), foetal neural stem cells and adult neural stem cells. hESCs are derived from the inner cell mass of the blastocyst from *in vitro* fertilization´s excess embryos [17]. *In vitro*, these cells can be kept in culture for many passages maintaining a normal karyotype (number and appearance of chromosomes), generating identical copies of themselves and potentially being differentiated into any (e.g. neural) cell lineage [18,19]. However, undifferentiated hESCs may generate teratomas upon transplantation [20]. Foetal neural stem cells are obtained from human foetal post-mortem tissue. *In vitro*, these cells can also be passaged extensively, however to a lesser extent as compared to hESCs, and can be efficiently differentiated into neurons and astrocytes [18]. *In vivo*, upon transplantation in the adult rodent brain, these cells generate large number of neurons with lower risk of teratoma formation [17,21,22]. Adult neural stem cells are derived from adult brain biopsy or post-mortem tissue. Both *in vivo* and *in vitro*, adult neural stem cells show a limited differentiation capacity compared to hESCs and foetal neural stem cells [23].

Two main cell-based strategies to treat neurodegenerative diseases involving the use of stem cells have been proposed: 1, delivery of bioactive molecules such as neurotrophic factors and neurotransmitters; and 2, approaches for cell replacement of neuronal and glial cells. I will describe recent reports on stem cell-based phase I clinical trials concerning both approaches:

Neurodegeneration proceeds with gradual neuronal cell loss and, subsequently, functional impairment. Stem cells can be used to deliver therapeutic molecules such as (a) neurotrophic factors and cytokines which may enhance regeneration, reduce cell damage and scar formation, and could stimulate neuronal process outgrowth and (b) enzymes for replacing mutated biochemical pathways [16]. One example of this approach is the clinical trial performed on infant patients suffering Batten's Disease, a fatal lysosomal storage disease in which a genetic defect leads to abnormal accumulations in lysosomes, leading to neuronal cell death [24]. Transplantation of human foetal neural stem cells (HuCNS-SC® StemCells, Inc) into immuno-deficient palmitoyl protein thioesterase-1 (PPT1) knockout mouse, which resembles the human disease [24], resulted in the preservation of hippocampal and cortical neurons as well as delayed motor

coordination loss [24]. The transplanted cells were able to migrate from the transplantation site and to produce the missing PPT1 enzyme, resulting in reduced lysosomal accumulation [25]. This experiments set the rationale for starting a clinical trial phase I study enrolling six paediatric patients with Batten's Disease in a dose increasing manner: three patients received a dose of 500 million cells, while in the case of the other three, one billion cells were transplanted. The surgery, involving several bilateral neural stem cell transplants was well tolerated and followed by 12 months of immune-suppression. Post-mortem analysis showed donor cell survival in one subject who died 11 months after transplant. This clinical trial phase I study showed for the first time human safety data with a neural stem cell product [16].

Another disease in which clinical trials following a stem cell therapeutic approach have been performed is Parkinson´s Disease (PD). This pathology is characterized by the loss of dopaminergic neurons in the substantia nigra pars compacta (SNc), which project to the striatum where motor function is regulated [26]. As dopaminergic neurons die, the levels of the neurotransmitter dopamine decline, leading to symptoms such as tremor, rigor and postural instability [26]. A number of patients suffering of PD have been subject of foetal cell and tissue transplantation in the caudate-putamen, where dopaminergic neurons project to. In some of them, a long-term relief has been reported [26]. Post-mortem analysis has revealed that an immature type A9 dopaminergic neuron may be responsible for these beneficial effects [27]. These studies have also shown that the transplanted cells may acquire pathological hallmarks of the disease, such as the formation of α-synuclein aggregates, indicating host-to-donor spread of pathology [28].

All together, stem cell-transplantation data indicates that neurodegenerative diseases can be treated using cell-based strategies. At the moment, basic research laboratories are developing alternative methods based on the use of somatic cells. One approach is the isolation of easily accessible (i.e. from skin) somatic cells from the patient, differentiation *in vitro* into the desired cell type and subsequently (autologous) transplantation into the diseased area. Alternatively and based on the related developmental cell origin (embryonic germ layers), the potential of cells present in the disease tissue as direct target for *in situ* reprogramming (i.e. astroglia to neuron) is presently explored. Both approaches aim at avoiding the use of stem cells which raise ethical issues; and risks which transcription factor-driven reprogramming may overcome.

1.2. **Cellular reprogramming**

1.2.1. **Induced pluripotent stem cells (iPS)**

Nuclear transplantation experiments in amphibians have shown that the nucleus of a terminally differentiated cell can be reversed to a pluripotent state, acquiring the ability to generate an entire animal [29]. This reprogramming approach, called somatic cell nuclear transfer (SCNT), has also been shown to be possible in mammals, and it is exemplified by the generation of "Dolly the sheep" [30]. These findings suggested that molecules present in an unfertilized egg can modify the epigenetic state of chromatin of a somatic nucleus and reactivate transcription of genes which are silenced in terminally differentiated cells. In 2006, a pioneering study revealed a set of transcription factors that could induce pluripotency (iPS) in embryonic fibroblasts, acquiring the potential to differentiate into other cell types [8]. These induced pluripotent cells (iPSCs) resemble embryonic stem (ES) cells morphologically (colony formation), display ES marker expression patterns, have the ability to form teratomas when transplanted into mice and, most rigorously, can give rise to an entire mouse [8]. Yamanaka´s group first used four transcription factors Oct4 (also known as POU5F1), sex determining region Y-related High Mobility Group-box 2 (Sox2), Krüppel-like factor 4 (Klf4) and myelocytomatosis oncogene (Myc) [8]. However, depending on the cell type of origin and the efficiency of reprogramming, some factors can be omitted. If Myc is not included, reprogramming takes place, albeit at lower efficiency [31]. Interestingly, human fetal and adult murine neural stem cells, which express Sox2 endogenously, can be reprogrammed by exclusively using Oct4 [32,33].

Indeed, Oct4 and Sox2, which interact with each other and form heterodimers, together with Nanog play an essential role in the development and maintenance of pluripotency in embryonic stem cells, activating and repressing the transcription of a core regulatory gene network [34]. In addition to direct control of transcription, these factors cooperate to regulate epigenetic modifiers and microRNAs, and bind to their own promoters conferring self-regulation of their own gene transcription levels [35]. iPS cells can be generated from adult human skin fibroblasts [36] allowing *in vitro* disease modeling and the development of cell replacement strategies. One example is the generation of motor neurons derived from spinal muscular atrophy (SMA) patient-specific iPS, which recapitulated the hallmarks of this pathology [37]. Also iPS from patients with other

neurological disorders such as amyotrophic lateral sclerosis (ALS) [38], Parkinson´s disease [39] and Schizophrenia [40] have been generated.

1.2.2. **Direct lineage conversion**

SCNT and iPS approaches have shown that the loss of developmental potential as differentiation proceeds can be overcome by exposing terminally differentiated cells to suitable reprogramming factors. This suggests the possibility to direct a cell from one lineage to a different one by selecting the appropriate combination of transcription factors which, by a single reprogramming step, will recapitulate their specific developmental role. In the following section, I will describe different examples of transcription factor-based direct conversions with special focus on the astroglia-to-neuron approach as a model for developing neuronal repair strategies.

MyoD and myogenic conversion

Based on the observation that the DNA demethylating agent 5-azacytidine could induce to a certain degree myogenic, chondrogenic and adipogenic phenotypes in immortalized mouse embryonic fibroblasts [41], a screening of cDNA libraries from 5-azacytidine-treated myogenic clones lead to the discovery of the basic helix-loop-helix transcription factor MyoD [42]. By forced expression, MyoD is able to convert primary mouse dermal fibroblasts in myocytes [43] and to induce the expression of skeletal muscle–specific genes in diverse cell types. However, while mesodermal cell types could fully down-regulate their lineage-specific genes, it did not occur when ectodermal (retinal pigmented epithelia) or endodermal (liver) cells were exposed to MyoD [44 45], suggesting that MyoD alone was not sufficient to achieve full muscle phenotype conversion. MyoD contains a histidine- and cystein-rich domain and a C-terminal amphipathic α-helix which are involved in the recruitment of Switch/Sucrose NonFermentable (SWI/SNF) chromatin-remodeling complexes to certain MyoD target genes; this property revealed a mechanism for lineage determination in muscle development and explains its ability to stimulate gene transcription in heterochromatin, which displays a condensed structure and is not transcriptionally active [46,47]. These findings demonstrate for the first time the ability of a single transcription factor to activate lineage-specific gene programs outside its normal cellular context.

B-cell to macrophage conversion

Experiments performed in the haematopoietic system have revealed that transcription factor-mediated direct conversion between mature cell types can be achieved [48]. Forced expression of the basic leucine zipper transcription factor CCAAT/enhancer binding protein (C/EBP) α or ß in spleen B cells mediates the up-regulation of the macrophage marker Macrophage-1 antigen (Mac1) within 4 days [48]. In addition, gene expression analysis of B-cell-derived Mac1-positive cells showed a Pax5-dependent down-regulation of seven B-cell genes as well as an up-regulation of five additional macrophage markers [48]. Functional macrophage properties were also reported by assessing the ability of reprogrammed B-cells to phagocytise fluorescent beads [48]. By means of an inducible fusion protein in which C/EBP is linked to the estrogen receptor (C/EBPα−ER), the conversion of B-cells into macrophages could be temporally controlled and led to nearly 100% conversion efficiency within two to three days [49]. Gene expression analysis revealed bidirectional changes in ~2,400 genes already three hours after induction, with morphological changes being observed within ten hours [49]. Since most of gene expression changes were independent of protein synthesis and the induction of a stable macrophage phenotype was achieved within 48 hours, this worked suggested that changes were caused directly by the activity of C/EBP [49].

ß-cell to endocrine cell conversion

By combination of gene expression analysis of pancreatic endocrine progenitors or mature beta cells [50] and loss of function studies of genes involved in beta cell specification and differentiation, it has been possible to decipher the set of transcription factors that are sufficient to convert *in vivo* exocrine cells into insulin-producing beta cells in mice, namely pancreatic and duodenal homeobox 1 (Pdx1), Ngn3 and musculoaponeurotic fibrosarcoma oncogene family protein A (MafA) [51]. Ectopic expression was achieved by infection with adenoviral vectors containing these three factors, resulting in the generation of insulin-producing cells throughout the pancreas, with an efficiency of 20% of the total co-infected cells being phenotypically beta cells [51]. Pdx1 is a homeobox-containing transcription factor expressed in pancreatic progenitors and mature endocrine cells [52]. When Pdx1 is ectopically expressed in adult murine liver cells it leads to insulin expression and up-regulation of several pancreatic genes [53] while Pdx1 deletion results in major defects in pancreas formation [54]. The basic helix-loop-helix transcription factor Ngn3 is an essential regulator of endocrine lineage

specification during pancreatic development[55]. In fact, the absence of Ngn3 expression results in the complete loss of cells of the endocrine lineage in pancreas and intestine [52]. Forced expression of Ngn3 can drive the transdetermination of hepatic progenitor cells present in the adult liver into pancreatic neo-islets, which are hormone-producing (e.g. insulin) cell clusters [56]. MafA, a basic leucine zipper transcription factor specifically expressed in islet beta cells, regulates insulin transcription by direct binding to the insulin promoter and its deletion does not interfere with beta cell specification [57]. In contrast, defects in insulin secretion, corresponding to a diabetic phenotype, can be observed when MafA is absent, indicating a role in late stages of beta cell differentiation [58]. When Pdx1, Ngn3 and MafA are ectopically expressed in the adult mouse pancreas by adenoviral transduction, insulin expression can be detected three days after infection and remains stable for a period of months. Interestingly, no cell division was required for this conversion. However, this combination of factors failed to reprogram mouse embryonic fibroblasts *in vitro* and skeletal muscle *in vivo* into a beta cell phenotype [51]. In summary, these findings provide an example of direct lineage conversion using defined factors in an adult organ with the advantage of no proliferation being necessary to achieve reprogramming.

Generation of inner ear hair cells

The inner ear contains five distinct regions of vestibular epithelia: the three cristae and the maculae of the utricle and saccule [60]. The mechanosensory receptor cells of the organ of Corti are the so called “hair cells” [60]. In non-mammalian vertebrates the auditory sensory epithelium consists of hair cell and glial-like “support cells", which are organized in an alternating manner [60]. In the mammalian auditory sense organ, namely the cochlea, hair cells are organized in a different pattern, with a single row of ‘‘inner’’ hair cells and three rows of ‘‘outer’’ hair cells [60]. The inner hair cells serve as primary sensory receptors, while the outer hair cells amplify sound partly through regulation of cochlear stiffness [60]. In mammalians, the support cells acquire different specialized morphologies [60]. In the inner ear, hair cells are surrounded by specialized support cells, the so called inner phalangeal cells [60]. The pillar cells line the space between the inner and outer hair cells (tunnel of Corti) and provide structural support to the epithelium [60]. It is believed that the development of the tunnel of Corti and the specializations of the hair and support cells may be an adaptation necessary for higher frequency hearing [59,60].

Spontaneous hair cell regeneration occurs in fish, amphibians and birds [61-63]. It has been shown that support cells can give rise to hair cells during adult stages by trans-differentiation through up-regulation of the bHLH transcription factor Atoh1 [64,65], which plays an essential role in hair cell development [66], and activation of the Notch-signalling pathway [67].

In mammalian vertebrates, regeneration of hair cells in the inner ear does not take place. Support cells are quiescent (G_0 cell cycle phase) in the mammalian inner ear and do not resume proliferation upon tissue damage [68]. Based on the findings from non-mammalian vertebrates, several groups have addressed the question whether forced expression of Atoh1 in non-sensory cells is sufficient to regenerate hair cells in the mammalian inner ear [60,65]. Indeed, over-expression of Atoh1 in support cells of the inner ear of the adult guinea pig may promote formation of new hair cells both in normal and lesioned organ of Corti, however, appearing only in non-sensory regions of the inner ear [69]. Further experiments revealed that the potential of Atoh1 to reprogram support cells into hair cells is restricted to a period of 6 days after lesion [70].

1.2.3. **Astroglia-to-neuron conversion**: **Why astroglia?**

During the early phases of murine neural development, the neural plate invaginates creating the neural tube which at embryonic stage 9 (E9) consists of a single layer of neuroepithelial cells lining the ventricle throughout the anterior-posterior axis. As neural development proceeds, the neural tube becomes regionalized and subdivided. The anterior part of the neural tube gives rise to the telencephalon which is then subdivided into a dorsal and a ventral part. The dorsal telencephalon develops into the hippocampus, the olfactory bulb and the neocortex. The ventral telencephalon gives rise to the basal ganglia and interneurons migrating to cortex, olfactory bulb and hippocampus [71]. Pyramidal neurons of the cortex arise from the dorsal ventricular zone, forming a six-layered structure, characteristic of the neocortex [72] (**Figure 1.1**). Neuronal differentiation in the murine neo-cortex peaks approximately at the second third of gestation.

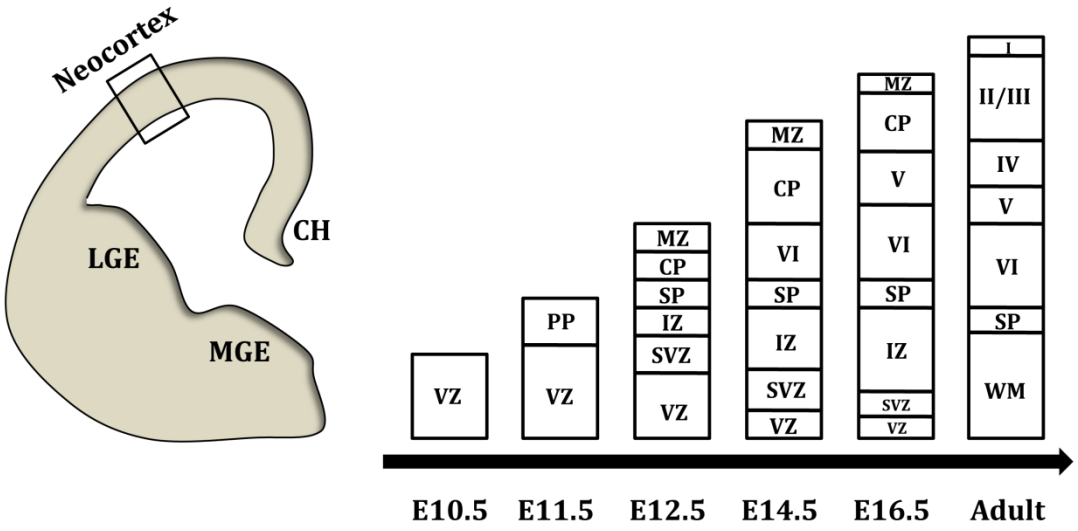

Figure 1.1: Schematic representation of the cortical layer formation. The cortical plate (CP), gives rise to the multilayered neocortex (layers I, II/III, IV, V, VI). E, embryonic day; MZ, marginal zone; SP, subplate; CH, cortical hem; IZ, intermediate zone; LGE, lateral ganglionic eminence; MGE, medial ganglionic eminence; SVZ, subventricular zone; VZ, ventricular zone; WM, white matter (Modified from *Molyneaux et al, 2007*).

An essential role during neurogenesis is played by the so called radial glial cells (RGCs). At the initial stage of neurogenesis (E9-10), neuroepithelial cells are transformed into radial glial cells. This process is characterized by the down-regulation of epithelial features such as up-regulation of markers such as Vimentin, Nestin, BLBP, GLAST, Glutamine synthetase, S100ß and GLT-1 [73-76]. Radial glial cells display a polarized morphology characterized by a cilium-bearing apical end contacting the ventricular fluid, with their basal domain extending towards the meninges and blood vessels [77] . During the neurogenic phase, two main functions have been described for radial glial cells: (1) they are used as a scaffold by migrating neurons from apical (ventricular area) to basal (outer layers) positions and, importantly, (2) serve as neuronal progenitors [74,77,78]. Some RGCs can give rise to neurons and glia, being then considered as multipotent [79]. They are also capable of self-renewing by symmetric division, giving rise to two RGCs, or asymmetric division, generating one RGC and a fate-restricted progenitor [80,81]. Thus, RGCs display defining stem cell hallmarks and, therefore, are considered as embryonic NSCs [3]. At the end of neurogenesis, radial glia generate astrocytes and later oligodendrocytes with differentiation phases peaking at birth and at first month of murine life respectively [82,83].

Interestingly, and in contrast to neurons and oligodendrocytes, astroglia retain the expression of some radial glia markers such as S100ß, GLAST, Glutamine Synthetase and GLT-1 [84]. In addition to their neurogenic and gliogenic functions, radial glia are

responsible for generating ependymal cells as well as some astro/radial glial cells which function as neural stem cells (NSCs) in the adult brain (aNSCs) [3,85,86]. Lineage relationship between RGCs and aNSCs can be suggested by the following arguments; given the heterogeneity of NSCs regarding both their location and the different progenies they give rise to, the subependymal zone (SEZ) is considered to be dorso-ventrally organized [9,11,87]. Such a regionalization is indeed found in the developing telencephalon [3]. Thus, it can be argued that different types of RGCs may be the founder cells giving rise to each class of adult generated neuron and glia. In further support of this idea, regionalized expression of certain transcription factors correlate between the embryonic and adult neurogenic areas. For example, the Drosophila distal-less (Dll) gene homeodomain transcription factor 2 (Dlx2), which is involved in interneuron specification in the developing ventral telencephalon [88] is also prominently expressed in the ventral SEZ [9]. Moreover, transcription factors expressed dorsally in the SEZ, such as the Paired box protein 6 (Pax6) and Neurogenin2 (Neurog2) [9,87] play important roles in the developing dorsal telenchephalon [136].

In further support of the direct relationship between RGCs and aNSCs, several signalling pathways (e.g. Notch and Sonic Hedgehog) mediating the transition from neurogenesis to gliogenesis in the developing cerebral cortex also play a major role in the specification of aNSCs [89].Notch is a trans-membrane receptor which upon ligand binding can be cleaved, releasing Notch´s intracellular C-terminal domain (NICD) into the cytosol and acts either as a transcriptional activator or repressor [90]. Notch signalling has been suggested to be involved in the maintenance of stem cell properties in RGCs since the expression of NICD1 and NICD3 increases the frequency of neurosphere formation from embryonic cortical progenitors [91,92]. Other studies showed that forced expression of hairy and enhancer of split (Hes)1 and 5 (downstream effectors of Notch) impairs neurogenesis in the developing cortex through repression of the proneural genes Neurogenin 1 (Neurog1) and mammalian homologue of achaete-scute 1 (Mash1) [93,94]. On the contrary, expression of an active form of Notch1 or Notch3 increases the generation of parenchymal astrocytes and ependymal cells [91,95]. Interestingly, activation of Notch signalling has been shown to be required for survival and proliferation of aNSCs [96]. Along this line, notch signalling has been suggested to determine the number of stem cells both *in vivo* and *in vitro* [97].

Another pathway playing a critical role in both RGCs and aNSC is Sonic hedgehog signalling. Upon ablation of ciliary genes in RGCs and, subsequently, defective Sonic

Hedgehog signalling, aNSCs are not formed [98]. There are suggestive evidences that a small population of RGCs in the developing brain may respond to the morphogen Sonic Hegdehog, establishing the two major neurogenic compartments in the adult brain [99]. In both areas of adult neurogenesis, Sonic hedgehog is required for maintenance and proliferation of adult stem cells [98,100,101].

In addition, aNSCs retain the expression of RGCs defining markers such as S100ß, GLAST, Glutamine Synthetase and GLT-1 [3,84,102]. Adult neural stem cells residing in the subgranular zone of the hippocampal dentate gyrus resemble morphologically RGCs due to their elongated radial morphology, while stem cells located at the subependymal zone of the lateral ventricule contact the ventricle via a single cilium, as RGCs do [103]. Interestingly, non-neurogenic parenchymal astroglia, which are originated from RGCs during development, share expression of proteins typically found in both neurogenic RGCs and aNSCs such as S100ß, GLAST, Glutamine Synthetase and GLT-1 [84]. Thus, if parenchymal astroglia are direct progeny of RGCs and share many features with both RGCs and aNSCs, it may be possible that these non-neurogenic glial cells harbor some degree of stem cell potential [84]. Under physiological conditions, astroglia carry out important functions such as regulation of synapse formation and homeostasis, blood brain barrier formation and maintenance, and metabolic support of neurons [104]. Notably, upon acute brain injury parenchymal astroglia up-regulate the expression of the glial acidic fibrillary protein (GFAP), which is also found in aNSCs in both neurogenic regions, and resume proliferation hence reactivating some stem cell properties [5,84].

Neurogenic transcription factors involved in astroglia-to-neuron conversion

Based on the fact that radial glial cells give rise to neurons during mouse cortical development [105,106] and the resemblance of stem cells residing in the adult neurogenic niches to astroglial cells [1,107], the group of M. Götz addressed the question whether astroglial cells from adult stages and non-neurogenic regions could be converted to neurons by forced expression of neurogenic fate determinants. Expression of Pax6 in astroglial cultures from postnatal mouse cortex resulted in up-regulation of neuronal markers [108] suggesting the potential of astroglia to adopt a neuronal phenotype. Further studies demonstrated the ability of other transcription factors with essential roles during nervous system development such as Ngn2 and Mash1 to instruct neurogenesis in postnatal astroglia *in vitro* [109,110]. These neuronal cells are capable of generating repetitive action potentials and receive synaptic inputs [109]. Later, by means of stronger

and persistent expression of Ngn2 or Mash1 and/or Dlx2 (a ventral telencephalic downstream effector of Mash1 [88]), through silencing-resistant retroviral constructs, astroglia-derived neurons were shown to form functional synapses [110]. By this approach, the neurotransmitter identity of the converted cells could be tightly controlled. Indeed, while Ngn2-expressing neurons are directed towards an excitatory glutamatergic phenotype, Mash1/Dlx2-expressing cells display an inhibitory GABAergic identity [110,111], recapitulating the function of these transcription factors during forebrain development. The efficiency of conversion by forced expression of Ngn2 is higher than following expression of Mash1 or Dlx2 alone. Combination of Mash1 and Dlx2, however, results in efficiencies close to 90%. Cell division is not required to achieve neuronal conversion following ectopic expression of neurogenic fate determinants, demonstrated by time-lapse video microscopy of transfected cells, indicating direct conversion across cell lineages without reverting to an intermediate progenitor stage. The astroglial identity of the cultures could be addressed by genetic fate mapping in tamoxifen-inducible GLAST:CreERT2/Z/EG transgenic mice [112] which allows identification of astroglial lineage based on gene reporter expression. Furthermore, astroglia derived from the injured cortex of adult mice could be converted to neurons, yet upon culturing in neurosphere conditions [110]. This work indicates the amenability of astroglial cells to adopt a neuronal phenotype upon forced expression of neurogenic transcription factors. Moreover, it suggests that the use of developmentally related cell lineages for the design of cell-based replacement strategies may be beneficial when aiming at fully functional conversions. In this particular case, it suggests the possibility to use cells present in the injured cerebral cortical tissue, by-passing transplantation steps.

Importantly, these experiments pointed at the essential role of the transcription factor Sox2, since its expression in both postnatal astroglia and neurospheres suggested a link between the use of a single transcription factor and the generation of functional neurons [110].

SRY-related HMG box 2 (Sox2): Role in neural development

Sox2 is expressed at high levels in progenitor and neural stem cells both during embryonic development and adulthood [113]. Ectopic expression of Sox2 in embryonic stem (ES) cells alters their differentiation towards neuroectoderm, displaying reduced mesodermal and endodermal fate commitment [114]. Constitutive expression of Sox2

inhibits neuronal differentiation thus maintaining their features of neural progenitors. In contrast, Sox2 inhibition results in precocious neuronal differentiation [115,116]. Furthermore, Sox2 plays a critical role in early development indicated by the embryonic lethality of Sox2 deletion in mice [117]. In order to study the functions of Sox2 in later stages than early embryonic, different genetic approaches involving conditional disruption have been generated. Crossing Sox2 floxed mice with Nestin-Cre resulted in survival up to neonatal stages, allowing the study of the role of Sox2 in the developing brain. Conditional deletion of Sox2 in neural progenitor cells results in enlargement of the lateral ventricles, indicating a role of Sox2 in maintaining neural progenitor cell populations during brain development [118]. An alternative conditional deletion approach results in the impairment of the neuronal program from E12.5 [119]. Sox2-deficient mice lived for few weeks after birth and showed minor brain defects, however the hippocampus lacked neural stem cells and therefore adult neurogenesis, resembling the effects of late Sonic Hedgehog (Shh) loss. Interestingly, GLI family zinc finger 2 (Gli2), a Shh downstream effector, regulates Sox2 levels in neural stem cells [120]. This suggests a positive feedback loop in which Sox2 activates Shh signaling, which in turn stimulates Sox2 expression through the activity of Gli2 [120]; thus maintaining an undifferentiated state in neural stem cells. In the adult brain, Sox2 is also expressed in neural stem cells present in the neurogenic niches, the subventricular zone [121] and the dentate gyrus of the hippocampus [122]. An enhancer deletion of the Sox2 gene results in a lower expression of Sox2 in heterozygous animals and consequently a reduction in the number of proliferating neural progenitors as well as several significant brain defects [121]. This finding suggests a critical role of Sox2 in stem cell maintenance in the neurogenic niches of the adult mammalian brain.

Molecular mechanism of action of Sox2

The neuroepithelium forms shortly after embryo implantation, temporally coinciding with the process of gastrulation [81]. Cells present in the neuroepithelium are referred as neural stem cells and give rise to the major cell types forming the CNS, namely neurons, astrocytes and oligodendrocytes [81,123]. Regulation of neural stem cell self-renewal and differentiation is controlled by multiple cell-intrinsic regulators and extracellular signals [123]. One of these intrinsic factors is the SRY-related HMG-box transcription factor Sox2 whose molecular mechanism in stem cell maintenance, self-renewal and differentiation is described.

The sex determining region of Y chromosome-box containing 2 (Sox2) belongs to the family of Sox proteins, characterized by the presence of a high-mobility group [124], its DNA binding domain formed by three L-shaped alpha helices which interact with the minor groove of DNA. This interaction widens the minor groove, resulting in DNA bending [125]. According to the model of activity in transcriptional regulation, binding of a Sox protein alone to a regulatory region of a gene does not activate gene transcription, but cooperation with a specific partner transcription factor which binds to a nearby site can create a functional complex, promoting transcriptional activation (**Figure 1.2**). A specific sequence flanking the Sox binding site and an available partner factor in the cell determines the activation of a lineage specific transcriptional program [126]. In ES cells, the complex formed by Sox2 and the class V POU (acronym derived from the names of three transcription factors, the pituitary-specific Pit-1, the octamer-binding proteins Oct-1 and Oct-2, and the neural Unc-86 from *Caenorhabditis elegans)* transcription factor Oct3/4 controls self-renewal and pluripotency [127]. The Sox2-Oct3/4 pair has been shown, together with other transcription factors, to induce pluripotency in somatic cells, giving rise to the so called induced pluripotent stem cell (iPSC) technology [8].

Sox2 expression remains high in the neural primordium and is regulated by an array of different enhancers, which reflect the local regulatory mechanisms during development [128]. During CNS development, Sox2 interacts with POU factors to activate genes characteristic of neural stem cells such as nestin [129]. As development proceeds, the N-3 enhancer is activated in the diencephalon and optic vesicles (retinal priomordium) in an overlapping pattern of expression with Pax6. Indeed, the delta-crystallin DC5 enhancer is activated by co-binding of Sox2 and Pax6 [130], forming an auto-regulatory circuit during retinal development [131]. Along this line, forced expression of Sox2 and Pax6 in non-ocular head ectoderm elicits ectopic lens placodal development [132]. Given that the Sox-partner interaction determines which of the different regulatory transcriptional programs become activated and play an essential role in cell specification, changes in one partner lead to step-wise transitions as development proceeds. One example is the transition from ES/inner cell mass state under control of Sox2 and class V POU (Oct3/4) factors and the neural stem cell state regulated by Sox2 and class III POU factors [133].

Another example is the shift from ventricular zone-located apical progenitors to subventricular zone-located basal neural progenitors in the developing spinal cord [129]. Both neural progenitors express the Nestin gene through Nes30, an intronic enhancer

activated by the combined action of group B Sox (e.g. Sox2) or group C Sox (e.g. Sox11) and class III POU (e.g. Brn2) factors [129]. In the developing spinal cord, ventricular progenitors co-express Sox2 and Brn2, with subventricular progenitors co-expressing Sox11 and Brn2. This shift may release proliferating Sox2-Brn2 neural progenitors from stem cell cycle, inducing the neurogenic mode when progenitors express Sox11-Brn2 [134].

Proneural activity of Mash1 and Ngn2: **Neocortical neurogenesis**

During mammalian early cortical development, neuroepithelial cells divide symmetrically giving rise to two identical cells, thus maintaining the pool of stem cells [77]. At the onset of cortical neurogenesis, a subset of neural progenitors becomes restricted to adopt a neurogenic fate [74]. This fate restriction is due to an increase in activity of proneural basic Helix-Loop-Helix (bHLH) transcription factors [135] and a reduction of Hes and Id factors [94], which antagonize the function of proneural proteins. Neurogenesis is controlled by two classes of transcription factors: (1) proneural factors (e.g. Neurogenins and Mash1) which initiate neurogenesis and specify the neuronal subtype and (2) differentiation factors (e.g. NeuroD) involved in terminal differentiation of neurons [136]. Both types are transcriptional activators which bind DNA as heterodimers together with E proteins, encoded by the E2A, E2-2 and HEB genes, also members of the basic Helix-Loop-Helix family of proteins [136]. E-Proteins (e.g. E47) are transcription factors involved in the regulation of neurogenesis versus gliogenesis during verterbrate nervous system development [137]. They form heterodimers with bHLH transcription factors such as Mash1 and Ngn2, cooperating to activate genes to induce neurogenesis in neural prescursors [136]. The core hexanucleotide motif CANNTG (E box) is recognized by the basic region of bHLH factors (**Figure 1.3**) [137].

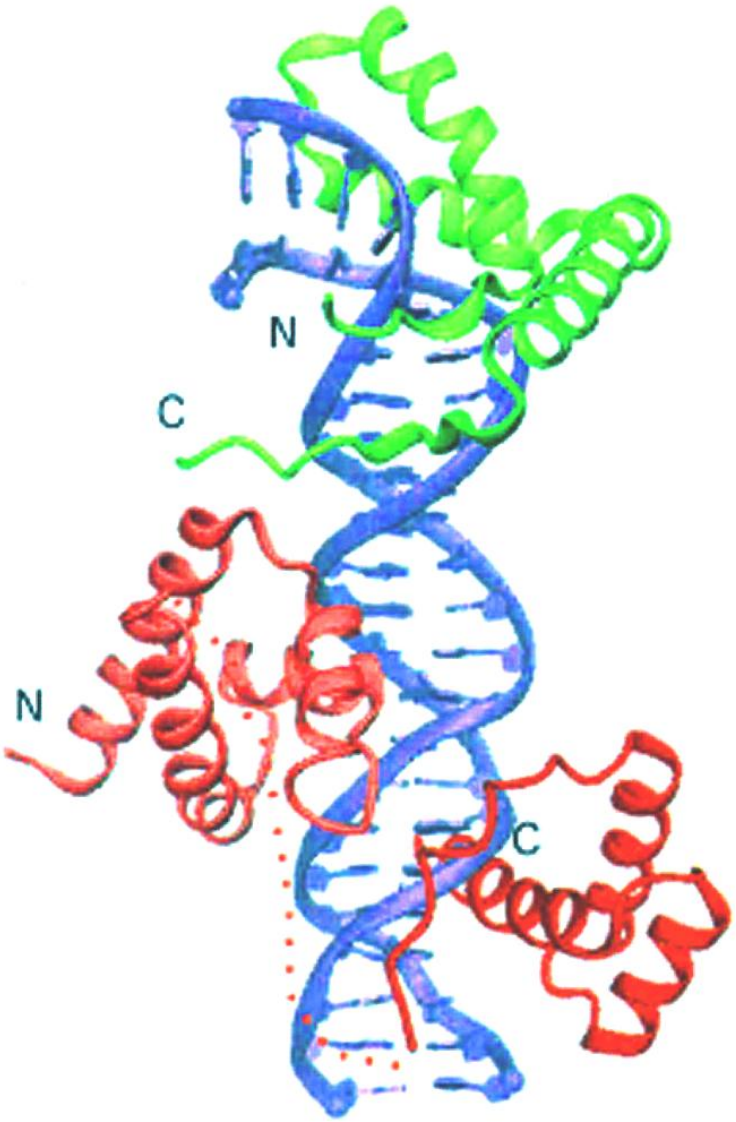

Figure 1.2: Crystal structure of the Oct1/Sox2/*FGF4* ternary complex. The centrally positioned POU-specific domain interacts with the HMG domain of Sox2. HMG domain of Sox2 (green); POU domain of Oct1 (red); Double stranded DNA (blue); (Modified from *Remenyi et al, 2003*).

Co-activators such as E1A binding protein(P300)/CREB-binding protein(CBP) and P300/CBP-associated factor (PCAF) bind to bHLH heterodimers and recruit the basal transcriptional machinery [137]. The acetylating activity of the co-activators promotes transcriptional activity by de-condensation of chromatin thus adopting an accessible structure for the transcriptional machinery [138].

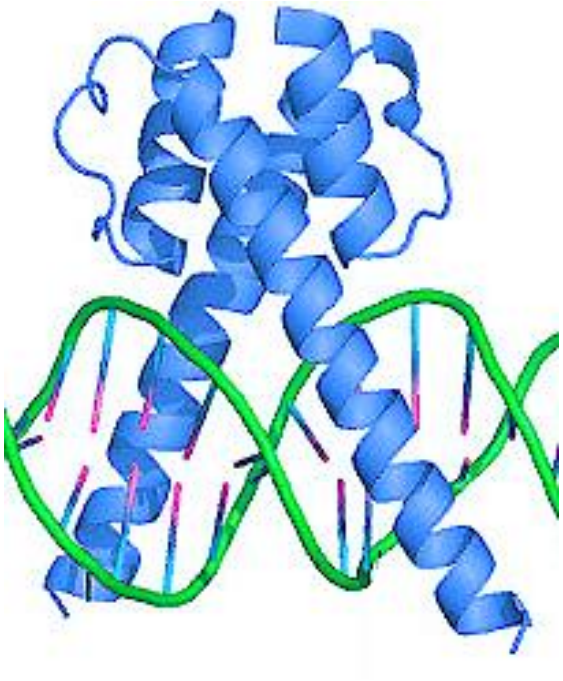

Figure 1.3: Structural model for the binding of bHLH transcription factors to DNA. bHLH transcription factor (blue); double stranded DNA (green); (Modified from *Nakahata et al, 2008)*.

Proneural protein activity in neocortical development

Proneural factors regulate the early steps of neurogenesis, including cell cycle control, neuronal commitment, subtype specification, migration of post-mitotic neurons and axonal growth [139-142]. Neurogenins (Ngn1 and Ngn2) are found expressed in the dorsal part of the telenchephalon, while Mash1 is expressed mainly at ventral positions and, in a lesser extent, dorsally [135] (**Figure 1.4**). Proneural bHLH factor expression is restricted to the ventricular and subventricular zone, being absent in the cortical plate, i.e. the final location of terminally differentiated neurons. Neurogenin activity gives rise to glutamatergic neurons, while Mash1 specifies GABAergic and cholinergic neuronal identity as well as oligodendrocytes [137]. GABAergic interneurons and oligodendrocytes found in the neocortex are born in the germinal zone of the ventral telencephalon and, following tangential migratory routes, reach their final destination at dorsal positions [143,144]. Mash1 regulates the GABAergic phenotype of progenitors in part through direct regulation of the Distal-less homeobox genes Dlx1 and Dlx2 (**Figure 1.4**) [145,146].

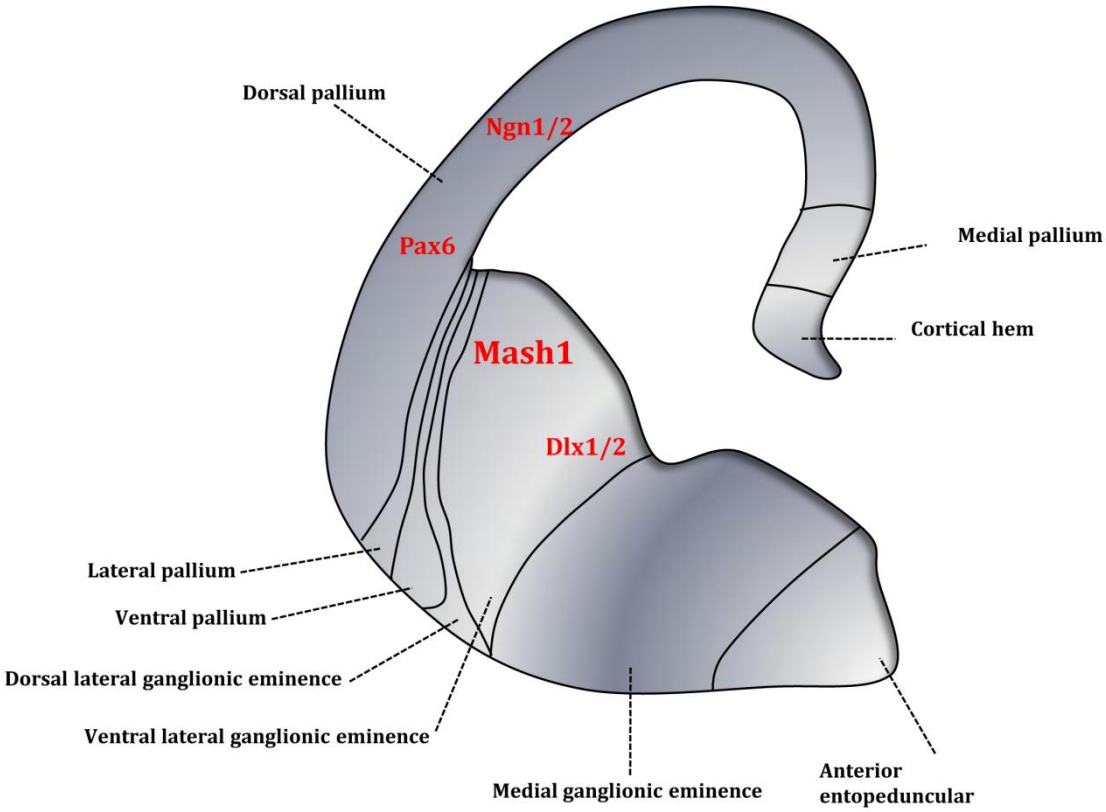

Figure 1.4: Genetic interactions underlying the regionalization of the mammalian telencephalon. Schematic coronal section through the telencephalic vesicles at E12.5 showing dorsal and ventral subdomains. Dorsal telencephalic progenitors express high levels of the bHLH transcription factors Ngn1 and Ngn2, and the homeodomain protein Pax6, whereas ventral progenitors express the bHLH protein Mash1 and the homeodomain transcription factors Dlx1 and Dlx2 (Modified from *Schuurmans and Guillemot, 2002*).

Loss-of-function studies have revealed the functions of these proneural proteins in telencephalic development. In the Ngn2 knock-out mouse, up-regulation of Mash1 at dorsal positions of the telencephalon can be observed, resulting in the generation of GABAergic neurons at dorsal positions [147]. Along this line and by knock-in strategy, inserting the Mash1 coding sequence in the Ngn2 locus promotes a change in cell fate in dorsal progenitors which adopt a GABAergic phenotype and migrate aberrantly from dorsal to ventral locations instead of radially. While their identity is altered, the number of neurons remains normal [148].

In the Mash1 knock-out mice, telencephalic ventral progenitors are lost, resulting in the subsequent absence of basal ganglia neurons and cortical GABAergic interneurons [149]. On the contrary, when Ngn2 replaces Mash1 at the Mash1 locus, no change in the phenotype of ventral progenitors can be observed [145,150]. These findings demonstrate the role of proneural proteins in neuronal subtype specification, while indicating that their

activities are cell-context dependent. *In vitro* gain of function experiments support the above mentioned *in vivo* findings; ectopic expression of Ngn1 in cultured cortical progenitors promotes neuronal differentiation [151]. Also Mash1 over-expression in mouse P19 embryonic carcinoma cells results in up-regulation of neuronal markers such as ßIII-tubulin and Neurofilament-M [152]. Moreover, *in vitro* retroviral transduction of both adult SVZ neural stem cells and cortical postnatal astroglia with Ngn2 or Mash1 results in the specification of glutamatergic or GABAergic neurons, respectively [13,110]. Mash1 and neurogenins activate Notch signaling by promoting expression of the Notch ligands Delta and Jagged, with Notch signaling activity being responsible for maintenance of the appropriate number of neural progenitors. Mash1 activates the transcription of the Notch ligand Delta1 by synergistically interacting with class III POU proteins (Brn1 and Brn2) on the Delta1 promoter[153]. By this mechanism, called lateral inhibition, differentiating neurons expressing Delta and Jagged inhibit neurogenesis in adjacent progenitors, thus maintaining the pool of multipotent neural progenitors[153,154]. Interestingly, in addition to its functions in cell cycle arrest and neuronal differentiation, Mash1 also regulates genes involved in cell cycle progression, including canonical cell cycle regulators and oncogenic transcription factors. This finding reveals a major role of Mash1 in the control of the neurogenic program by coordinating the progression of neural progenitors through proliferation, cell cycle exit and differentiation[135].

Neuronal differentiation by bHLH activity

Terminal neuronal differentiation is controlled by other group of bHLH proteins, including neuronal differentiation (NeuroD), NeuroD2 and NeuroD6 [155]. These are transcriptional activators and bind to E-box hexanucleotide motifs. They are expressed in the cortical plate but not in the ventricular zone [156], contrary to proneural bHLH proteins. No phenotype can be observed in the neocortex of the single or double knockouts, indicating a large redundancy among these factors and possibly the existence of undiscovered terminal differentiation factors [157-159].

Proneural bHLH factors inhibit astrogliogenesis

The expression levels of proneural proteins peaks during neurogenesis, with astrocyte differentiation being characterized by a decrease in proneural gene activity. In fact, over-expression of proneural proteins in cortical progenitors *in vitro* inhibits

astrogliogenesis [151]. In support of this observation, neural progenitors isolated from Mash1 or Ngn2 knock-out mice tend to give rise to astrocytes rather than to neurons [139]. Ngn1 blocks cytokine-induced astrocyte formation by disruption of the Signal transducer and activator of transcription 3(Stat3)/ homolog of protein SMA and mothers against decapentaplegic MAD (Smad)/CBP transcriptional co-activator complex, indicating a way to regulate transcription independent of its DNA binding activity [151]. These findings indicate that proneural proteins may have both activator and repressor transcriptional activities.

The transition of neural precursors cells (NPCs) from neurogenic to astrogenic fate is controlled by the polycomb group complex (PcG) which restricts the neurogenic competence of NPCs and promotes the fate transition of NPCs by changing the epigenetic state of *ngn* gene loci during development [160]. In fact, the chromatin state of the *ngn* promoter gradually becomes closed as development proceeds, with transcription of *ngn* genes being reduced at the onset of gliogenesis [160]. The complex ring finger protein 1(Ring1B)/Polycomb Repressor Complex 1(PRC1) suppresses *ngn1* expression at late stages of neocortical development, eliminating the ngn-mediated repression of astrogenic genes [160].

REST-VP16

An additional reprogramming strategy is based on the role of the repressor element 1 (RE1)-silencing transcription factor (REST)/neuron-restrictive silencer factor (NRSF) in neural tissue. REST/NRSF is a transcriptional repressor that regulates the transitions from pluripotent to neural stem/progenitor cell and from progenitor to mature neuron[161]. In the transition to neural progenitor cell, REST is degraded to levels that maintain neuronal gene chromatin in an inactive state yet poised for expression [161]. As progenitors differentiate into neurons, REST and its co-repressors dissociate from the RE1 site, activating transcription of neuronal genes [161]. Based on this knowledge, the use of a fusion protein in which the repressor-recruiting domain of REST is replaced by the transcriptional activation domain of the herpes virus protein (VP16) [162]. This approach allows for activation of the target genes that REST is normally repressing thereby promoting neuronal differentiation [163].

1.3. **Pericytes as a target for neuronal direct conversion**

1.3.1. **Introduction**

Originally discovered by Charles-Marie Benjamin Rouget in 1873, pericytes or Rouget cells were described as contractile cells surrounding the endothelial cells of capillaries. The term pericyte was introduced by Zimmerman in 1923 due to their location, as they are perivascular cells adjacent to blood microvessels [164]. The definition of a mature pericyte as a cell embedded within the vascular basement membrane of microvessels, i.e. capillaries, pre-capillary arterioles, collecting venules and post-capillary venules, relies on the electronmicroscopical analysis of this cell type [165]. Due to this technical limitation, the identification of pericytes and their distinction from other perivascular cells such as vascular smooth muscle cells (vSMCs), fibroblasts, macrophages, etc. is still challenging. Therefore, most of the literature refer to a mixture of mural cells types of diverse developmental origins associated to blood microvessels, which can be defined by location, morphology and gene expression profile.

1.3.2. **Location and morphology of pericytes**

Pericytes are found ubiquitously associated to microvessels throughout the mammalian organism, extending cytoplasmic processes along the abluminal side of the endothelial tube (**Figure 1.5**). The soma of pericytes is commonly found at branching point of capillaries, extending processes in a Y-shape maner along each branch. Most pericytes synthesise and share a common basement membrane with endothelial cells [166] but many examples of incomplete or absent BM coverage can also be found [167]. Pericyte and endothelial cells communicate to each other through peg-socket junctions, the pericyte fingers (peg) being inserted into invaginations (socket) of the endothelial cells. These junctions, found in membrane evaginations are rich in tight and gap junctions [168]. Another types of contacts between pericyte and endothelial cells are adhesion plaques, which are fibronectin-rich and resemble adherent junctions [169], and N-cadherin adhesion junctions [170].

1.3.3. **Pericyte coverage**

The proportion of endothelial coverage by pericytes and its ratio is variable and organ-specific. In normal tissues, the endothelial-pericyte ratio varies from 1:1 to 10:1 and the pericyte coverage of the abluminal surface of endothelial cells represents between 70% and 10% [165]. These differences can be correlated to the intrinsic properties of the vascular barrier. For instance, the blood brain barrier, with a very tight control of vascular permeability, displays the highest pericyte coverage with a 1:1-3:1 endothelial cell-pericyte ratio, covering 30% of the endothelial surface [171]. In contrast, in skeletal muscle, where the permeability of the vascular bed is higher, the ratio appears to be 100:1 [167]. Large coverage of pericytes is also found in the lower limbs [165] and in tissues with reduced endothelial turn-over [167].

1.3.4. **Pericyte identification**

No single specific maker to unambiguously identify pericytes has so far been described. In addition, all molecular markers are dynamic in their expression depending upon species, local anatomy, developmental stage, pathology, in vitro culturing, and can be also expressed by other cell types. Some of the validated markers are PDGFRß (platelet-derived growth factor receptor-beta) a receptor tyrosine kinase [172,173]; NG2, a chondroitin sulfate proteoglycan [174,175]; CD13 (alanyl aminopeptidase), a type II membrane zinc-dependent metalloprotease [176]; Desmin, an intermediate filament [177]; CD146 (also MCAM), melanoma cell adhesion molecule [178]; and αSMA, alpha-smooth muscle actin [179]. NG2 serves as a good example for the heterogeneity of pericyte marker distribution as it can be found expressed by arteriolar and capillary perivascular cells but it is absent on venular pericytes [180].

1.3.5**. Pericyte functions**

Through physical and chemical interaction with endothelial cells, pericytes promote vessel stability. Both cell types synthesize and secrete growth factors that promote their mutual survival. Mutant mice deficient for PDGF-B/PDGFRß lack mural cells on the vasculature resulting in endothelial hyperplasia, abnormal endothelial ultrastructure, as well as increased capillary diameter and transendothelial permeability [181]. Capillary constriction mediated by pericytes in response to the addition of vasoactive substances

and neurotransmitters has been reported both *in vivo* and *ex vivo* [182,183]. However, convincing evidences for in vivo control of blood flow by pericytes at the capillary level are lacking, in part due to the difficulties to identify pericytes in living specimens.

1.3.6. **Developmental origin of pericytes**

Lineage-tracing experiments have revealed that mural cells have diverse developmental origins, exemplified by vSMCs present on the aorta and its proximal branches which are originate from the secondary heart field, neural crest, mesodermal somites and splanchnic mesoderm [184]. By generation of chick-quail chimeras, a neuroectodermal origin for mural cells in the head region has been suggested [185,186]. Additional support for a neural crest origin of mural cells in the CNS has been provided by marker expression analysis in mice (**Figure 1.5**) [187]. In contrast, mural cells found in lung, liver, heart and gut have a mesodermal origin [188-191].

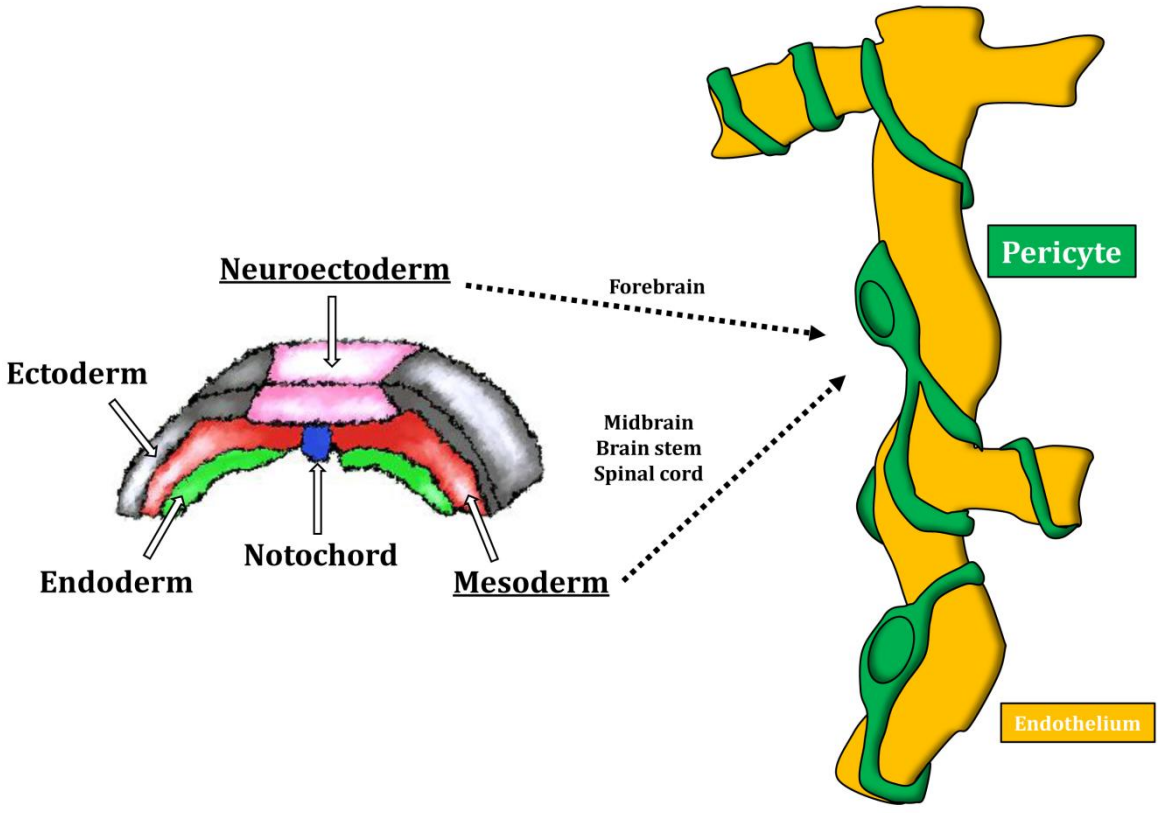

Figure 1.5: Origin of pericytes in the CNS. The embryonic sources of pericytes include (1) neuroectoderm-derived neural crest cells, which give rise to pericytes of the forebrain and (2) mesoderm-derived mesenchymal stem cells, which give rise to pericytes in the midbrain, brain stem and spinal cord (Modified from *Winkler, Bell and Zlokovic, 2011).*

1.3.7. **Pericytes at the blood-brain barrier**

The vascular bed in the CNS is characterized by a high resistance to the passive transport of molecules and cells present in the blood. The neurovascular unit is the structure that confers this impermeability to the healthy CNS and is formed by the tight interaction of endothelial cells, pericytes and astrocytes. The brain vasculature is fully enwrapped by processes called astrocyte endfeet. Also microglia and neurons take part of the blood-brain barrier (BBB) by contacting astrocyte´s end feet with their cytoplasmic processes (**Figure 1.6**) [192]. Brain vessels harbor pericytes that seem different to pericytes found at other organs and display brain-specific marker expression [193]. Based on genetic manipulations of the PDGF-B/PDGFRß signaling pathway in mice, the role of brain pericytes during development and adulthood has been recently addressed. During embryogenesis, around a week before astrocyte formation, endothelial cells invade the CNS and pericytes are recruited to the nascent vessels, playing an essential function in the regulation of the blood-brain barrier formation through interactions with endothelial cells [194].

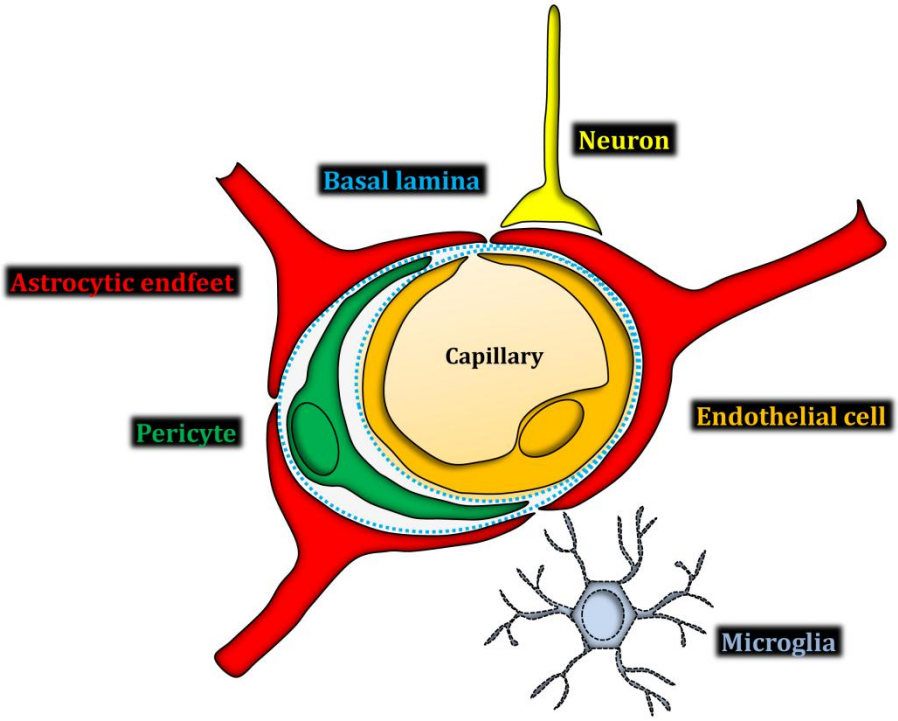

Figure 1.6: Cellular constituents of the blood–brain barrier. The barrier is formed by capillary endothelial cells, surrounded by a basal lamina and astrocytic perivascular endfeet. Astrocytes provide the cellular link to the neurons. The figure also shows pericytes and microglial cells (Modified from *Abbott et al, 2006*).

Experiments with adult viable pericyte-deficient mouse mutants have demonstrated the role of pericytes in the regulation of permeability of the blood-brain barrier. Pericytes regulate blood-brain barrier-specific gene expression patterns in endothelial cells and induce polarization of astrocyte end-feet surrounding CNS blood vessels [195]. Thus, progressive pericyte loss in the aging brain may lead to an increased vessel permeability and, subsequently, to neurodegeneration [196]. At the physiological level, control of the local blood flow in the brain in response to neuronal activity may occur by pericyte-mediated capillary constriction, as suggested by *ex vivo* experiments performed on cerebellar and retinal tissue [197,198]. Pathological situations such as brain ischemia/reperfusion-mediated oxidative stress promotes capillary constriction by pericytes, adding supportive evidence for a role of pericytes in blood flow control in the brain [199].

1.3.8. **Pericyte role in fibrosis**

Tissues respond to injury through processes of wound healing and repair in order to maintain their original structure and functionality. Chronic injury, however, results in excessive generation of extracellular matrix components and, subsequently, in scar formation and organ malfunction [200]. Myofibroblasts are αSMA expressing cells involved in the process of fibrosis. Some studies of fibrogenesis in liver and kidney have suggested that pericyte may be precursors of myofibroblasts under pathological conditions [201,202]. The role of the pericyte as a non glial component of the scar in spinal cord injury has been addressed recently. The use of GLAST-CreER transgenic mice, previously reported to allow labeling of astrocytes [112], has been shown to label a subset of pericytes lining blood vessels in the spinal cord parenchyma [203]. Ultrastructural analysis confirmed the location on these cells within the basal laminae, between endothelial cells and astrocytes, with the recombined cells representing around 10% of the total pericyte population in the adult spinal cord. These cells also expressed markers characteristic of pericytes such as PDGFRß and CD13. The authors demonstrated that, upon injury, a specific pericyte subtype gives rise to scar-forming stromal cells, surprisingly, outnumbering astrocytes. Interfering with the generation of progeny from these cells by targeted deletion for *ras* genes (necessary for cell cycle progression during mitosis) resulted in failure to form a scar in the injured tissue [203], revealing the ability of pericytes to proliferate in the adult spinal cord upon certain stimuli.

1.3.9. **Pericyte plasticity**

One remarkable aspect of pericytes from different organs is their ability to differentiate *in vitro* into diverse cell types such as adipocytes, osteoblasts, chondroblasts, myoblasts, etc. suggesting a multipotent stem cell phenotype [204,205]. The similarities with bone marrow (BM) mesenchymal stem cell cultures have led to the idea that pericytes may be indeed the organ–specific BM mesenchymal stem cell counterparts [206]. A deeper analysis of this issue will be carried out in the discussion part of this thesis.

2. RESULTS

2.1. Characterization of cultures from the adult human cerebral cortex

In order to assess the potential of somatic cells from the adult human cerebral cortex to be used in cell-based replacement strategies for neuronal repair I collected brain tissue directly from the operation room and proceeded to culture cells isolated from it. These specimens were derived from surgical approaches through the cerebral cortex to deep-seated non-malignant lesions such as epileptic foci and non-ruptured vascular lesions. Only non-diseased tissue was used in this study; furthermore, no patients with tumors were selected for this work. It remains open whether patients suffering epilepsy present abnormalities in areas where no pathological hallmarks of the disease can be detected which could lead to unexpected phenomena *in vitro.* Specimens were mostly derived from temporal cerebral cortex but included also frontal and parietal tissue due to its location, adjacent to the hippocampus, a region which is often the focus of epileptic seizures. The tissue samples could easily be identified as cortex due to its characteristic convolutions which confers the gyrencephalic appearance to the human brain. The age of the patients, in the range of 18 to 65 years old, did not result in obvious changes in proliferation or morphology upon culturing. In contrast to reports claiming the isolation and expansion of progenitor cells from white matter of the adult human brain as neurospheres [207], I performed adherent monolayer cultures to avoid the isolation of neural stem cells. Attempts to culture cells from adult human brain can be found in the literature [208], however lacking a systematic characterization of the main population of protoplasmic proliferative cells that can be expanded from these samples and applying the recurrent term *fibroblast* to a cell type for which no well characterized marker is known. Astroglia can be also found in cultures from adult brain tissue when mild dissociation procedures are applied, however they seem to lack the ability to proliferate, a limiting condition that makes this cell type not suitable for retrovirally-mediated transduction (gene delivery method for over-expression purposes). One cell type which so far has not attracted much attention as a potential player in cell-replacement strategies is the pericyte, which is part of the neurovascular unit, the blood-brain barrier (BBB), and can be isolated from adult human brain autopsy tissue and subsequently cultured *in vitro* [209]. In this thesis, I provide evidence for the perivascular nature of the main cell type with the ability to proliferate in the presence of serum upon mechanical dissociation

of healthy adult cerebral cortical tissue while excluding a major contribution of other cell lineages.

2.1.1. **Immunocytochemical analysis**

Astroglia from human adult brain *in vitro*

Two major populations can be detected by immunocytochemical methods in adherent cultures from adult human cerebral cortex, namely astroglia and pericytes, which can be distinguished from each other by their distinct morphology and marker expression. Due to their size and characteristic morphology, astroglial cells can be readily visualized under the fluorescence microscope. Although astrocytes represent a minor proportion of the total cell number it is worthwhile including a section in this thesis to address the diversity of this lineage in the adult human cortex, revealed indirectly by *in vitro* culturing. Only when performing mild dissociation (together with a trypsinization step) of cortical tissue it is possible to isolate this cell type, suggesting that they are very sensitive to mechanical rupture.

Astrocytes are characterized by the presence of thin elongated and ramified processes, radiating from the cell body in a stellate manner, however differences in shape, branching complexity as well as in marker expression can be observed in cultured astroglial cells. In the adult human cerebral cortex four distinct GFAP-positive astrocyte morphologies have been described: a, protoplasmic; b, interlaminar; c, polarized; and d, fibrous [210]. Astroglial cells present in the cultures were visualized by immunostaining using various markers typically labeling astrocytes such as the intermediate filaments GFAP, Nestin and Vimentin; cytoplasmic proteins like S100ß and Glutamine Synthetase [84] and receptors such as the neurotrophin receptor $p75^{NTR}$ [211] (**Figures 2.1**, **2.2**). I found great heterogeneity in the expression of these astroglial markers, with GFAP being prominently expressed by most cells displaying astroglial morphology although with differences in intensity, indicating a clear diversity among the GFAP-positive population. Interestingly, cells with lower levels of GFAP often displayed higher levels in the expression of S100ß and Glutamine synthetase (**Figures 2.1**, **2.2**).

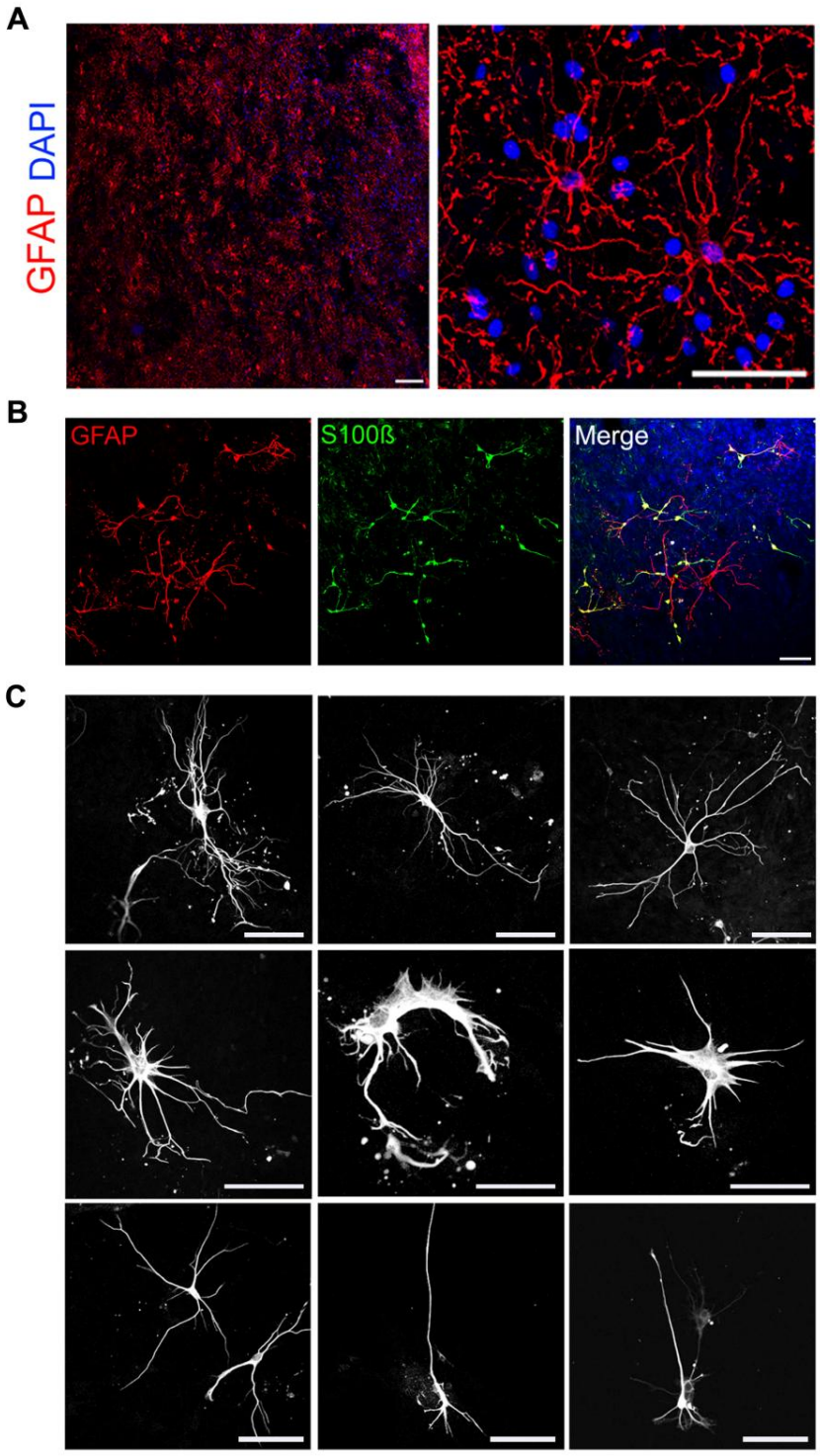

Figure 2.1: Cultured astroglia from adult human cerebral cortex. A, Immunohistochemistry reveals abundant GFAP-positive astrocytes in adult human cortical tissue samples prior to culturing (**left,** overview; **right,** high magnification view**)**; GFAP (red), DAPI (blue). **B**, Adult human astroglia immunostained for GFAP (red) and S100ß (green) *in vitro*; DAPI (blue). **C**, Examples of GFAP-positive astroglia *in vitro*. Scale bars: 100µm.

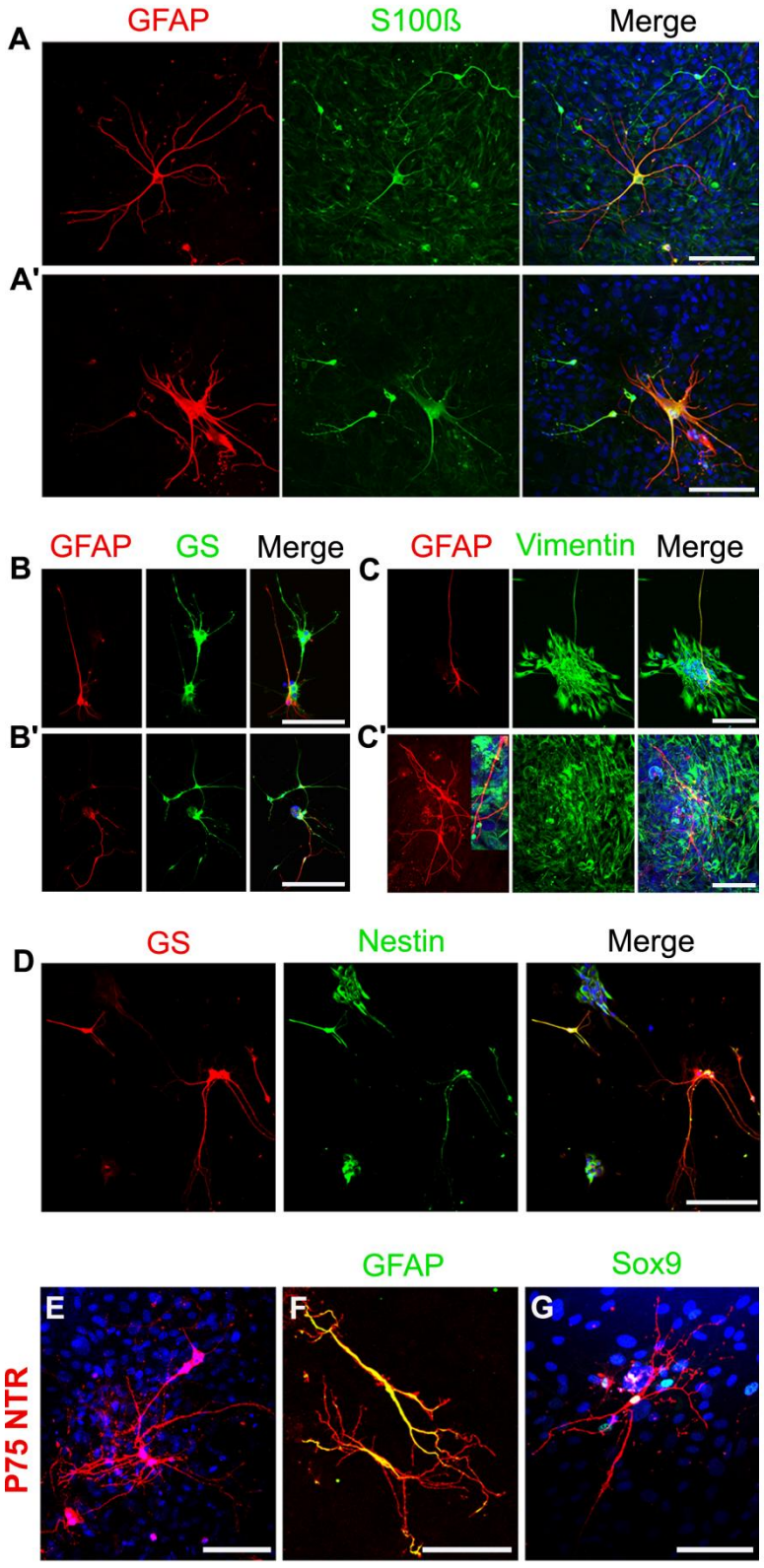

Figure 2.2: Marker expression diversity among astroglia derived from adult human cerebral cortex. A-A', GFAP (red)**,** S100ß (green), DAPI (blue). **B-B'**, GFAP (red)**,** Glutamine synthetase GS (green), DAPI (blue). **C-C',** GFAP (red), Vimentin (green), DAPI (blue). **D**, Glutamine synthetase GS (red), Nestin (green), DAPI (blue). **E**, P75 neurotrophin receptor P75NTR (red), DAPI (blue). **F**, P75NTR (red), GFAP (green). **G**, P75NTR (red), Sox9 (green), DAPI (blue). Scale bars: 100µm.

In regard to Nestin and Vimentin expression, also certain variability could be observed, with the expression levels of these filaments being inversely proportional to the size and complexity of the cells (**Figure 2.2**). I could then identify two types of astroglia in these cultures which correspond morphologically to fibrous and polarized astrocytes, according to the number of processes emerging from their cell bodies (**Figure 2.1**). I did not find protoplasmic astrocytes, characterized for bearing on average forty radial processes with high degree of branching [210]. In contrast, fibrous astrocytes, displaying a stellate morphology with fewer primary processes, are less branched than protoplasmic astrocytes, allowing a clear identification. Polarized astrocytes display a unipolar neuron-like morphology and they are smaller in size in comparison to fibrous astrocytes. Given the length of the main process of the interlaminar astrocytes, it is very unlikely that upon dissociation their integrity could be preserved, thus explaining their absence in culture. Despite the fact that no proliferation assay was performed, the scarcity of astrocytes in these cultures suggests their inability to proliferate in vitro. This data shows the feasibility of culturing adult astroglia from the human cerebral cortex, highlighting the diversity of this cell lineage both in morphology and in marker expression.

Perivascular cells from human adult brain *in vitro*

Upon dissociation of adult human cerebral cortical tissue and culturing in the presence of serum for a period of 2-3 weeks, proliferating protoplasmic cells originating from sphere-like structures (**Figure 2.5**) can be readily detected in the culture flask. They are morphologically very different from astrocytes and have been previously identified as fibroblasts [208]. I performed immunocytochemical analysis for the expression of markers of perivascular cells [205], namely platelet–derived growth factor receptor ß (PDGFRß), Vimentin, α-Smooth muscle actin (SMA), NG2, CD146, CD13, Sox9 and Nestin resulting in a major proportion of the analyzed cells being immunoreactive (**Figure 2.4**, **2.5**). Pericytes are mural cells located at perivascular positions, which typically express PDGFRß and NG2, among other markers, however with a high degree of heterogeneity depending on their localization and size of the blood vessel (**Figure 2.3**). Upon culturing, the vast majority of the cells express PDGFRß, clearly recognized as a membrane bound protein, and Vimentin, an intermediate filament expressed by cultured pericytes and fibroblasts. Also NG2, SMA, CD146 and CD13 expression could be detected although at variable levels and distribution among the expanded cell population (**Figure 2-4**). Nestin could be detected in the majority of cells; however it is also

expressed by glial and neural stem cells (data not shown). NG2 is as well expressed by glial cells, but co-localization with SMA indicates a perivascular identity.

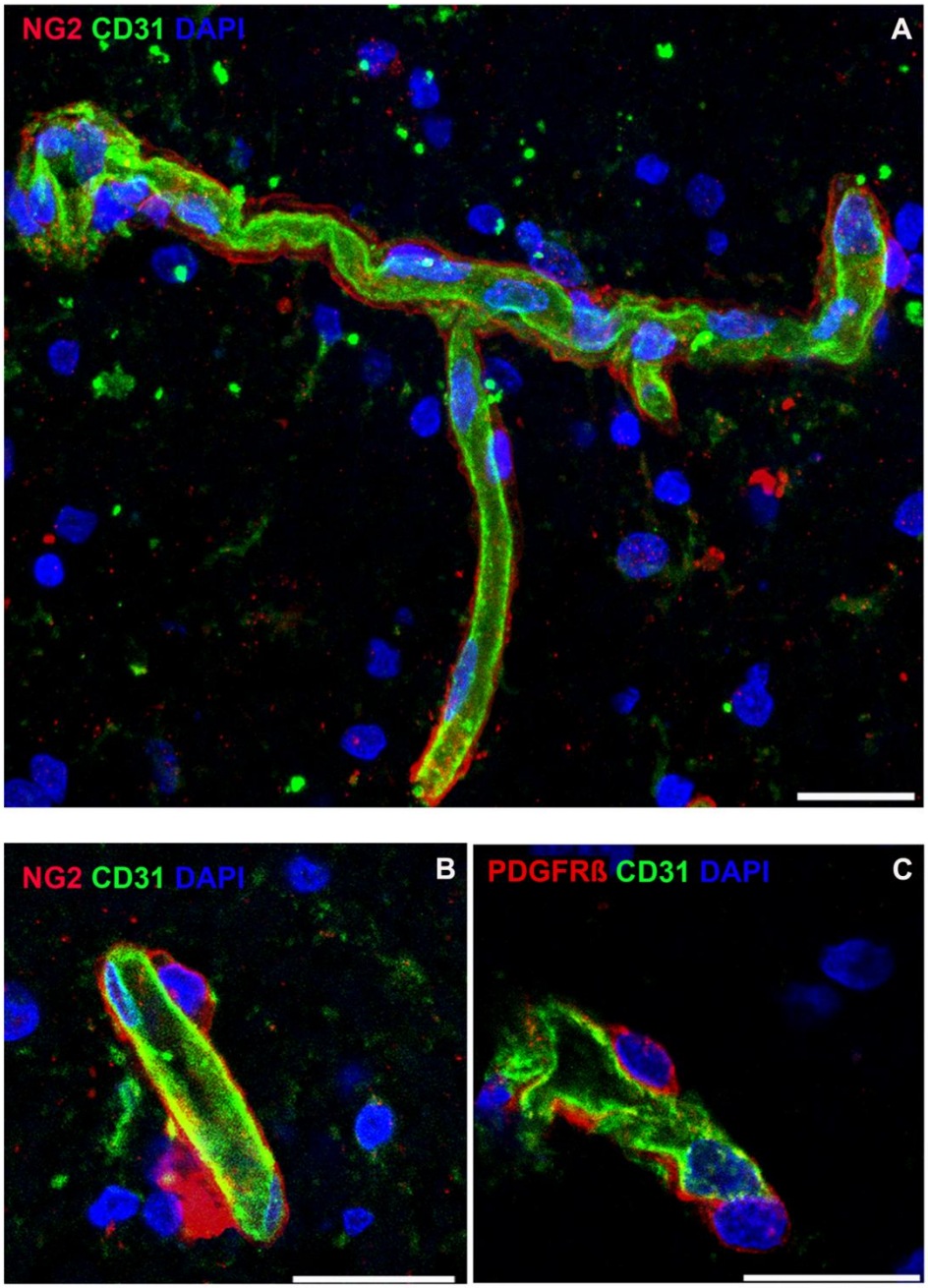

Figure 2.3: Marker expression characterization of perivascular cells from the adult human brain *in vivo*. PDGFRß expression in microvessel-associated cells in the adult human cerebral cortex. **A, B,** NG2 expression in microvessel-associated cells in the adult human cerebral cortex. **C,** PDGFRß expression in microvessel-associated cells in the adult human cerebral cortex, Microvessels were visualized by CD31 (green) immunoreactivity; DAPI (blue). Scale bars. 50 µm.

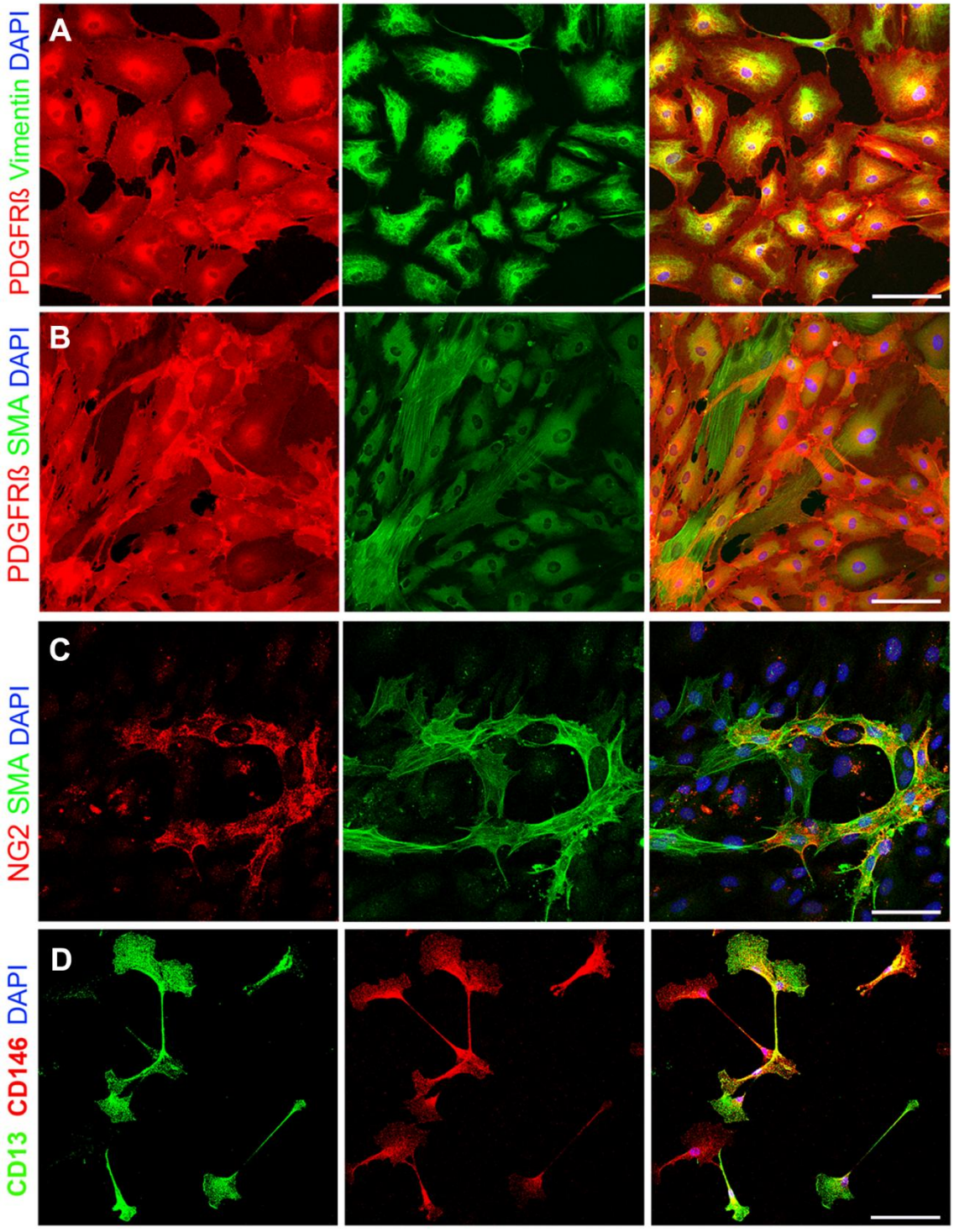

Figure 2.4: Immunocytochemical analysis for pericyte marker expression in cell cultures obtained from adult human cerebral cortical tissue. **A,** PDGFRß (red), vimentin (green), DAPI (blue). **B** PDGFRß (red), α-smooth muscle actin (SMA, green), DAPI (blue). **C,** NG2 (red), SMA (green), DAPI (blue). **D,** CD13 (green), CD146 (red), DAPI (blue). Scale bars: 100µm.

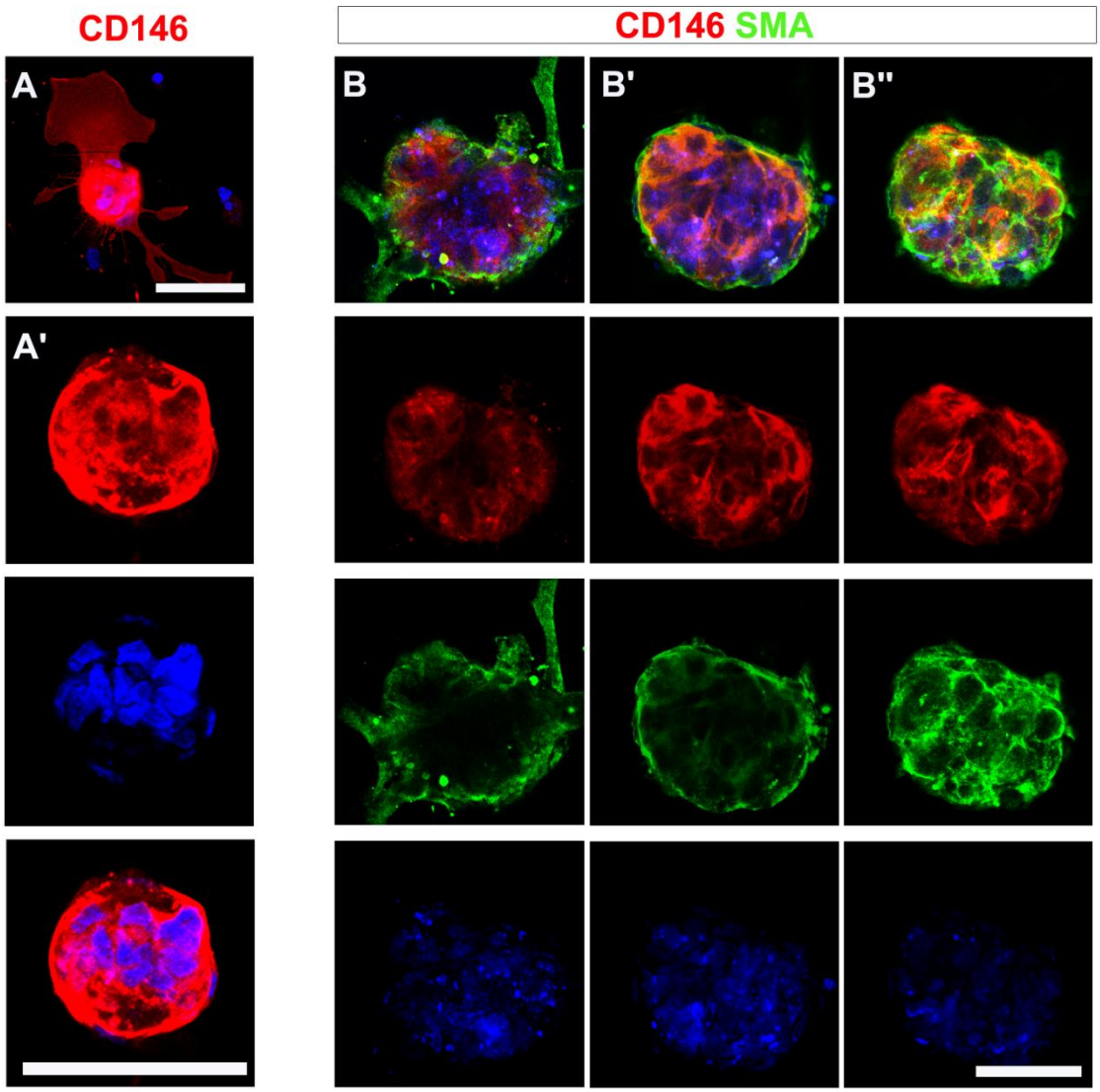

Figure 2.5: *In vitro* sphere-like aggregates in cell cultures derived from adult human cerebral cortex. A, Accumulation of DAPI-positive nuclei in a sphere-like aggregate on top of a CD146-positive proteoplasmic cell. **A'**,Confocal section through a CD146-positive sphere-like aggregate (shown in **A**); CD146 (red), DAPI (blue). **B-B''**, 3 confocal slices from the bottom to the top of a sphere containing CD146- and SMA-positive cells; CD146 (red), SMA (green), DAPI (blue). Scale bars: 100µm.

By the use of antibodies raised against proteins typically expressed by pericytes, I could demonstrate the major contribution of protoplasmic cells of perivascular origin in cultures isolated from adult human cerebral cortex.

2.1.2. **Identity of cell cultures from adult human brain assessed by qRT-PCR**

In order to confirm the cellular composition of the cultures, messenger RNA (mRNA) was extracted from cell cultures derived from four patients at three different stages, from starting point right after expansion up to passage number two. By quantitative RT-PCR experiments, the relative proportion of mRNA corresponding to a selection of proteins

could be estimated. This technique allowed the confirmation of the perivascular identity of the cultures as well as determined the presence of cell lineages which might have not been detected by immunocytochemical analysis. As control, mRNA was extracted from cerebral tissue corresponding to two patients from which cell cultures were derived and used in this analysis.

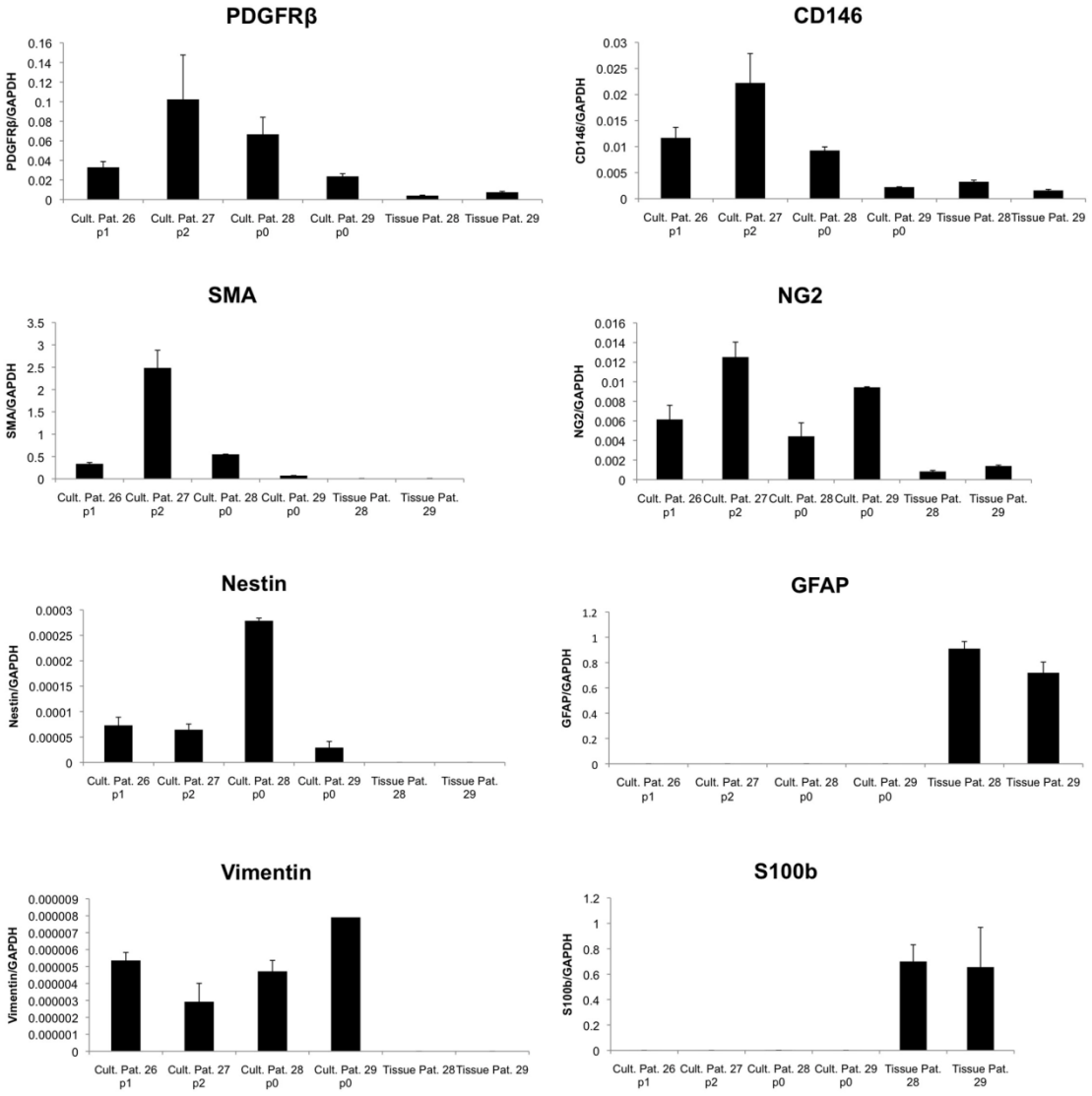

Figure 2.6: **Gene expression analysis in adult human cerebral cortical cultures.** Real-time quantitative RT-PCR analyses for expression of various mRNAs in cultures derived from different patients and different passages. Expression was normalized to mRNA levels of GAPDH and compared to the expression within the human tissue from which cells were isolated. Messenger RNAs analysed include some characteristic for pericytes (PDGFRß, CD146, α-smooth muscle actin (SMA), NG2 (gene name Cspg4), intermediate filaments which are also expressed in pericytes (NESTIN, VIMENTIN) and astroglia specific mRNAs (GFAP, S100ß).

The amount of mRNAs for the pericyte markers PDGFRß, CD146, SMA and NG2 (**Figure 2.6**) was examined at three different culturing stages (passages). The enrichment of perivascular mRNAs could be explained by an increase on expansion in the number of cells pericytic origin, an induction of the higher expression due to the culture conditions, or both. In any case, the relative proportion of these transcripts is remarkably high, even exceeding the levels of the housekeeping gene, i.e. mRNA levels for SMA (**Figure 2.6**). Notably, all mRNAs analyzed showed lower levels in the transcripts extracted directly from cortical tissue, evidencing enrichment for pericytic mRNAs upon culturing. Taken together, this data demonstrates the enrichment of mRNA expressed by pericytes and indirectly suggests a proliferating behavior of pericytes *in vitro* since the levels compared to original tissue samples dramatically increase as the cells expand in number.

Despite the potential presence of astroglial cells in the cultures derived from cortical tissue, the lack of mRNA for GFAP and S100ß (**Figure 2.6**) in the analyzed samples reveals the virtual absence of astrocytes when tissue dissociation is carried out in standard conditions (excluding trypsin) indicating that this cell lineage does not participate as a cellular component of the cultures. In contrast, the amount of transcripts extracted from the original tissue reveals a strong contribution of astrocytes within the organ, highlighted when comparing to the levels of perivascular mRNAs. This data indicates that astroglia cannot be expanded under these culture conditions. Furthermore, mRNA levels for intermediate filaments such as Vimentin and Nestin were analyzed (**Figure 2.6**), resulting in an increase upon culturing. Of note, they were absent in the tissue samples, suggesting that neither tumor formation nor reactive gliosis [84] had occurred within the tissue prior to culturing. It has been described that pericytes *in vitro* up-regulate the expression of mRNA for these intermediate filaments [209] which, in contrast to classical pericyte markers, seems to decrease in level upon passaging.

One major concern is the presence of neural stem cells in the cultures from adult cortical tissue which would undergo neuronal reprogramming much more efficiently than any other cell lineages such as pericytes, potentially generating confusion when interpreting results. For this reason, qRT-PCR was carried out on the samples for the detection of mRNAs typically expressed by neural stem cells such as SOX1 and SOX2 (**Figure 2.7**). All cultures were devoid of transcripts for these neural stem cell markers, arguing against the presence of cells with the intrinsic ability to generate neurons.

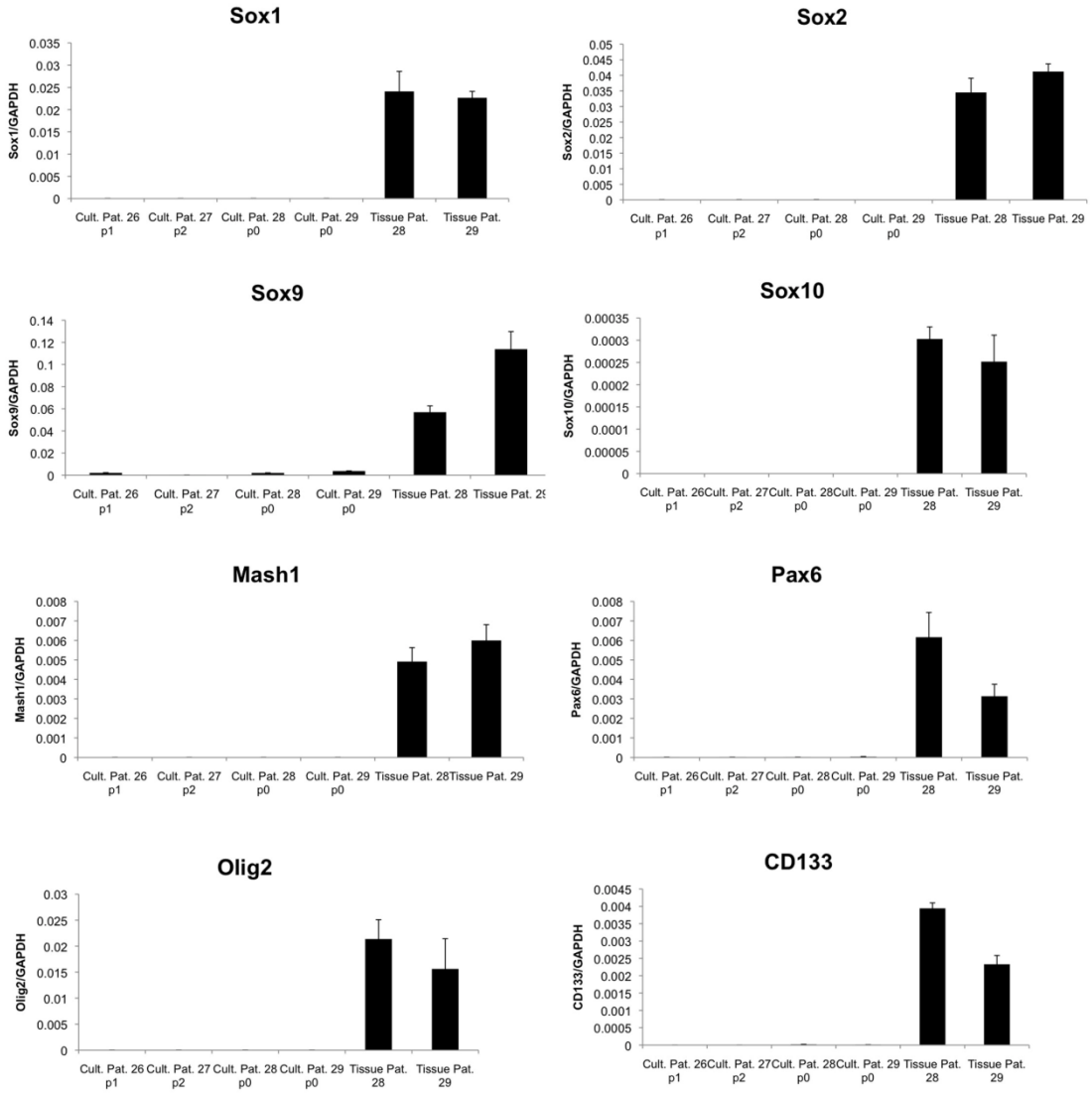

Figure 2.7: Absence of neural stem cell and progenitor gene expression in adult human cerebral cortical cultures. Real-time quantitative RT-PCR analyses of genes characteristic of neuronal stem or progenitor cells (SOX1, SOX2, OLIG2, ASCL1 (Mash1), PAX6, CD133/Prominin1), oligodendrocytes (OLIG2, SOX10) or neural crest progenitors (SOX10). Expression was normalized to mRNA levels of GAPDH and compared to the expression within the human tissue from which cells were isolated.

The tissue samples contained mRNAs for SOX1 and SOX2, consistent with the described expression of SOX2 in adult cortical astrocytes [212] and in subtypes of adult postmitotic neurons, including pyramidal cells of the cerebral cortex, some striatal neurons and many thalamic neurons [121].

Other member of the SOX family, SOX10, whose expression marks neural crest-derived cells and the oligodendrocyte lineage in the brain [213], could not be detected at the mRNA level, however abundantly expressed in the cortical tissue samples (**Figure 2.7**). The repressor bHLH transcription factor OLIG2 was also analyzed by RT-PCR to exclude

the presence of oligodendrocyte progenitor cells (OPC) in the cultures, since a potential neuronal fate under certain conditions has been reported for this cell type [214]. Indeed, while high expression levels of this mRNA were found in the cortical tissue, no expression was detected in the cultures, excluding the possibility for a major cellular contribution of this lineage (**Figure 2.7**). Furthermore, examination of the expression of markers for neural progenitors or precursor cells committed to a neuronal lineage was required to exclude additional cells with intrinsic potential to generate neurons. In fact, a marker of stem cells such as CD133/Prominin or Pax6 and Mash1 mRNAs, which are expressed by neural progenitors, could not be detected at any passage confirming that the cultures were devoid of neuronal progenitors (**Figure 2.7**).

SOX9, another SOX family member can be found labeling diverse cell types such as astrocytes, chondrocytes, etc and its expression may also be found in pericyte cultures when exposed to certain culture media [215]. Compared to control samples, the levels of SOX9 mRNA in the cultures at all analyzed passage stages were very low (**Figure 2.7**).

Due to the intimate contact of pericytes and endothelial cells forming the capillaries it is possible that the latter could be also taking part in the cellular composition of the cultures. For this reason, the levels of mRNA for CD34 which labels cells of endothelial and hematopoietic lineage were analyzed (**Figure 2.8**). Despite a certain amount of CD34 mRNA present in the culture samples, a clear reduction is observed upon passaging, indicating that an initial minor contribution of these cell types at an early time point of culturing does not persist at late stages.

The neurotrophin receptor $p75^{NTR}$ labels, among other cell types, neuroectodermal lineages, such as neural crest-derived cells [216]. While p75 mRNA can be readily detected in all samples, it seems that culturing promotes a down-regulation of this receptor (**Figure 2.8**).

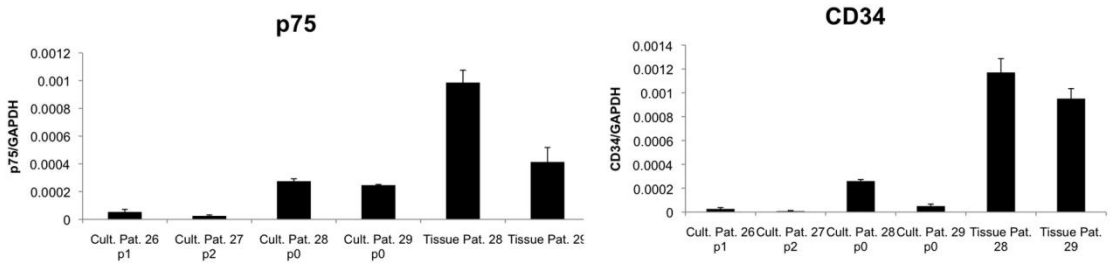

Figure 2.8: Gene expression analysis in adult human cerebral cortical cultures. Real-time quantitative RT-PCR analyses for expression of two mRNAs in cultures derived from different patients and different passages. Expression was normalized to mRNA levels of GAPDH and compared to the expression within the human tissue from which cells were isolated. Messenger RNAs analysed consist of p75 neurotrophin receptor and and endothelial/hematopoetic lineage specific mRNA (CD34).

2.1.3. **Cellular composition of cultures from adult human brain assessed by FACS**

In order to estimate the relative proportion of pericytes within the cultures, and taking advantage of their surface marker expression, fluorescence activated cell sorting (FACS) was performed. After isolation and expansion, cells from adult human cerebral cortical tissue were detached from the culture dish and incubated in suspension with fluorescence-conjugated antibodies against proteins expressed by pericytes within the cell membrane, at its external surface. The use of membrane-bound proteins as markers for sorting allows further culturing without significant cell death. For control, isotype (same species as subject antibodies) fluorescence-conjugated antibodies were used and the gates properly established in order to eliminate data from cell debris, dead cells, and clumps of 2 or more cells. Subcellular debris and clumps can be distinguished from single cells by size to avoid false positives (**Figure 2.9**). Antibodies against PDGFRß, CD146 and CD13 were used to detect pericytes and CD34 for identification of endothelial/hematopoietic cells. Single or double analysis was performed, combining one pericyte marker with CD34. Consistent with the data obtained from the immunocytochemical and qRT-PCR analyses, I found that a major proportion of the cells present in the cultures expressed PDGFRß, in some occasions above 90% (**Figure 2.9**). Given that PDGFRß expression was restricted to perivascular location in the histochemical analysis of cerebral cortical tissue used to prepare the cultures (**Figure 2.3)**, it is very likely that these cells in culture are indeed of pericyte origin. However, in order to accumulate additional evidence further analysis was performed on cells isolated from 6 patients at different passages (P0 to P4) in comparable experimental conditions with PDGFRß, CD146 and CD13 antibodies (**Figure 2.9**). Around 70% of the cell

population showed PDGFRß expression, while CD146 and CD13 were found to be expressed to a lesser extent, representing around 40% of the total analyzed cells. While this data shows some heterogeneity within the cultures, it is worthwhile mentioning that it is well accepted in the literature that expression of markers by pericytes is highly dynamic, especially *in vitro* [217].

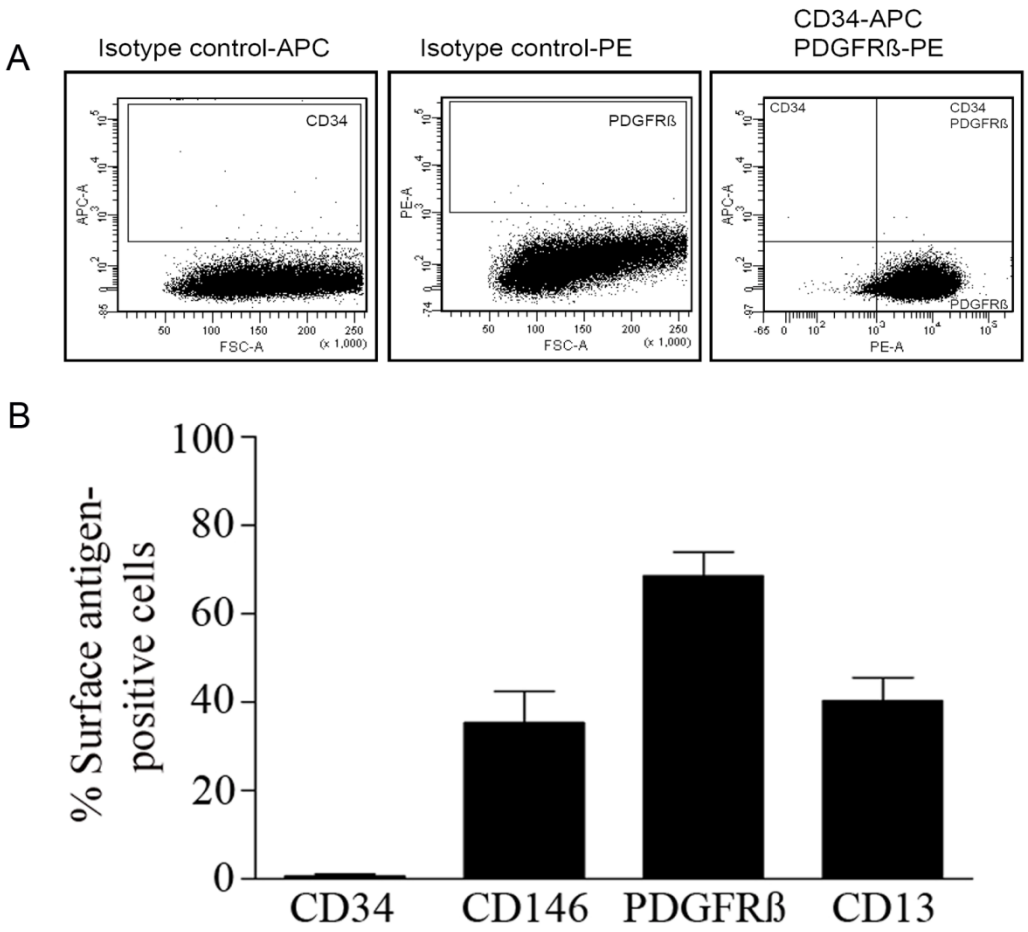

Figure 2.9: FACS analysis of cell cultures from adult human cerebral cortex: A, Example of FACS analysis from an adult human brain culture based on PDGFRß expression. Depicted are the isotype controls for establishing the gating conditions for sorting the PDGFRß- and CD34-positive (left and middle panel) and the PDGFRß-positive (right) populations. **B,** Histogram shows the percentage of cells positive for cell surface markers characteristic of pericytes. Cells isolated from 6 different patients were used (n=6). Error bars show SEM.

In addition, variability in the expression levels can be clearly observed by immunocytochemical methods. Since FACS analysis was performed in a very stringent manner to avoid false positives, it is likely that low expressing cells are excluded from positive ones. Of note, the proportion of CD34 positive remained below 1% (**Figure 2.9**), adding further evidence for the absence of endothelial/hematopoietic cells in the cultures despite the detection of low levels of CD34 mRNA. Taken together, these data

demonstrate that cells with a pericytic nature represent the major population within the cultures while excluding the presence of astroglia, oligodendrocytes, neural progenitors and neural stem cells. Moreover, while low amounts of endothelial/hematopoietic mRNA can be detected in the samples (**Figure 2.8**), the contribution at the cellular level is shown to be lower than 1% (**Figure 2.9**).

2.2. **Candidate reprogramming transcription factors**

2.2.1. **Design of reprogramming Mash1- and Ngn2-expressing constructs**

It has been shown that astroglia can be directed to a neuronal phenotype by forced expression of neurogenic fate determinants such as Neurogenin2 and Mash1 (also known as Ascl1), relying in retrovirally-mediated gene transfer through the use of Moloney Murine Leukemia Virus (MMLV)-derived vectors in which expression was driven by the long terminal repeat (LTR). These viral sequences also mediate retroviral integration into the host genome via a LTR specific integrase [218,109].

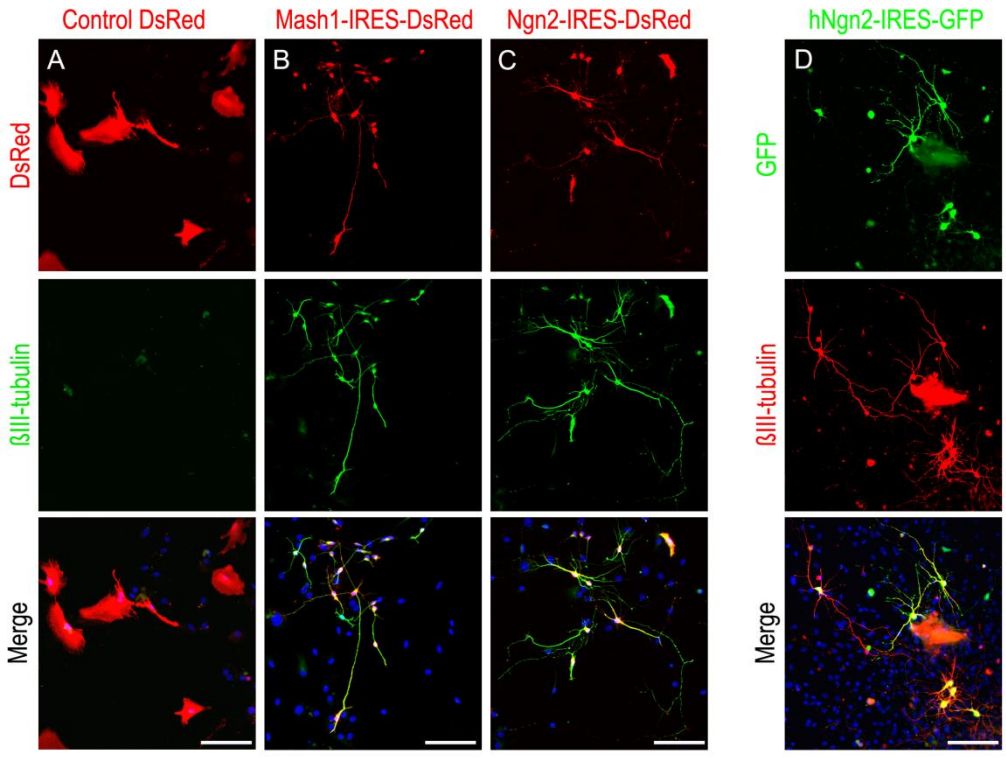

Figure 2.10: ***In vitro*** **conversion of mouse postnatal astroglia into neurons by forced expression of CAG-Mash1-IRES-Dsred, CAG-Ngn2-IRES-Dsred or pMX-humanNeurog2-IRES-GFP**. **A,** Control transduced astroglia; DsRed (red), ßIII-tubulin (green) DAPI (blue). **B,** CAG-Mash1 transduced astroglia adopt a neuronal phenotype; DsRed (red), ßIII-tubulin (green), DAPI (blue). **C,** CAG-Ngn2 transduced astroglia; DsRed (red), ßIII-tubulin (green) DAPI (blue). **D**, pMX-humanNeurog2 tranduced astroglia; GFP (green), ßIII-tubulin (red) DAPI (blue). 5 days post-infection; Scale bars: 100µm.

However, astroglia-derived neurons generated by this approach lacked the ability to establish functional synapses. It was speculated that expression of the reprogramming factors should occur at faster rate and higher level to achieve a fully mature neuronal conversion. For this reason, I generated new retroviral constructs in which expression was driven by an alternative promoter, the so called CAG, a combination of the cytomegalovirus (CMV) early enhancer element and chicken beta-actin promoter [219], which has been shown to drive expression at higher levels in mammalian expression vectors and are less prompted to silencing. I subcloned the cDNA corresponding to rat Mash1 and mouse Ngn2 from the vectors originally used in the astroglia to neuron conversion. While rat and human Mash1 share high homology at the protein level (99%), suggesting that the rat cDNA may activate transcription in human cells, the lower similarities between mouse and human Ngn2 (81%) led me to subclone the human Ngn2 cDNA into a retroviral vector in order to ensure reprogramming efficacy in the context of human cells. In all cases, the sequence of the neurogenic fate determinant was followed by an internal ribosomal entry sequence (IRES) and a reporter gene, either DsRed or GFP. The use of reporter is required for detection of transduced cells for electrophysiological recording.

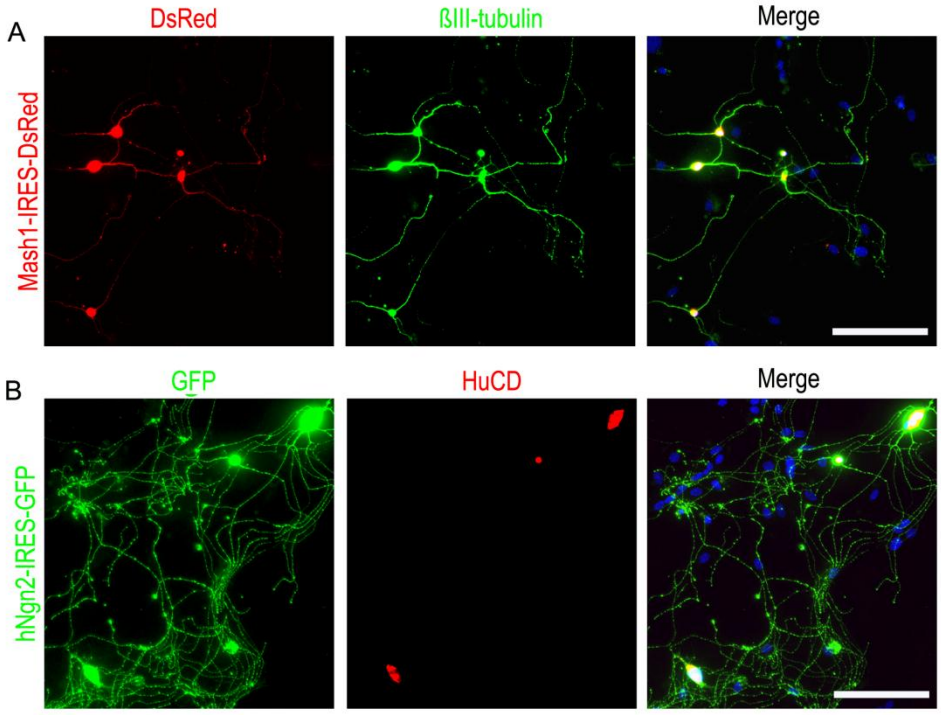

Figure 2.11: Long term expression of neurogenic transcription factors does not impair neuronal differentiation. Mouse postnatal astroglia transduced with **A**, Mash1-IRES-Dsred or **B**, pMX-humanNeurog2-IRES-GFP. **A**, DsRed (red), ßIII-tubulin (green), DAPI (blue). **B**, GFP (green), HuCD (red), DAPI (blue); 30 days post-infection. Scale bars: 100µm.

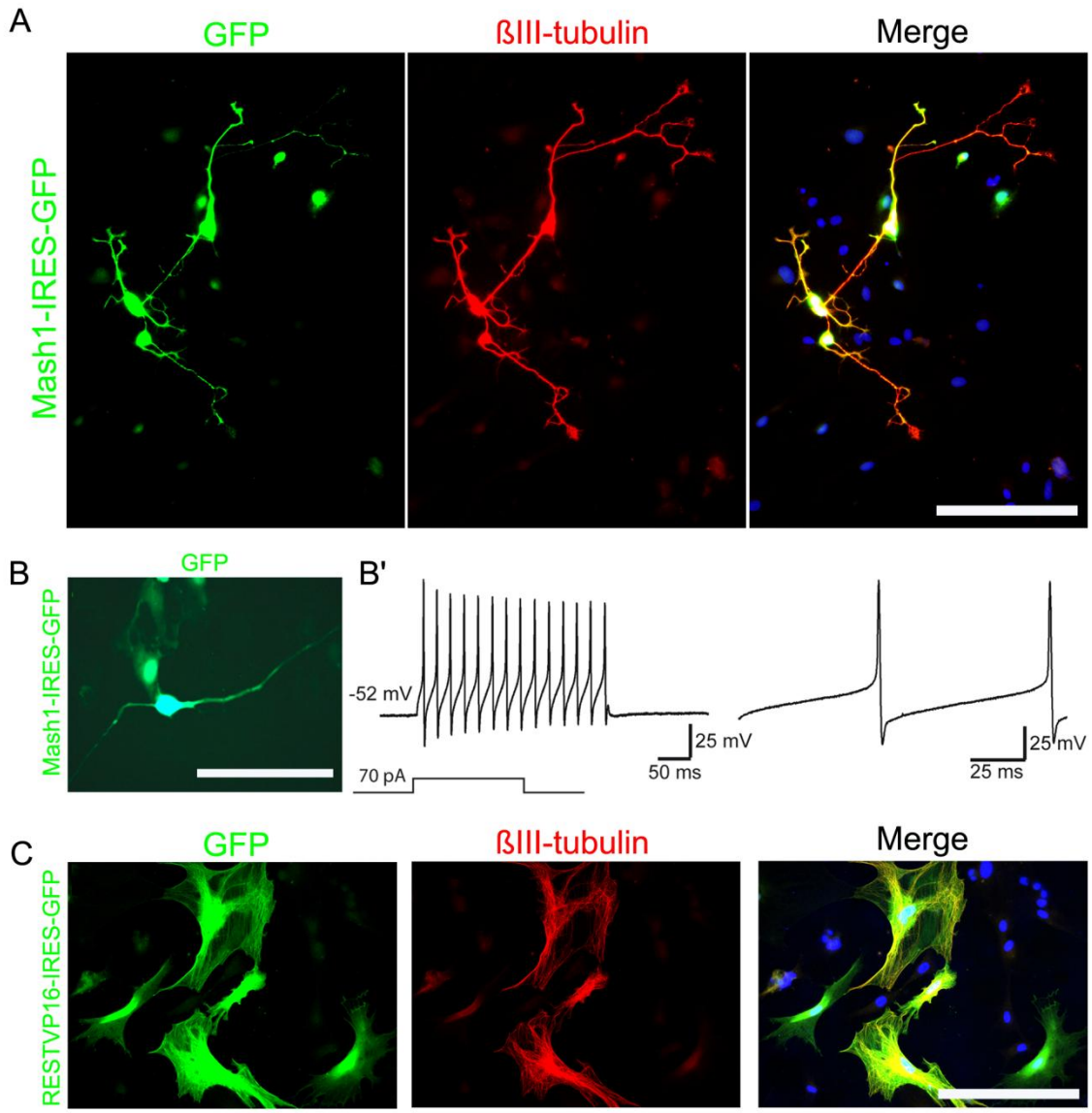

Figure 2.12: In vitro conversion of cells isolated from the rat cerebral cortex of late postnatal age into neurons by forced expression of Mash1. A, Cells transduced with pCLIG-Mash1-IRES-GFP give rise to ßIII-tubulin (red) positive cells, DAPI (blue); 12 days post-infection. **B-B',** Mash1-positive cells (GFP) fire repetitive action potentials upon depolarizing step-current injection; 14 days post-infection. **C**, Cells transduced with pMX-REST:VP16-IRES-GFP fail to induce a neuronal phenotype in cells isolated from the cerebral cortex of late postnatal rat but express ßIII-tubulin; 12days post-infection; GFP (green), ßIII-tubulin (red), DAPI (blue). Scale bars: 100µm:

I then proceeded to test the ability of the CAG retroviral constructs to convert postnatal astroglia to neuron (P5). As expected, Mash1 transduced cells adopted a neuronal morphology (round cell soma extending long thin processes) and up-regulated the expression of the neuronal marker ß-III-tubullin (class III member of the beta tubulin protein family [220]) within 5 days after infection (**Figure 2.10**). Interestingly and despite the lower homology between species in comparison to Mash1/Ascl1, the human Ngn2 construct showed similar efficacy as mouse Ngn2 in converting mouse astroglia to neurons (**Figure 2.10**). The generated neurons displayed distinct morphologies upon

expression of either transcription factor (**Figure 2.10**) In addition, analysis after long term differentiation periods (30 days) showed no toxicity due to over-expression of the neurogenic fate determinants, as healthy HuCD-expressing mature neurons [221] could be found within the cultures (**Figure 2.11**). Since the goal of this project is to generate neurons from cells derived from later developmental stages (ultimately, adult human tissue), I tested the ability of retroviral constructs to induce neurogenesis in cells isolated from the cortex of rats at later postnatal stages (P25) in a similiar manner as from early postnatal mouse. Neither mouse (with 97% homology with rat Ngn2) nor human Ngn2 (82%) expression resulted in the generation of cells with neuronal morphology or up-regulation of ß-III-tubulin, suggesting differences in reprogramming efficacy of this transcription factor among species and developmental stages. In contrast, transduction of rat cortical cultures with Mash1 led to the generation of cells with bipolar elongated morphology; their neuronal identity was confirmed by immuno-cytochemistry (**Figure 2.12**). Further characterization by means of electrophysiological recordings, showed the ability of Mash1-expressing cells to fire trains of actions potentials, indicating the potential of Mash1 to elicit functional neurogenesis in other *in vitro* cellular contexts than early postnatal mouse astroglia (**Figure 2.12**).

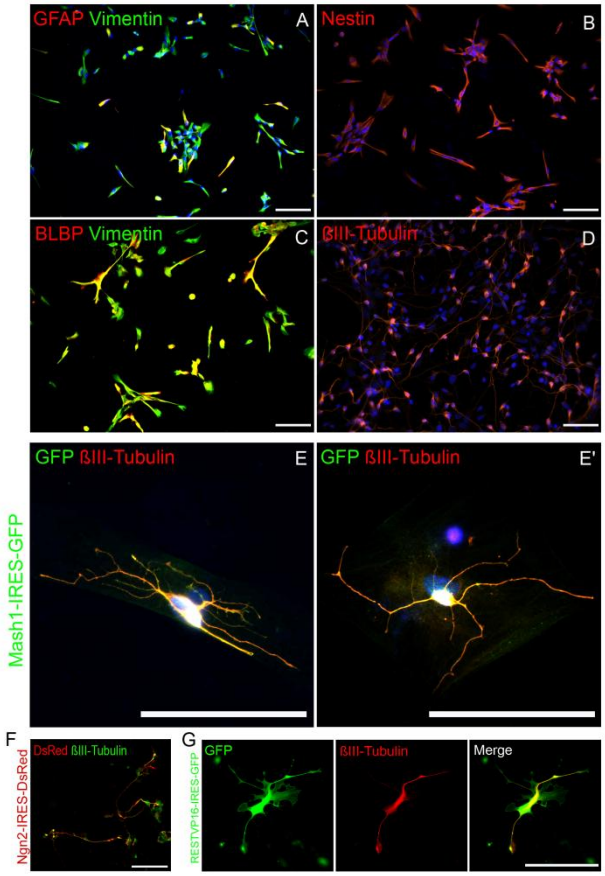

Figure 2.13: Astrocyte cultures from fetal human brain parenchyma transduced with Mash1 give rise to neuronal cells. A, B, C, D, Marker expression characterization of cultures from fetal (20 week old) brain tissue. **A,** GFAP (red), Vimentin (green). **B,** Nestin (red). **C,** BLBP (red) Vimentin (green). **D**, ßIII-tubulin (red). **E-E',** 2 examples of cells transduced with pCLIG-Mash1-IRES-GFP, giving rise to cells with neuronal morphology and ßIII-tubulin expression; GFP (green), ßIII-tubulin (red). **F,** Cells transduced with CAG-Ngn2-IRES-DsRed adopt a neuronal morphology and up-regulate ßIII-tubulin; DsRed (red), ßIII-tubulin (green). **G,** Human fetal astrocytes fail to adopt a neuronal phenotype upon REST-VP16 expression; GFP (green), ßIII-tubulin (red). DAPI (blue); Scale bars: 100µm.

Along this line and to test the ability of Mash1 to convert human cells to neurons, I obtained cultures of astrocytes derived from fetal (5 months of gestation) brain parenchyma and transduced them with Mash1 or Ngn2. After a period of 10 days I could observe the appearance of cells with small soma and branched processes, positive for ß-III-tubulin expression, indicating that Mash1 (and to a lesser extent also Ngn2) could induce a neuronal phenotype in cells of human origin (**Figure 2.13**). Ultimately, their functional neuronal properties could be assessed by electrophysiological recordings, displaying the ability to fire a single action potential. In order to reveal the origin of their electrical properties, the voltage-gated sodium channel antagonist tetrodotoxin (TTX) [222] was applied to the cells, resulting in blocking of the inward sodium current and so corroborating their truly neuronal identity (**Figure 2.14**). It is worthwhile mentioning that the cultures showed a tendency to generate cells of presumptive neuronal identity at early passages (p1-p2) (**Figure 2.13**), yet this phenomenon was no longer observed at later stages (p3-p5). Despite the use by the provider company of the term "astrocyte" based on the expression of GFAP by ≥95% of the cells, the presence of radial glia, which possesses neurogenic potential, cannot be excluded in the cultures. Indeed, the cells present in these cultures showed immunoreactivity for GFAP, BLBP, Vimentin and Nestin, highly suggestive of a radial glia identity (**Figure 2.13**). Regardless of the diversity of cell types in this sample, the ability of Mash1 and Ngn2 to promote neurogenesis in cells of human origin could be demonstrated.

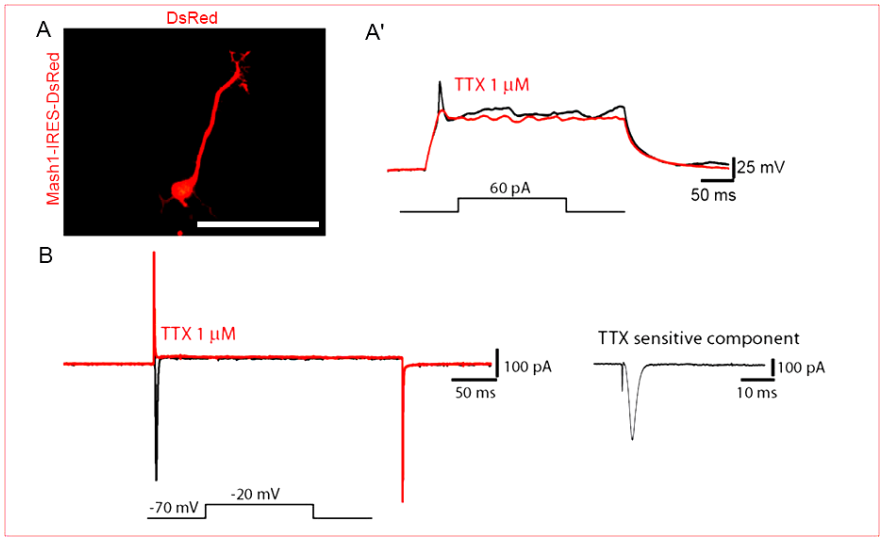

Figure 2.14: Mash1 expression induces a functional neuronal phenotype in astrocyte cultures from human fetal brain parenchyma. A, Cell transduced with CAG-Mash1-IRES-DsRed**. A',** In current-clamp mode, a cell transduced with Mash1 fire a single action potential, blocked by the sodium channel antagonist Tetrodotoxin TTX. **B**, the TTX-sensitive sodium inward current is shown is voltage-clamp mode.

2.2.2. **E47**

Over-expression of E47, one splice variant of the E2A gene, has been shown to prevent inhibition of neurogenesis by gliogenic cues in the spinal cord when co-expressed with Mash1 [223]. For this reason, I generated a retroviral construct encoding for E47 in order to test its neurogenic potential by over-expression *in vitro*.

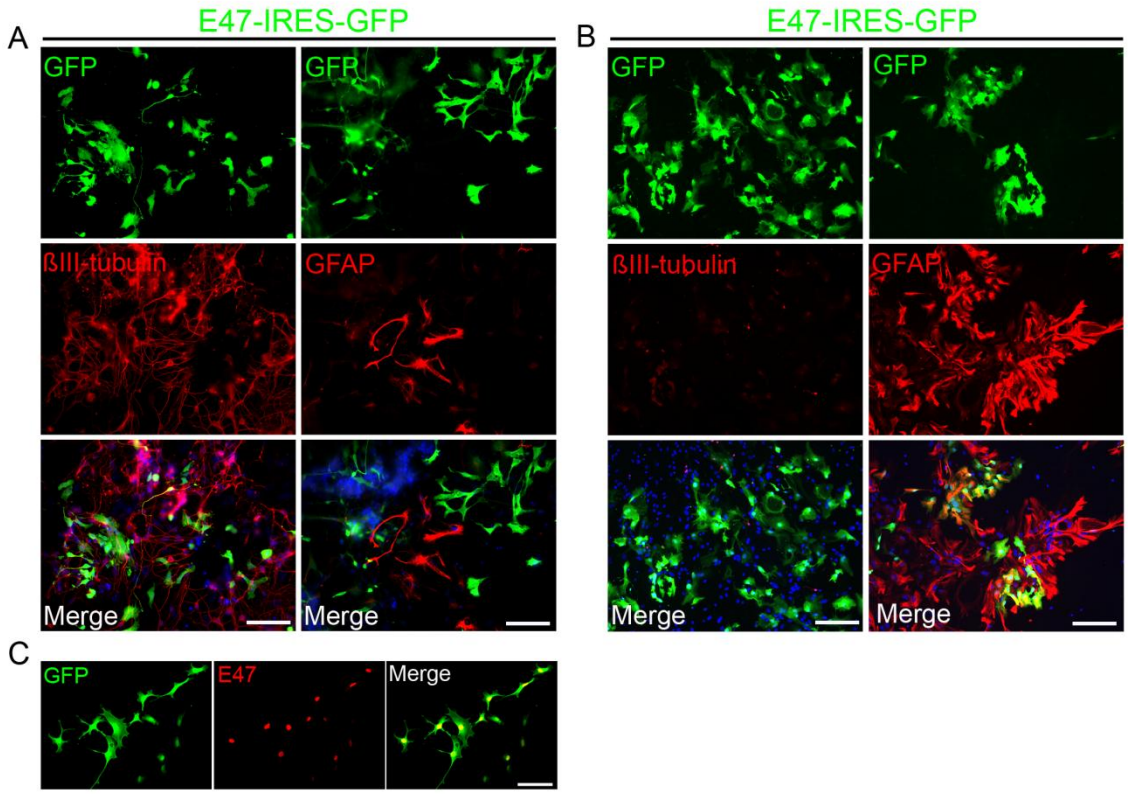

Figure 2.15: Forced expression of E47 in mouse embryonic cortical cultures and postnatal astroglia. **A,** Cultures from E14 mouse cortex transduced with pMX-E47-IRES-GFP (green), analyzed for the expression of ßIII-tubulin (left) or GFAP (right). **B,** Mouse postnatal astroglia from the cerebral cortex transduced with pMX-E47-IRES-GFP (green) analyzed for the expression of ßIII-tubulin (left) or GFAP (right). **C,** Confirmation of E47 protein expression in cells transduced with pMX-E47-IRES-GFP; GFP (green) E47 (red). DAPI (blue); Scale bars: 100µm.

I assessed the neurogenic activity of E47 in neural progenitor cell cultures isolated from mouse embryonic cortex at embryonic day 14 (**Figure 2.15**). Upon retroviral transduction, cells positive for the reporter gene (GFP) did not show a marked tendency to undergo neurogenesis, being most of the E47-expressing cells negative for neuronal markers. Interestingly, many E47-trasnsduced cells were also negative for the astroglial marker GFAP. Since the function of E-proteins is context-dependent, I analyzed the activity of E47 when over-expressed in cultures of mouse postnatal astroglia (**Figure**

2.15). Similarly as in embryonic cultures, the over-expression of E47 alone did not induce a neuronal phenotype in astroglial cells. On the contrary, reporter positive cells displayed high levels of GFAP expression, suggesting that E47 alone does not elicit obvious changes in the identity of mouse cultured cells. Therefore I proceeded to combine the expression of Mash1 and Ngn2 together with E47 (data not shown). I observed no major changes in the reprogramming effect compared to Mash1 or Ngn2 alone. More interestingly, these experiments provided useful information in regard to the possibility of use of different factors by combination of retroviral constructs, demonstrating the feasibility of this approach.

2.2.3. REST-VP16

The use of a fusion protein in which the repressor-recruiting domain of REST is replaced by the transcriptional activation domain of the herpes virus protein VP16, allows for activation of the target genes that REST is normally repressing and therefore, promoting neuronal differentiation [163]. The human cDNA for REST was used to generate REST-VP16 fusion protein, allowing for retroviral transduction of fetal human astrocyte cultures. The REST-VP16 positive cells, which could be detected by expression of a reporter gene (GFP), up-regulated the expression of ß-III-tubulin and underwent morphological changes to some extent yet they did not acquire a convincing neuronal morphology, indicating an incomplete neuronal reprogramming. Occasionally, these cells became polarized, extending two processes opposite to each other, with a cell body of polygonal/protoplasmic shape (**Figure 2.13**). Further assessment of the reprogramming ability of REST-VP16 on late postnatal rat cortical cultures resulted in no major changes in the morphologies of the infected cells; however, immuno-reactivity for ßIII-tubulin within the cytoplasm of the reporter-positive cells confirmed the ability of this fusion protein to stimulate the expression of neuronal genes [224] (**Figure 2.12**).

2.3. *In vitro* neuronal conversion of adult human brain perivascular cultures

2.3.1. Generation of neuronal cells following co-expression Mash1 and Sox2

Following the characterization of the cells present in the cultures obtained from adult human brain tissue, I proceeded to assess the response of cells of perivascular nature to forced expression of Mash1 or Ngn2. Consistent with the data obtained by immunocytochemistry, qRT-PCR and FACS techniques I found that the majority of cells transduced with a control retroviral construct encoding for Dsred displayed high expression of the pericyte marker PDGFRß (**Figure 2.16**). Given the ability of retroviral particles to transduce exclusively cells during mitosis, I could reveal the proliferative nature of the perivascular-derived cells within the cultures.

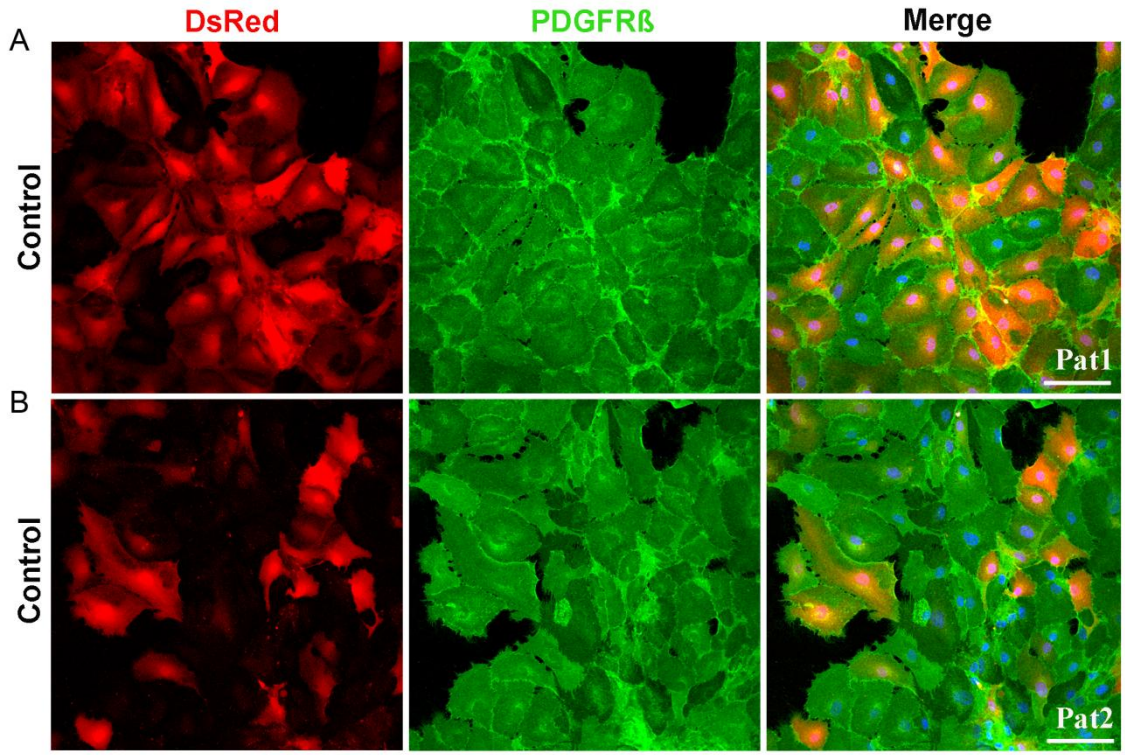

Figure 2.16: PDGFRß-positive cells isolated from the adult human cerebral cortex can be targeted with retroviral vectors. A, B, Cells isolated from 2 different patients transduced with a control retroviral construct expressing DsRed(red) display PDGFRß (green) expression. 5DPI; DAPI (blue); Scale bars: 100µm.

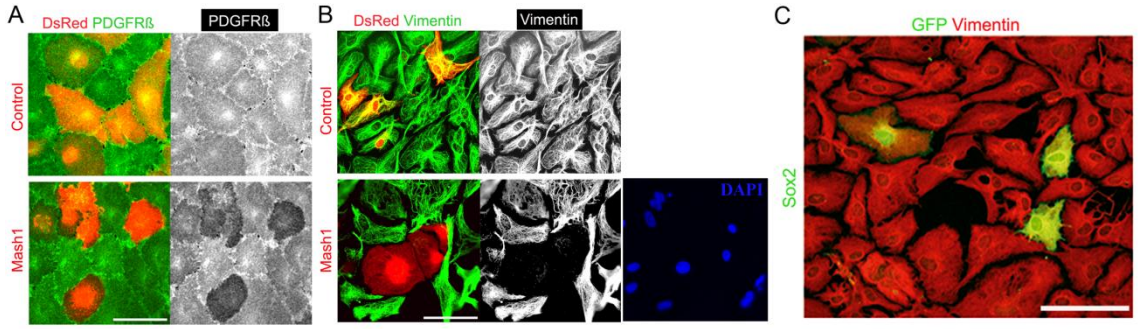

Figure 2.17: Down-regulation of pericyte markers after forced expression of Mash1 in cell cultures from adult human cerebral cortex. **A,** Control virus and Mash1-coding virus transduced cells derived from adult human cortex *in vitro* and stained for the pericyte-marker PDGFRß. The left panels show expression of DsRed protein (red, indicative of transduction) and PDGFRß (green). Right panels show down-regulation of PDGFRß (white) expression after forced Mash1 expression, but not in controls; 22 days post infection (DPI). **B,** Down-regulation of vimentin in Mash1- but not control-transduced cells; 24 DPI. **C,** Forced expression of Sox2 does not alter the cellular morphology nor vimentin expression in cultures prepared from the adult human cerebral cortex. Sox2-IRES-GFP (green); vimentin (red); 21 DPI. DAPI (blue); Scale bars: 100µm.

Interestingly, upon retrovirally-mediated expression of Mash1, a down-regulation in the fluorescence intensity corresponding to PDGFRß-immunoreactivity could be readily observed among infected reporter-positive cells (**Figure 2.17**).

Indeed, in one experiment 86% of control virus infected cells (n= 161) remained positive for PDGFRß expression after 22 days, while the proportion of PDGFRß-positive cells upon Mash1 transduction showed a reduction to 23% of the total infected cells (n=219). Forced expression of Mash1 in perivascular human cultures promote a change in cell identity, assessed by down-regulation of a defining marker for pericytes. In order to confirm the change in phenotype, I transduced cells with Mash1 and analyzed for the expression of Vimentin, which is expressed by brain pericytes in culture [209].

Mash1-positive cells displayed a strong reduction in the expression of vimentin, which could not be observed among control transduced cells, corroborating the partial reprogramming effect of Mash1 under this culture conditions (**Figure 2.17**). However, as in control cultures, no expression of neuronal markers could be detected in confluent perivascular cultures (**Figure 2.18**). The normal appearing nucleus, assessed by 4',6-diamidino-2-phenylindole (DAPI) nuclear DNA staining, indicated that the down-regulation of pericyte markers upon Mash1 expression did not correlate with cell death (**Figure 2.17**). In addition, both control- and Mash1-transduced cells could be cultured for periods of several weeks, suggesting no negative effect on survival after prolonged retroviral expression.

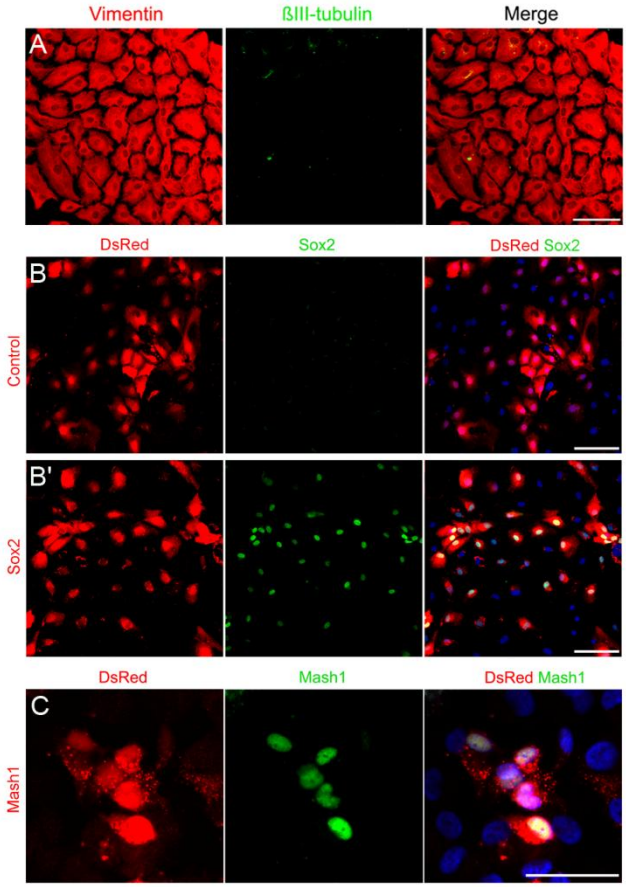

Figure 2.18: Cultures of adult human cerebral cortex are devoid of βIII-tubulin and Sox2 protein. A, Immuno-cytochemical analysis of cultures from adult human cerebral cortex exhibits no ßIII-tubulin-immunoreactive cells (green). Vimentin (red) staining reveals the protoplasmic morphology of these cells. Passage 2; 2DIV. Scale bar: 100µm. **B,** immuno-cytochemical analysis reveals no endogenous protein expression of Sox2 in proliferative cells, assessed by transduction with a control retrovirus; 2DPI. Following transduction with a Sox2-encoding retrovirus, Sox2 protein expression is readily detectable in the nuclei of the transduced cells; 21DPI. Same confocal settings were used in both conditions. Scale bars: 100µm. **C,** Mash1 expression is confirmed by immuno-cytochemical analysis. Cells transduced with Mash1-IRES-DsRed exhibit nuclear staining for Mash1 protein (green); 30DPI; Scale bar: 50 µm. DAPI (blue).

Of note, the observation that upon Mash1 expression cells did not change in morphology could be correlated with the growth of perivascular cells in a confluent manner since, at lower cell densities, a consistent change in the shape of some Mash1-positive cells took place. Within a period of 10-12 days round cells of 15-20 µm in diameter appeared within the Mash1-transduced cell population (**Figure 2.20**). Importantly, these cells up-regulated the expression of the neuronal marker ß-III-tubulin, indicating that, under these conditions, Mash1 could elicit a further response in direction to a neuronal phenotype than in confluent cultures. Following DAPI staining, the nucleus of Mash1-expressing cells appeared normal, indicating no Mash1-induced toxicity and subsequent cell death (**Figure 2.18**). The long periods of culturing (up to 8 weeks) in which these cells could be detected, further demonstrate that the Mash1-reprogramming effect does not promote apoptosis. However, none of the cells acquired a neuronal morphology, indicating that Mash1 alone was not sufficient to elicit a neuronal phenotype in perivascular cells isolated from adult human cortical tissue. Of note, Ngn2 was not able to generate changes in cell identity or morphology.

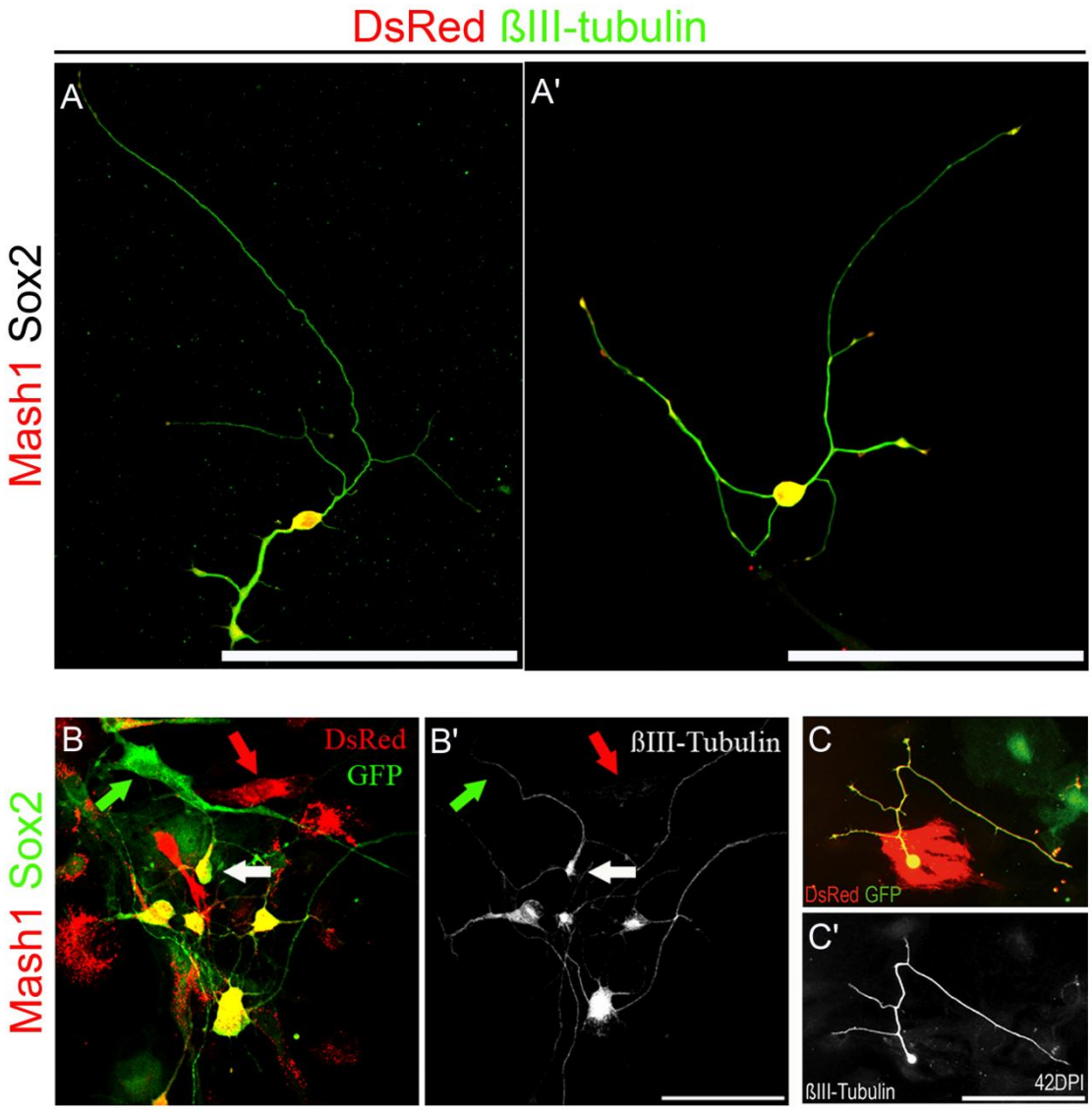

Figure 2.19: In vitro conversion of adult human brain pericyte-like cells into neurons. A-A', Induction of a neuronal phenotype following co-expression of Mash1-IRES-Dsred and Sox2 (no reporter) in cultures from the adult human cerebral cortex 21 days post infection and **B-B',** Mash1- IRES-Dsred and Sox2- IRES -GFP 12 days post infection; **C-C'**, Combined expression of Mash1 and Sox2 results in the generation of cell with neuronal morphologies 42 post infection. **A-A', B-B',** DsRed (red), ßIII-tubulin (green). **C-C'**, DsRed (red), GFP (green) ßIII-tubulin (white). Scale bars: 100µm.

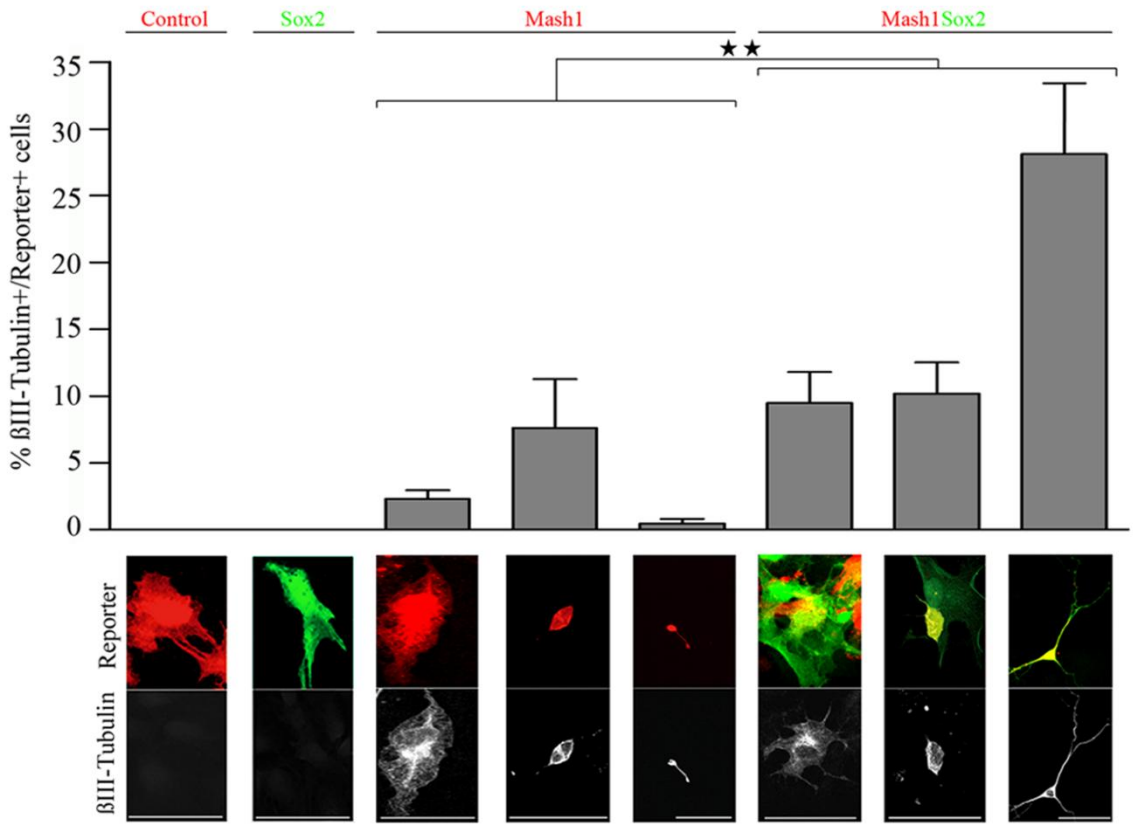

Figure 2.20: Quantification of the effect on ßIII-tubulin expression and morphology following DsRed only for control, Sox2, Mash1 and combined Sox2 and Mash1 expression. Cells were categorized for exhibiting a flat polygonal, round morphology without processes, or neuronal morphology. Insets below the histogram show examples of reporter-positive cells and their corresponding expression of ßIII-tubulin. Each value represents the mean of ßIII-tubulin- positive cells from 6 different patients. For each patient and treatment at least 3 experimental replicates were analysed. For each condition > 1000 cells were analysed. Error bars are SEM. Scale bars: 100µm.

Therefore, additional factors acting in a synergistic manner might be necessary to achieve full neuronal reprogramming. In the process of searching for factors playing essential roles in neurogenesis I came across Sox2, a transcription factor expressed from early stages during development [127], becoming restricted to neural tissue [117] and remaining expressed up to adulthood in the neurogenic niches of the mammalian brain [113]. In ES cells, Sox2 governs the pluripotency transcriptional network in synergism with Oct4, interacting physically and thereby regulating the expression of pluripotent stem cell-specific genes [34]. Accordingly, these genes have been shown to induce a pluripotent state in cells (e.g. skin fibroblasts) isolated at adult stages [8], including of human origin [225], indicating that Sox2 has the ability to induce transcriptional activation when the right partner transcription factors are available.

Also, previous work has suggested that the presence of endogenous Sox2 expression may facilitate neuronal conversion of mouse postnatal astroglia by neurogenic fate determinants [110] . Bearing in mind that no Sox2 expression could be detected at the

protein or mRNA level in perivascular cell cultures from adult human brain (**Figures 2.7 , 2.18**), I hypothesized that co-expression of Mash1 and Sox2 might enhance the efficiency of neuronal reprogramming. Retroviral expression of Sox2 alone did not elicit any changes in morphology or cell identity, assessed by normal expression of vimentin (**Figure 2.17**) and absence of ßIII-tubulin protein (**Figure 2.20**), or changes in proliferation (data not shown), consistent with the requirement of a partner transcription factor to allow transcriptional activity by Sox2 [132]. Initially, I used a retroviral vector encoding for Sox2 which lacked expression of a reporter gene. Combination of Mash1 and Sox2 (no reporter) resulted in the generation of cells with neuronal morphology positive for ßIII-tubulin expression (**Figure 2.19**); given the absence of a reporter, a construct containing a reporter gene (Dsred or GFP) was constructed which allowed for the detection of Sox2-expressing cells (**Figures 2.18, 2.19**). Notably, in cultures derived from 6 patients forced expression of Mash1 and Sox2 significantly increased the proportion of ßIII-tubulin positive cells from 10%±4 SEM in Mash1-only transduced cells (n=1238 cells analyzed) to 48%±9 SEM in Mash1/Sox2 co-transduced cells (n=1500 cells analyzed) (**Figure 2.20**).

Strikingly, upon Mash1/Sox2 co-expression cells with identifiable neuronal morphology were detected within the ßIII-tubulin–positive population. Confocal microscopy analysis revealed that these cells extended thin processes in the range of 100-200µm long emerging from a elliptic cell soma of approximately 15-20 µm in diameter, morphological features of neurons. In order to assess the reprogramming efficiency of the Mash1/Sox2 combination, I established 3 morphological categories among the reporter-positive cells expressing ßIII-tubulin, namely a, flat-polygonal; b, round; and c, neuronal. Since control or Sox2-only expressing cells did not display ßIII-tubulin expression, no quantification or categorizing was carried out on them. I found that within two weeks following transduction, most of the Mash1 only-positive cells expressing ßIII-tubulin adopted a round morphology.

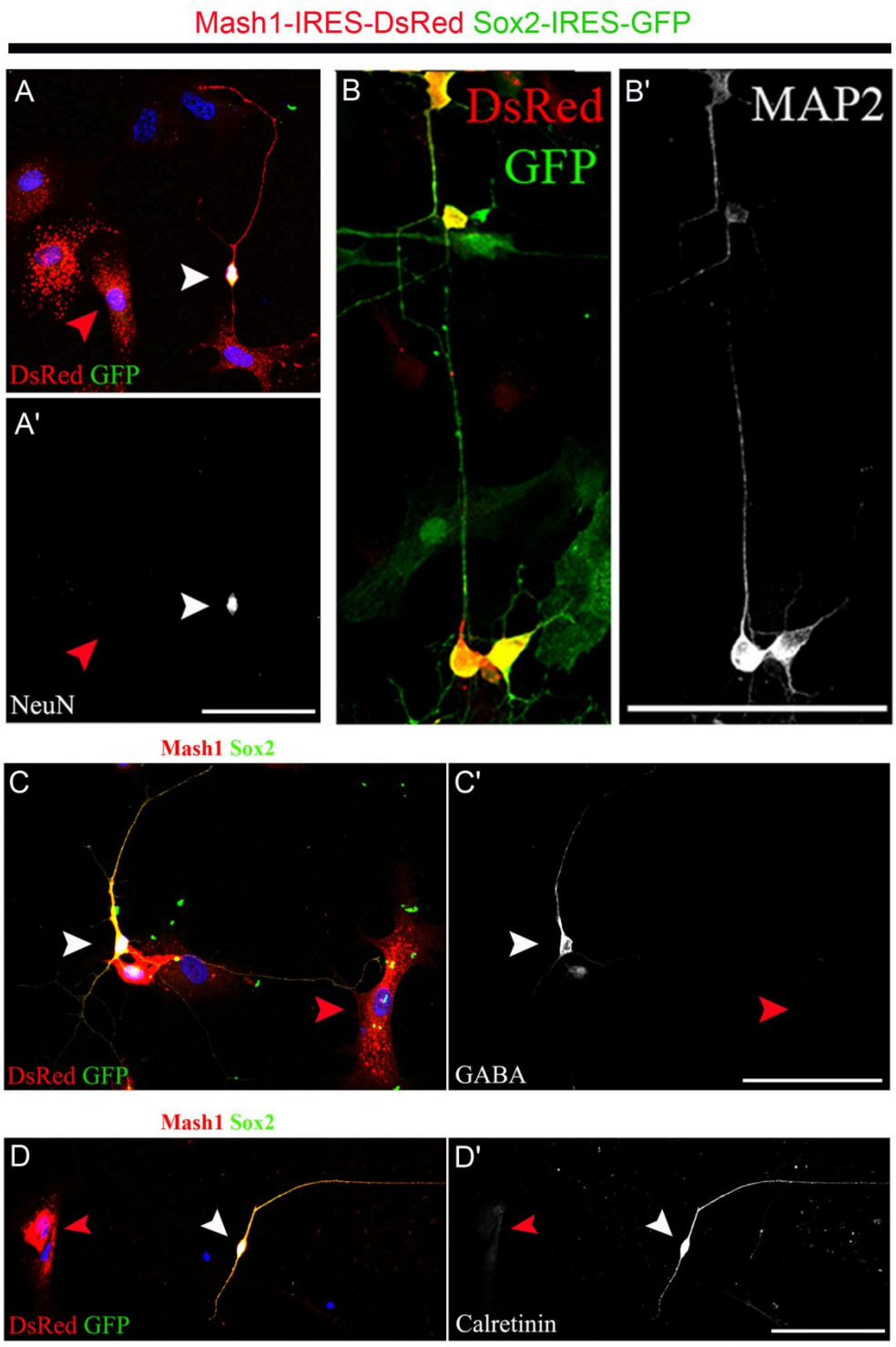

Figure 2.21: In vitro conversion of adult human brain pericyte-like cells into mature neurons. A-A', Cells transduced with Mash1 and Sox2 (white arrowhead) express the neuronal marker NeuN (white). Note the NeuN-negative Mash1-only expressing cell (red arrowhead); 42 days post infection (DPI). **B-B',** Cells transduced with Sox2 (green) and Mash1 (red) express the neuronal marker MAP2 (white). **C-C', D-D',** Adult human pericyte-derived neurons express the inhibitory neurotransmitter GABA and calretinin following expression of Sox2 and Mash1**. C,** GABA immunoreactivity following Sox2 (green) and Mash1 (red) co-expression. **C'**, GABA (white); 42 DPI. **D,** Calretinin immunoreactivity following Sox2 (green) and Mash1 (red) co-expression in co-culture with E14 mouse cortical neurons. **D'**, Calretinin (white); 35 DPI. DAPI (blue); Scale bars: 100µm.

Virtually none of the cells displayed neuronal processes, indicating a poor reprogramming efficiency by Mash1-alone. In contrast, in addition to an increase in the

total number of cells expressing ßIII-tubulin, a significant proportion among the double-transduced cells (28%±5 SEM) displayed a complex neuronal morphology (**Figures 2.19, 2.20**), demonstrating that the combined expression of Mash1 and Sox2 can elicit a neuronal phenotype in non-neuronal somatic cells isolated from the adult human neocortex. When cultured for periods longer than 4 weeks, markers of mature neurons such as the microtubule-associated protein MAP2 [226] and the neuronal nuclear antigen NeuN [227] could be detected in double-transduced cells (**Figure 2.21**). While MAP2 expression was found along cell soma and processes, NeuN was confined to the nucleus, consistent with the expected expression profile of these neuronal markers, adding further evidence for a truly neuronal conversion upon Mash1/Sox2 expression.

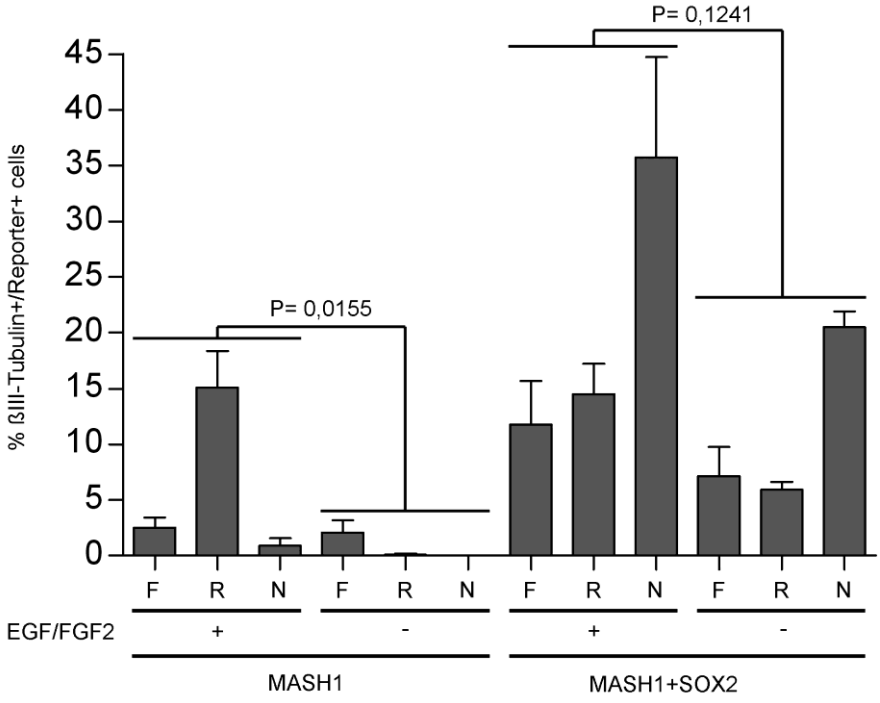

Figure 2.22: Efficient neuronal reprogramming of adult human pericyte-like cells by combined expression of Sox2 and Mash1 following expansion with or without EGF and FGF2 treatment. Histogram shows the number of ßIII-tubulin-positive among reporter-positive cells following expression of Mash1-only or Mash1 and Sox2 in combination, with (+) or without (-) the addition of EGF and FGF in the culture medium during expansion and prior to retroviral transduction. Cells were categorized for exhibiting a flat (F), round without processes (R) or neuronal (N) morphology. For each patient and treatment at least 3 experimental replicates were analysed. Statistical significance between culture conditions was tested by Student t-test and p-values are shown. Error bars are SEM.

Further immunocytochemical characterization of the induced neuronal cells suggested the acquisition of an inhibitory interneuron phenotype based on the expression of the inhibitory neurotransmitter γ-aminobutyric GABA [228] and the calcium-binding protein

calretinin [229]. All analyzed double-transduced cells with neuronal morphology showed expression of GABA (14/14 cells), with a subpopulation of these cells (11/18 cells) being immunoreactive for calretinin. Lack of expression of the glutamatergic lineage marker Tbr1 by Mash1/Sox2-induced neurons adds further evidence for the acquisition of an interneuron phenotype (data not shown).

2.3.2. **EGF/FGF influence on Mash1/Sox2 induced neuronal reprogramming**

To determine whether soluble factors may influence the reprogramming efficiency upon forced expression of Mash1 and Sox2, I cultured adult human brain perivascular cells in the presence or absence of the mitogens epidermal growth factor (EGF) and fibroblast growth factor 2 (FGF2), which are required for the expansion of neural stem cells as neurospheres and have to be removed from the culture medium to allow neuronal differentiation [13]. I did not find obvious differences in morphology between cells cultured with or without these mitogens. The cells were exposed to the mitogens during the expansion phase, with EGF and FGF2 being removed just after retroviral transduction. To assess the reprogramming efficiency following treatment with these mitogens, I analyzed the ßIII-tubulin-positive cells among the reporter-positive cells based on their morphology (a, flat; b, round; c, neuronal) and compared Mash1-only versus Mash1/Sox2-combined expression in the presence or absence of EGF and FGF2 (**Figure 2.22**) While the proportion of Mash1-only transduced cells that up-regulated ßIII-tubulin was higher when expanded with EGF/FGF2, virtually none of them adopted a neuronal morphology, indicating that these mitogens do not have a direct influence in neuronal differentiation upon expression of Mash1 alone.

Similarly, the analysis of Mash1/Sox2 expressing cells revealed that only the total number of ßIII-tubulin-positive cells was increased upon treatment with EGF/FGF2 but not the number of cells that acquired morphological hallmarks of neurons. In both conditions, the proportion of neuronal cells was equivalent, representing approximately half of the total ßIII-tubulin positive cells, with the differences between both analyzed conditions being statistically not significant. The mitogens EGF and FGF2 may influence the susceptibility of cells to be targeted with retroviral vectors, which could indicate differences in their proliferative behaviour (i.e. cell cycle length) as these can only integrate into the genome of host cells during mitosis, resulting in an increase in the total number of cells that could be successfully transduced.

2.4. **Membrane properties of human pericyte-derived neurons**

The synergistic action of Mash1 and Sox2 induces, in adult human brain perivascular cell cultures, the generation of cells expressing neuron-specific proteins. However, in order to claim that this conversion is indeed driving the fate of these cells to a truly neuronal identity, a functional electrophysiological analysis of their membrane properties is required.

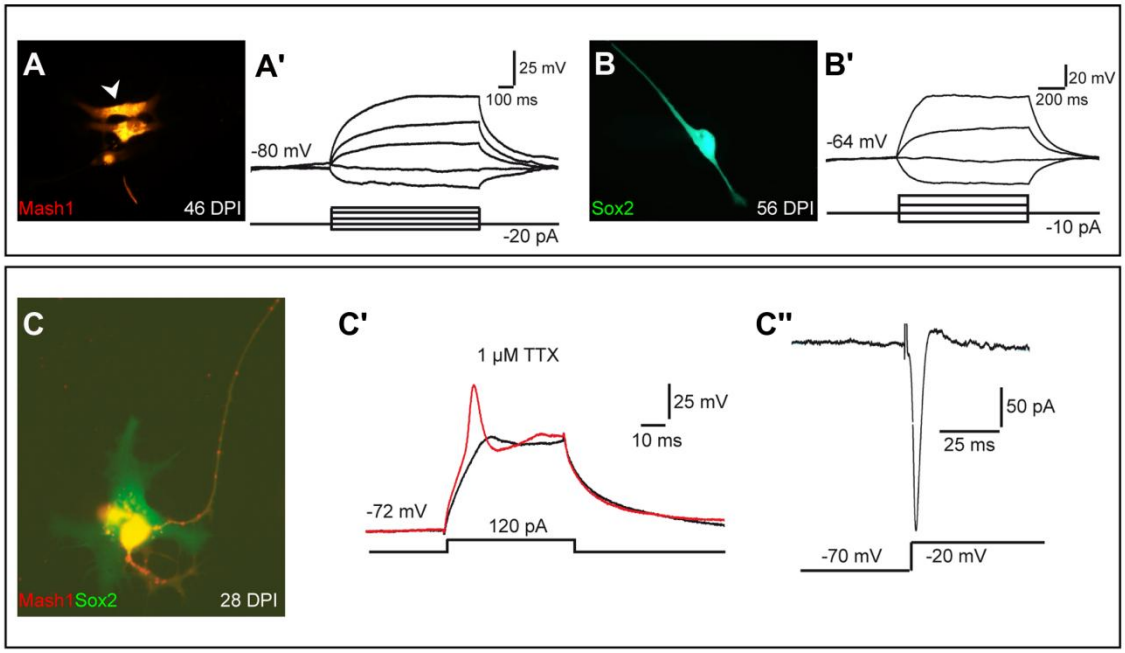

Figure 2.23: Membrane properties of neurons derived from pericyte-like cells of the adult human cerebral cortex. A, Example of a Mash1-only expressing cell. **A',** current-voltage relation of the same cell (arrowhead), following step-depolarisation. Note the passive response of the cell. **B,** example of a Sox2-only expressing cell. **B',** passive current-voltage relation of the same cell. **C,** example of a cell co-expressing Sox2 and Mash1 (yellow). **C',** following a step-current injection, the cell fires a single action potential (red trace) that is blocked by TTX (black trace). **C'',** TTX-sensitive sodium currents recorded in voltage-clamp.

Therefore, the ability of these cells to fire action potentials, a defining characteristic of neurons and muscle cells was analyzed. To this purpose, I took advantage of the whole-cell patch-clamp recording technique that allows the study of excitable cells, such as neurons and muscle cells, I started testing the electrical membrane properties of Mash1 (n=7 cells) and Sox2 (n=6) singly transduced cells. In all cases and consistent with the

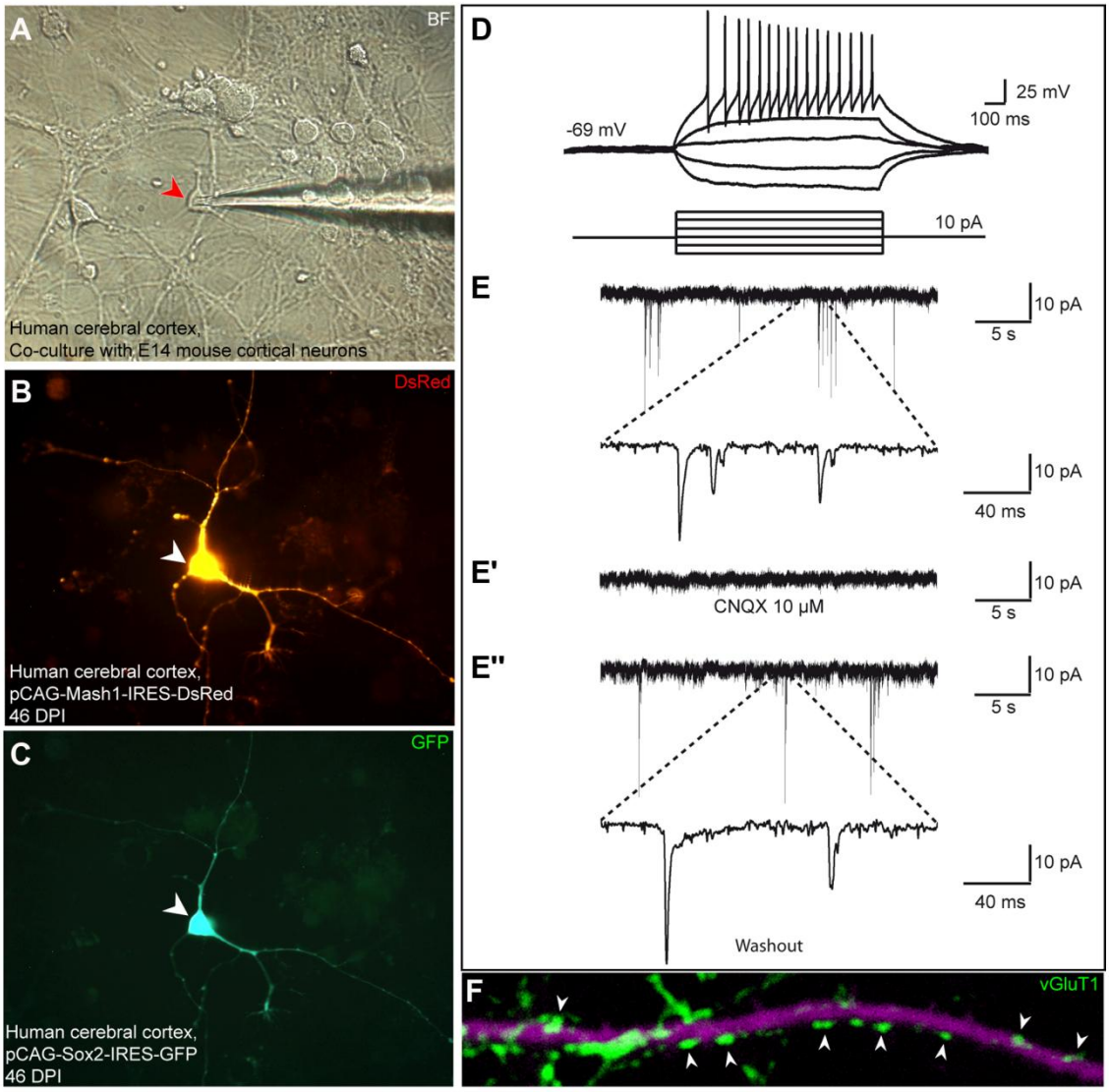

Figure 2.24: Membrane properties of neurons derived from pericyte-like cells of the adult human cerebral cortex co-cultured with mouse embryonic cortical neurons. A, bright field micrograph depicts a human PdN (red arrowhead) after 26 days of co-culture with E14 mouse cerebral cortical neurons, 46 days following retroviral transduction. **B,** DsRed fluorescence indicating transduction with Mash1 and DsRed-encoding retrovirus. **C,** GFP fluorescence indicating transduction with Sox2 and GFP-encoding retrovirus. **D,** Step current injection in current-clamp results in repetitive action potential firing. **E,** the graph depicts spontaneous synaptic events recorded from the same PdN as shown in D. The enlarged trace shows individual synaptic events. **E',** The synaptic events are blocked by the application of CNQX (10 µM). **E'',** Recovery of spontaneous synaptic input following washout of the CNQX. **F,** High magnification view of a single dendrite from a pericyte-derived neuron (magenta) illustrates the high density and the distribution of vGluT1-immunoreactive puncta (green).

lack of morphological features of neurons of these cells, step-current injection did not elicit any action potential firing even at longer periods of culturing (**Figure 2.23**), indicating that neither factor alone induces neuronal electrical properties. In sharp contrast, around 70% of the double-transduced cells (12/17 cells from 5 different patients) analyzed in current-clamp mode responded with the generation of a single action potential upon depolarizing current injection, which could be blocked by the

sodium channel antagonist tetrodotoxin (TTX) (**Figure 2.23**). In addition, in voltage-clamp these cells exhibited mode a clearly recognizable sodium current (**Figure 2.23**). These observations undoubtedly reveal a functional neuronal phenotype induced by the combined action of Mash1 and Sox2. However, the high input resistances as well as low action potential and peak sodium current amplitudes reflect the presence of low number of ion channels at the neuron´s membrane and therefore immature neuronal properties, even at prolonged time in culture (**Figure 3.2**). Considering the requirement of environmental cues in addition to the intrinsic mechanisms to promote maturation of neurons, it was hypothesized that cell-cell contact mechanisms and the action of soluble factors secreted from neighboring neurons might stimulate differentiation/maturation, creating more suitable physiological conditions. To test this possibility, human Mash1/Sox2-induced neurons were co-cultured together with neurons from mouse embryonic (E14) cerebral cortex. Under this conditions, an obvious increase in morphological complexity could be observed among the human neurons (**Figure 2.24**) but more importantly, they acquired the ability to fire chains of action potentials, adding further evidence for a neuronal identity as only functional neurons are capable of generating such a response upon current injection (**Figure 2.24**). Importantly, these induced human neurons were found to receive functional glutamatergic inputs from the co-cultured mouse embryonic neurons, as spontaneous synaptic activity could be detected (**Figure 2.24**). The glutamatergic identity of these synapses could be revealed by treatment with the α-amino-3-hydroxy-5-methyl-4-isoxazole-propionic acid (AMPA)/ kainate receptor antagonist 6-cyano-7-nitroquinoxaline-2,3-dione (CNQX), which blocks glutamate-mediated synaptic transmission [230] (**Figure 2.24**). These findings demonstrate that Mash1/Sox2-induced human neurons are indeed functional as they express transmitter receptors, are capable of assembling a postsynaptic compartment and can be recognized by other neurons as functional targets. In order to confirm the physical interaction between human and mouse embryonic neurons, immunocytochemical analysis for the expression of the vesicular glutamate transporter 1 (VGlut1), typically found at the presynaptic terminals of glutamatergic neurons [231], was performed. Consistent with a functional glutamatergic input, the surface of dendrites of the Mash1/Sox2-induced human neurons were found to be decorated with Vglut1-positive puncta, indicative of physical cell-cell contacts from surrounding glutamatergic neurons (**Figure 2.24**). In sum, these data demonstrates that neurons generated upon transduction of adult human brain perivascular cells with Mash1 and Sox2 and co-

cultured with embryonic neurons acquire properties of functional neurons such as repetitive action potential firing and the ability to integrate into neuronal networks.

2.5. **Direct evidence of neuronal conversion**

Despite the high frequency of PDGFRß-positive cells infected by the retroviral vectors, other cells types could also be targeted and converted to neurons upon expression of Mash1 and Sox2, creating confusion in regard to the cell type subjected to neuronal reprogramming. In one experiment, FACS analysis revealed that a proportion of 97% of cells expressing the PDGFRß were found in the culture dish, indicating that virtually all expanded cells had a perivascular origin (**Figure 2.9**). In this particular culture, the combined expression of Mash1 and Sox2 resulted in the generation of 47% cells expressing ßIII-tubulin, displaying 26% of them a convincing neuronal morphology (n=203 cells). This experiment strongly suggested that the PDGFRß-positive population was the origin of the neurons; however, in order to unequivocally confirm the perivascular origin of the reprogrammed cells neuronal conversion was monitored by live-imaging (**Figure 2.25**). First, cultured cells were sorted based on their surface expression of PDGFRß (**Figure 2.25**) and left to recover for a period of 48hours. After this time, cells were transduced with retroviral vectors encoding for Mash1 and Sox2, which allowed for visualization of the infected cells by fluorescence (Dsred and GFP, respectively), and subsequently imaged by time-lapse video microscopy (**Figure 2.25**).
After 3 days, expression of the reporter genes became apparent and the fate conversion of the transduced cells could be then monitored. Phase contrast image acquisition was carried out every 5 minutes; however, due to fluorescence toxicity, a frequency of 7,5 hours between every acquired fluorescence image was necessary to avoid cell death. Interestingly, PDGFRß-positive cells display high mobility in culture, a situation that reduced the rate of successful imaging as many of the cells disappeared from the field of view. One important piece of information in regard to any reprogramming process is the timing of acquisition of cell lineage-specific hallmarks.

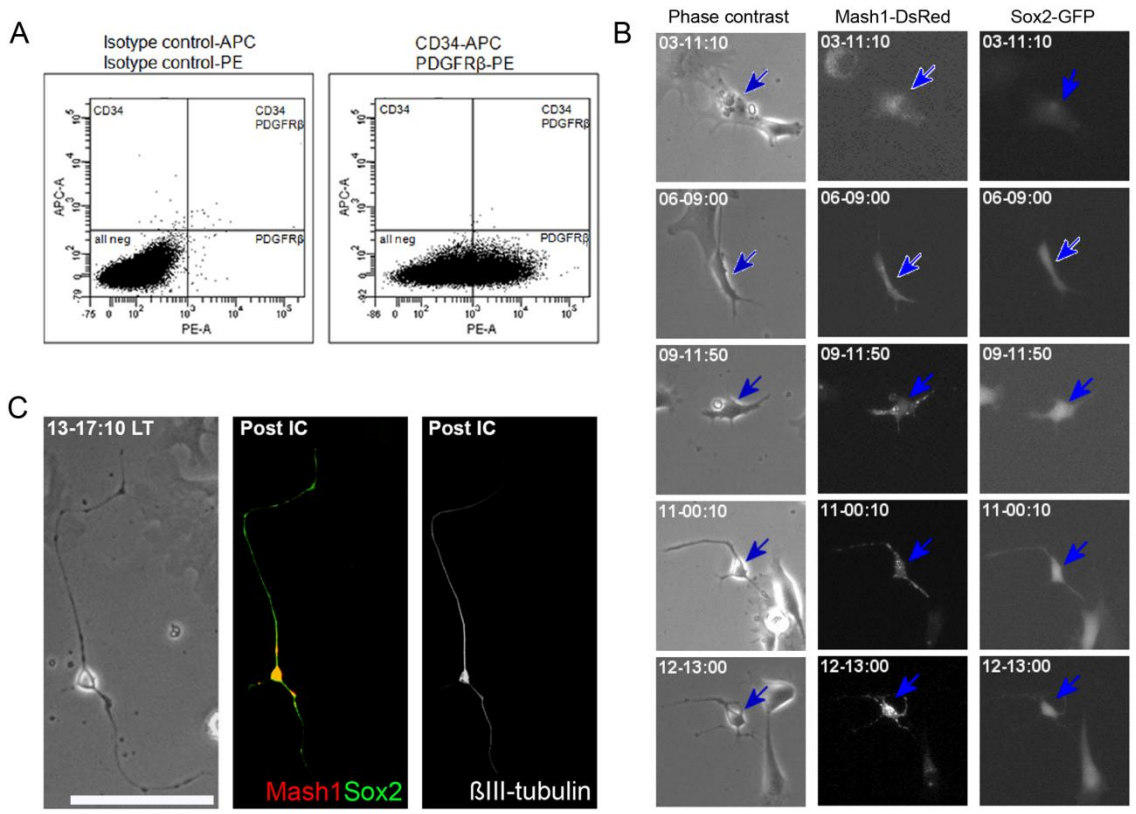

Figure 2.25: Direct evidence of neuronal reprogramming by live-imaging of FACS-sorted PDGFRβ-positive cells from cultures of the adult human cerebral cortex. A, Left panel: FACS plot depicting the isotype controls for the analysis of PDGFRβ- and CD34-expression in a culture derived from adult human cerebral cortex. Right panel: FACS plot depicting PDGFRβ- and CD34-positive as well as negative fractions. CD34-negative/PDGFRβ-positive cells were sorted. **B,** Live imaging of the conversion of a PDGFRβ FACS-sorted cell (blue arrow) into a neuron following co-expression of Sox2 and Mash1. Pictures show phase contrast and fluorescence (Mash1-IRES-DsRed and Sox2-IRES-GFP) images at different time points (Days-Hours:Minutes) during the reprogramming process. Note the change of the co-transduced cell from a protoplasmic to neuron-like morphology. **C**, Depicted is the last recorded time point in phase contrast (LT) and the post-immunocytochemistry (Post IC) of the reprogrammed cell for GFP (green), DsRed (red) and ßIII tubulin (white).

For a period of 10 days, all double-transduced cells exhibited high mobility and as well as erratic changes in morphology, in all cases remaining protoplasmic. Importantly, at day eleven some analyzed reporter-positive cells adopted a stable polarized morphology. Within the next two days, the fate conversion reached a state in which the morphological features of a neuron were obvious, namely a small elliptic cell soma and long thin processes emerging from it (**Figure 2.25**). In addition, these cells adopted a stable behavior, displaying a reduced mobility and, in the example, extending two opposite processes. To confirm the neuronal identity of the reprogrammed cells, immunocytochemical detection of ßIII-tubulin after imaging was performed (**Figure 2.25**).

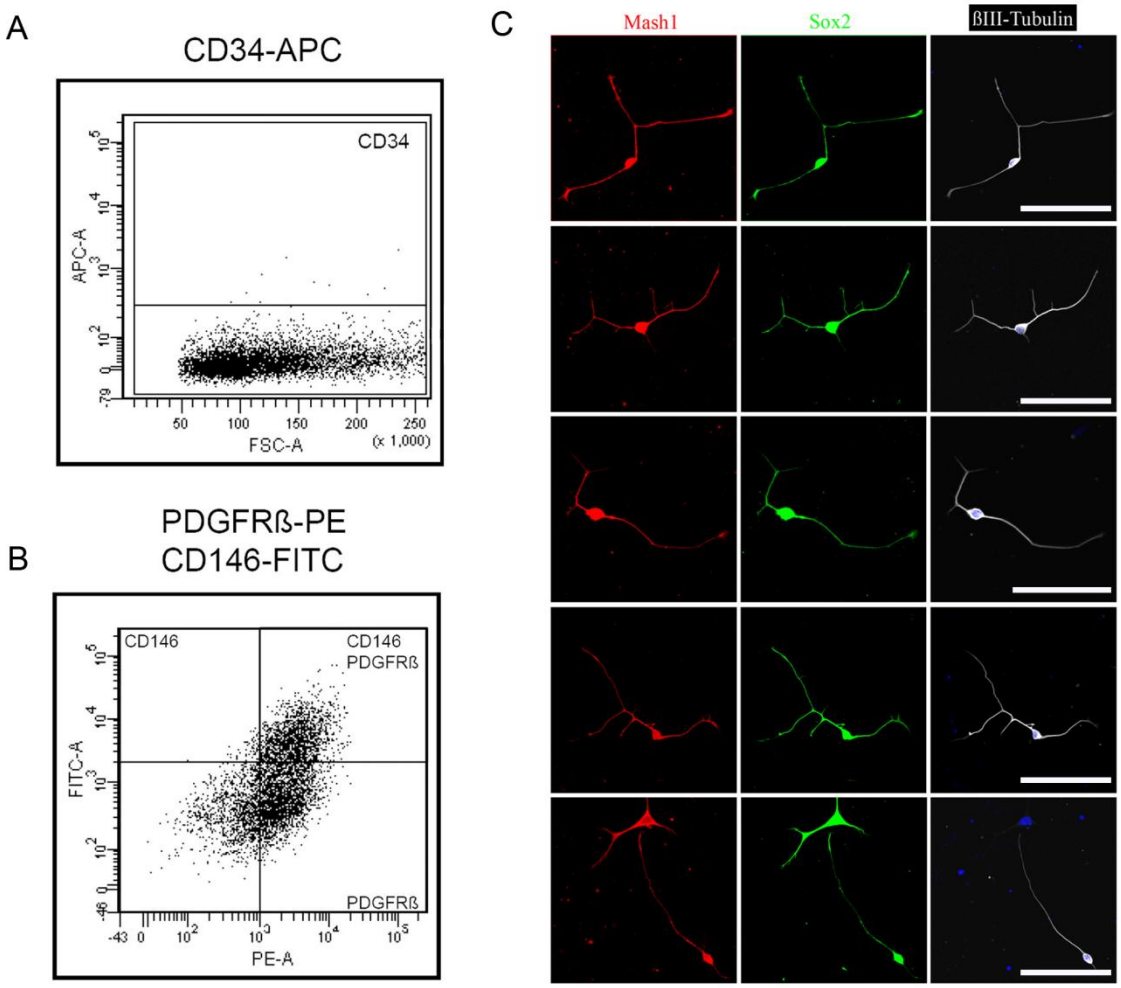

Figure 2.26: FAC-sorted cells positive for both PDGFRß and CD146 give rise to neuronal cells upon forced expression of Mash1 and Sox2. A, FACS plot depicting CD34-expression in a culture derived from adult human cerebral cortex. **B**, The CD34-negative population was resorted based on the double expression of PDGFRß and CD146. **C,** Sorted cells were subjected to Mash1/Sox2 induced neuronal reprogramming. 5 Examples of neuronal cells from PDGFRß/CD146 double positive pericyte-derived cells; Mash1-IRES-Dsred (red), Sox2-IRES-GFP (green), ßIII-tubulin (white). DAPI (blue); Scale bars:100µm.

While none of the Sox2-positive cells (n≥300 cells) expressed the neuronal marker, 7% of Mash1-only (n=88 cells) and 20% (n=366 cels) were immunoreactive, indicating similar reprogramming efficiencies as in unsorted cultures. No morphological characterization was carried out due to the relatively short differentiation period (fourteen days). Considering that at day fourteen some cells were still undergoing the acquisition a neuronal fate, this experiment suggests that the reprogramming process did not occur in a synchronous manner throughout the culture. Following the onset of reporter expression, none of the analyzed cells underwent cell division, providing strong

evidence for direct conversion from adult human non-neuronal somatic cells into pericyte-derived neurons. The use of time-lapse video microscopy demonstrates that FAC-sorted proliferative protoplasmic PDGFRß-positive cells isolated from the adult human brain undergo a dramatic change in morphology within a period of 14 days, adopting a neuronal phenotype upon the combined expression of Mash1 and Sox2. To exclude that some cell populations expressing PDGFRß could belong to cell lineages other than of perivascular origin, FACSorting was performed based on the combined surface expression of PDGFRß and CD146 (**Figure 2.26**). In contrast to the previous approach, cells were expanded for a period of 14 days after sorting, followed by retroviral transduction and subsequent live monitoring. Importantly, many cells with neuronal morphology and expression of ßIII-tubulin could also be found in a similar period of time (**Figure 2.26**), adding further evidence for a pericyte origin of the neurons present in the culture dish, excluding preexisting neuronal cells.

2.6. *In vitro* conversion of adult mouse brain pericytes

With the purpose of corroborating the results obtained with adult human cells I examined the potential of perivascular cells isolated from the cerebral cortex of adult wild type mice to give rise to neurons upon Mash1/Sox2 co-expression, focusing on the origin of the reprogrammed cells. I proceeded to culture cells from gray matter of the adult murine cerebral cortex. Special care was taken to remove all traces of meninges, since potential fibroblast growth could interfere with culturing of perivascular cells. I processed the tissue by mechanical dissociation in a similar manner as I did for the human samples. Cellular clones arising from protoplasmic cells were detected earliest five days after plating. Typically, these clones are characterized by the presence of a sphere-like structure, composed by a variable number of cells, from which protoplasmic cells arise, consistent with the observations in adult human brain perivascular cultures (**Figure 2.5**). Indeed, immunocytochemical analysis revealed that the cells forming these clones may have a perivascular origin, since they expressed NG2 (**Figure 2.28**), a marker of pericytes *in vivo* (**Figure 2.27**). Although oligodendrocyte progenitor cells (OPC) also express NG2, this possible identity is unlikely due to the fact that OPC are stellated *in vitro*, bearing thin processes arising from a small cell soma, and not protoplasmic, as perivascular cells appear.

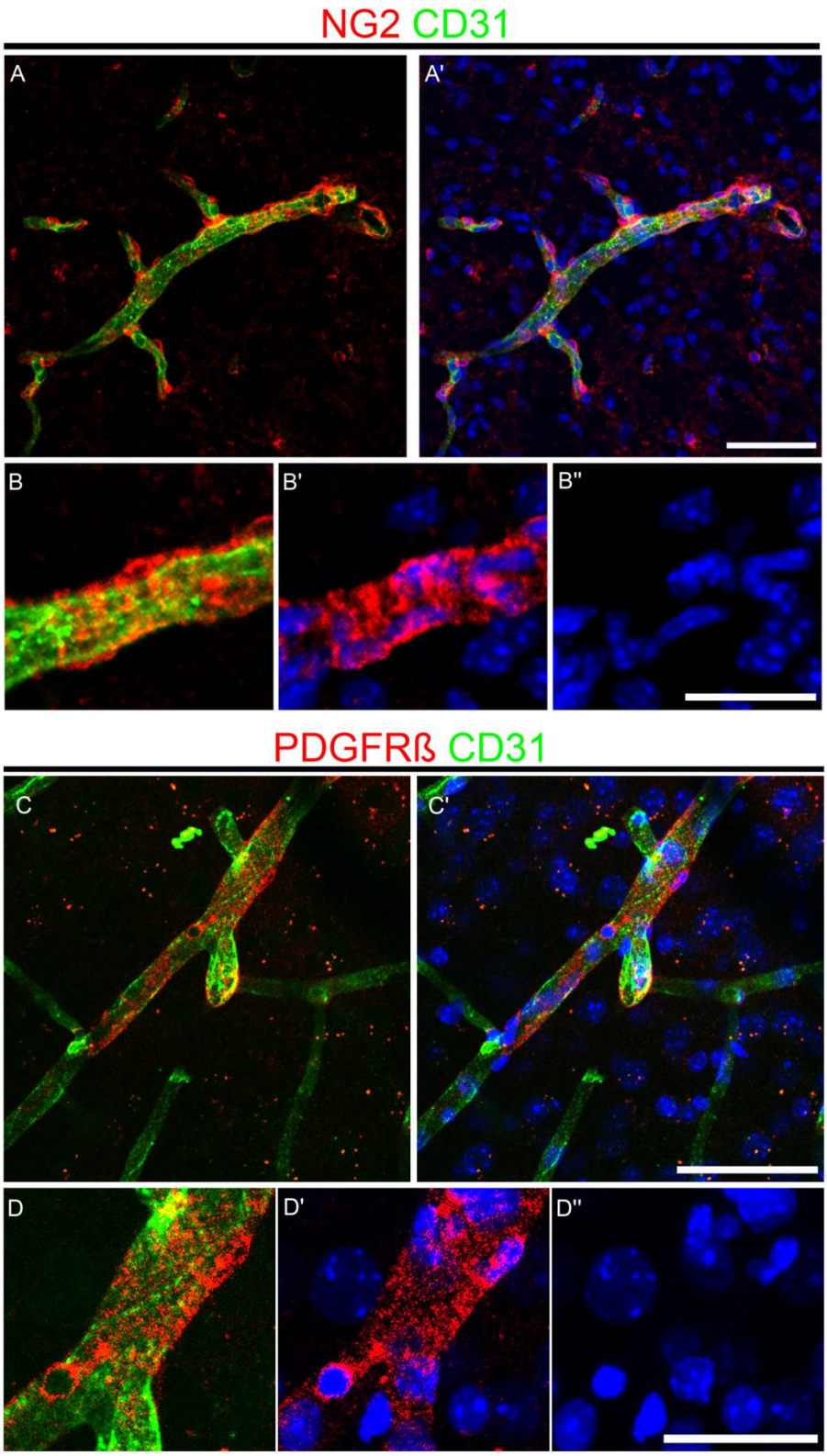

Figure 2.27: Pericyte localization in the adult cerebral mouse cortex. A-A', NG2 (red) expression in microvessel-associated cells in the adult mouse cerebral cortex. **B-B'',** Higher magnification. **C-C',** PDGFRß (red) expression in microvessel-associated cells in the adult mouse cerebral cortex. **D-D'',** Higher magnification. Microvessels were visualized by CD31 (green) immunoreactivity; DAPI (blue). Scale bars: 50µm.

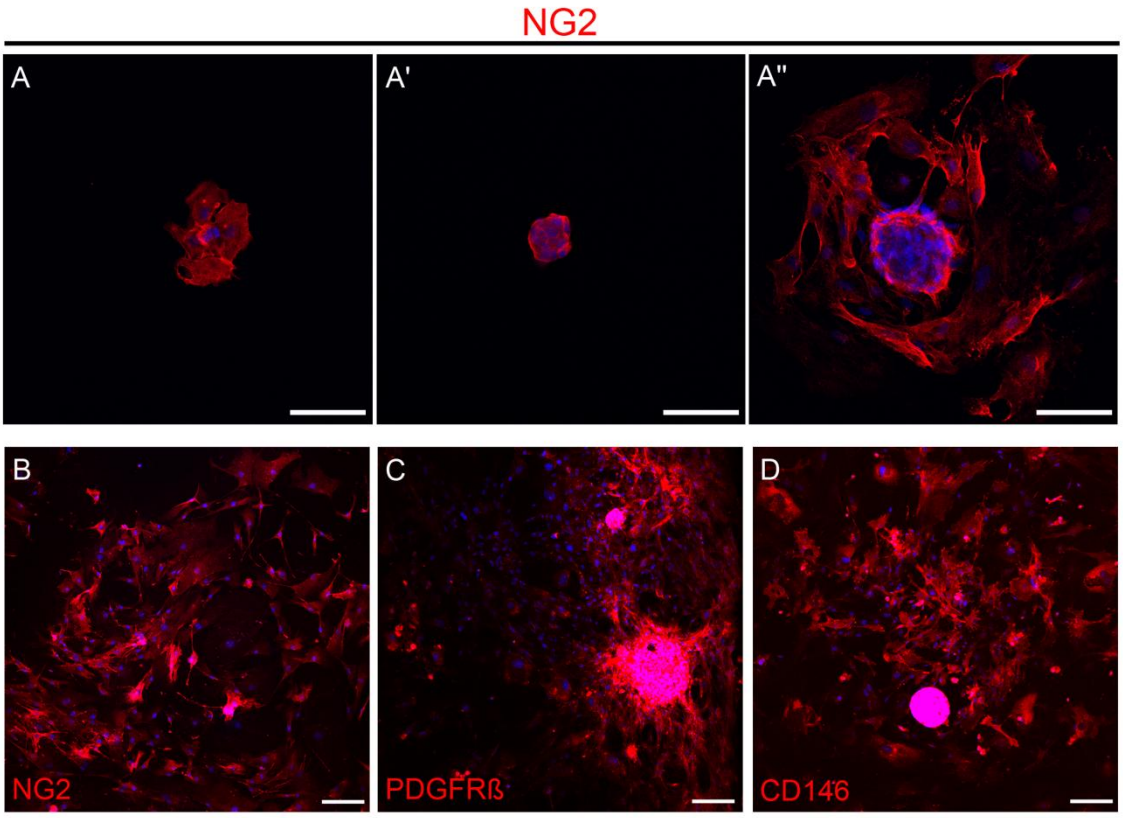

Figure 2.28: Characterization of cultures from adult mouse gray matter containing pericyte-derived cells. A-A'', NG2 immunoreactive cells plated at low density form clones (5, 7, 12 days after plating, respectively). **B, C, D,** Protoplasmic cells display expression of pericyte markers 20 days after plating. **B**, NG2 (red). **C**, PDGFRß(red). **D,** CD146 (red). DAPI (blue); Scale bars:100µm.

In a period of 2-3 weeks, a few clones generated large number of protoplasmic cells, displaying expression of pericyte markers such as NG2 and CD146 (**Figure 2.28**); likewise PDGFRß (**Figure 2.28**), also expressed by pericytes within the brain (**Figure 2.27**), was found to be expressed in cells arising from sphere-like structures (**Figure 2.28**).

These cultures were also analyzed by RT-PCR for the expression of several pericyte markers (Acta2/αSMA; Axl, receptor tyrosine kinase; Rgs5, regulator of G protein signaling 5 and PDGFRß) confirming the presence of perivascular cells within the culture dish (**Figure 2.29**). These protoplasmic cells were trypsinized and transduced with retroviral constructs (**Figure 2.30**), demonstrating their proliferative nature; however, mouse cells could not be passaged more than two times, in contrast to the ability of human cells to be passaged up to ten times.

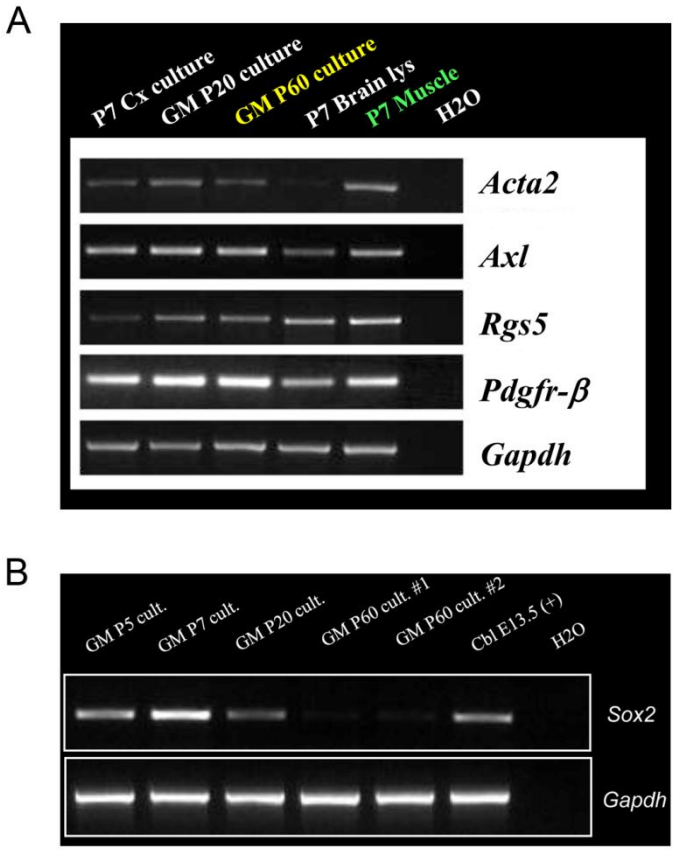

Figure 2.29: Characterization of cultures from adult mouse cerebral cortex by RT-PCR. A, mRNA expression of mRNA for several pericyte markers in cultures from gray matter (GM) of the cerebral cortex of postnatal P5, late postnatal P20, and adult P60 mice was analyzed. For comparison, mRNA from brain and muscle isolated at postnatal stages P7 was used. **B**, Sox2 mRNA levels were analyzed in cultures from gray matter obtained at different developmental stages (P5, P7, P20 and P60). As positive control, cerebellar tissue from embryonic day E13,5 was used.

I repeated the reprogramming approach applied to the human cells, namely to infect with retroviral contructs encoding for control (reporter gene DsRed/GFP), Sox2, Mash1 or Mash1/Sox2 in combination, to analyze for the expression of ßIII-tubulin and to distribute the reprogrammed cells into three morphological categories (a, flat; b, round; c, neuronal) (**Figure 2.30**). While control or Sox2-alone expressing cells did not up-regulate ßIII-tubulin (**Figure 2.30**), 41% ± 10 SEM of Mash1-only cells displayed immunoreactivity for the neuronal marker, with a small proportion of them acquiring a neuronal morphology. Strikingly, combination of Mash1 and Sox2 gave rise to a significant increase in the proportion of ßIII-tubulin expression among double reporter-positive cells to 92% ± 3 SEM. More importantly, the majority of them (72% ± 7 SEM) were identified as neurons by morphology (**Figure 2.30**).

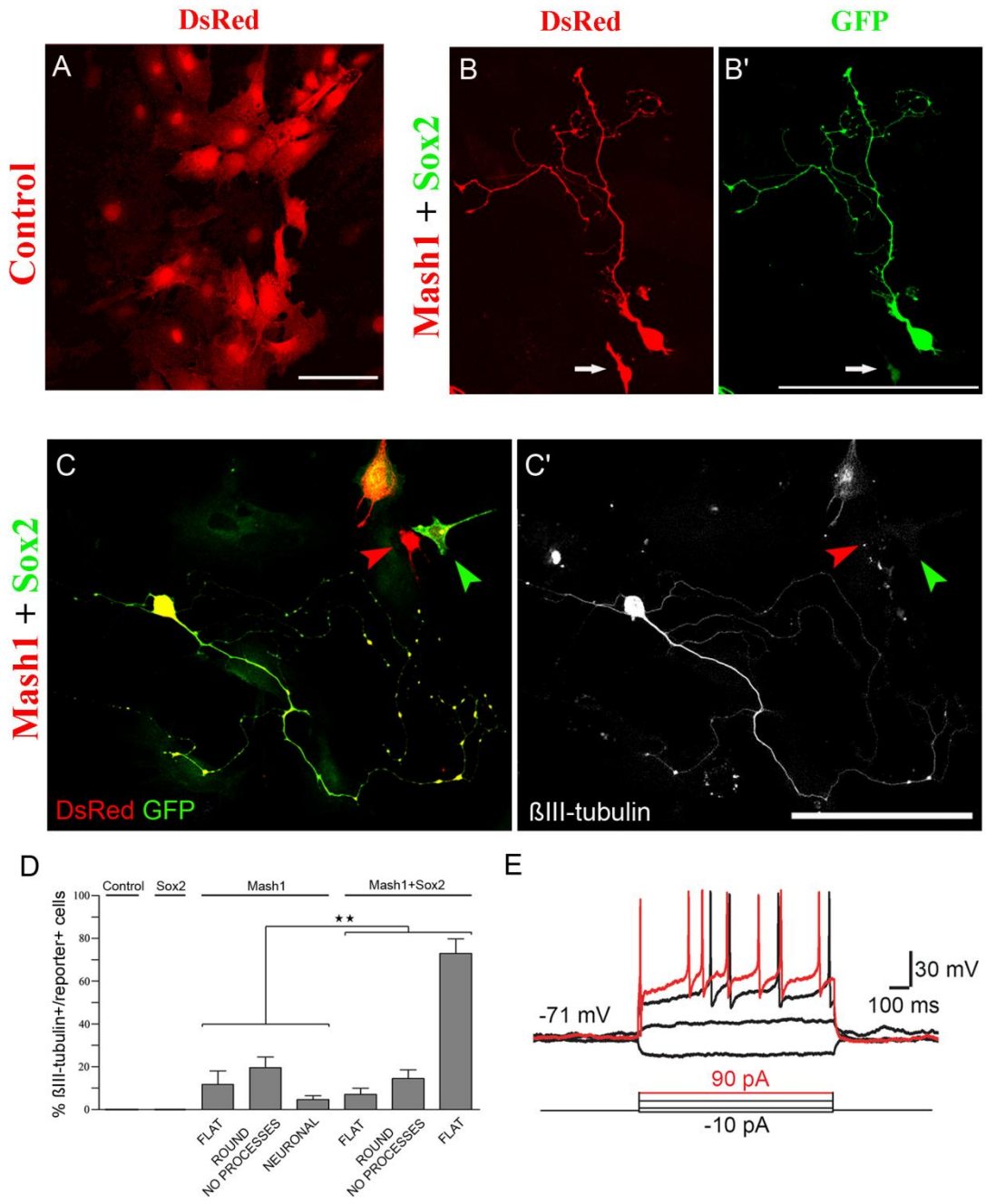

Figure 2.30: **Induction of a neuronal phenotype following co-expression of Sox2 and Mash1 in cell cultures from the adult mouse cerebral cortex. A,** Cells transduced with a control retroviral construct expressing DsRed do not undergo morphological changes, remaining flat and polygonal. **B-B',** In sharp contrast, a Mash1 (CAG-Mash1-IRES-DsRed) single-transduced cell (arrow) display a round morphology with a short process. Mash1 and Sox2 (CAG-Sox2-IRES-GFP) double-transduction results in the generation of a neuronal morphology, characterized by a round cell body and long branched processes; 14DPI; Scale bar: 100µm. **C-C',** Note that cells expressing Mash1 (red arrowheads) or Sox2 (green arrowheads) only are devoid of βIII-tubulin (white). Mash1(Dsred), Sox2(GFP); Scale bar: 100 µm. **D,** Quantification of the effect on βIII-tubulin expression and morphology following DsRed, Sox2, Mash1 or combined Sox2 and Mash1 expression in cultures from adult mouse cerebral cortex. Cells were categorized for exhibiting a flat polygonal, round without processes, or neuronal morphology. Histogram depicts the percentage of βIII-tubulin-positive among the reporter-positive cells (n=4). Error bars are SEM. Control and Sox2-positive cells were analysed by counting >100 cells per experimental replicate, of which none were ßIII-tubulin immunoreactive. **E,** Example of action potential firing of a Sox2 and Mash1 co-transduced cell in response to current injection in current-clamp.

The formation of neurons by forced expression of Mash1 and Sox2 is more efficient in mouse cells compared to the results obtained from human cells, in regard to the proportion of responding cells as well as to their ability to acquire morphological hallmarks of neurons.

In order to demonstrate that these cells were indeed neurons, electrophysiological recordings were performed. In current-clamp mode, step-current injection in Mash1/Sox2 induced-neuronal cells elicited action potential firing, evidencing their truly neuronal identity (**Figure 2.30**). The analyzed reprogrammed mouse neuronal cells displayed more mature electrophysiological properties as human cells did in a similar period of time, adding support for an ease in reprogramming of mouse cells (**Figure 2.30**). Although neurons could be generated from adult mouse cortical cultures, the identity of the cells prior reprogramming had to be addressed. The use of mice allows for genetic fate mapping and since NG2 appeared to be expressed by these cells, I searched for a mouse line in which cells expressing NG2 could be labeled, allowing for detection and identification prior reprogramming. The knock-in strategy used to generate transgenic NG2-EYFP mice [232] allows for fluorescence labeling of NG2-positive cells *in vivo* and also in culture (**Figure 2.31**). In fact, a large number of EYFP positive cells could be found in cultures from gray matter isolated from heterozygous NG2-EYFP mice.

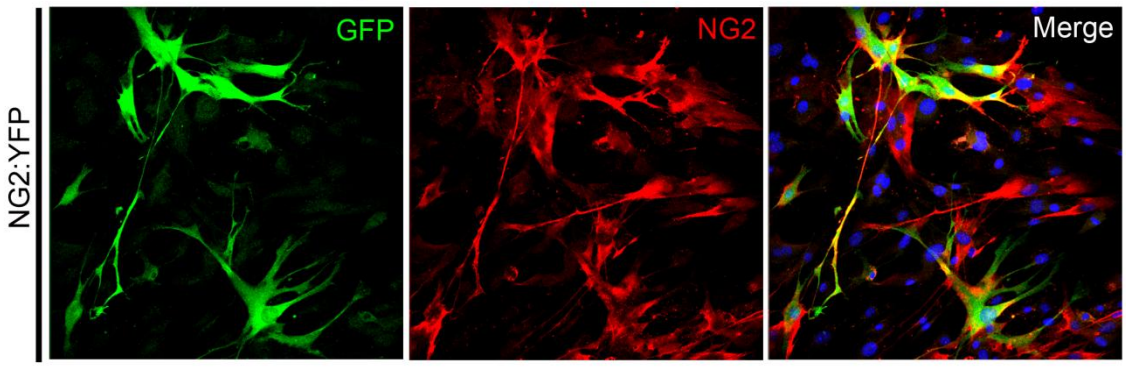

Figure 2.31: Reporter positive cells isolated from the cerebral cortex of NG2:YFP mice can be cultured. YFP-positive cells (GFP green) are immunoreactive for NG2 (red); DAPI (blue); 12 days in vitro.

However, due to the control of reporter expression by the NG2 promoter, labeling of NG2-positive cells was transient and progressive loss of fluorescence intensity throughout the culturing period took place, indicating that the expression of NG2

fluctuates *in vitro.* Although the use of this mouse line confirmed that a large proportion of the cells could indeed be of perivascular origin, no stable fate mapping could be achieved to demonstrate that the generated neurons were originally NG2-positive cells. In addition, as other cell types express this marker, no definitive proof for a pericyte identity could be provided using this transgenic knock-in mouse line. To unequivocally determine the origin of the reprogrammed cells from pericytes I took advantage of a transgenic mouse line which expresses an inducible Cre recombinase (CreERT2) under the control of the tissue non-specific alkaline phosphatase (TN-AP) promoter [233].

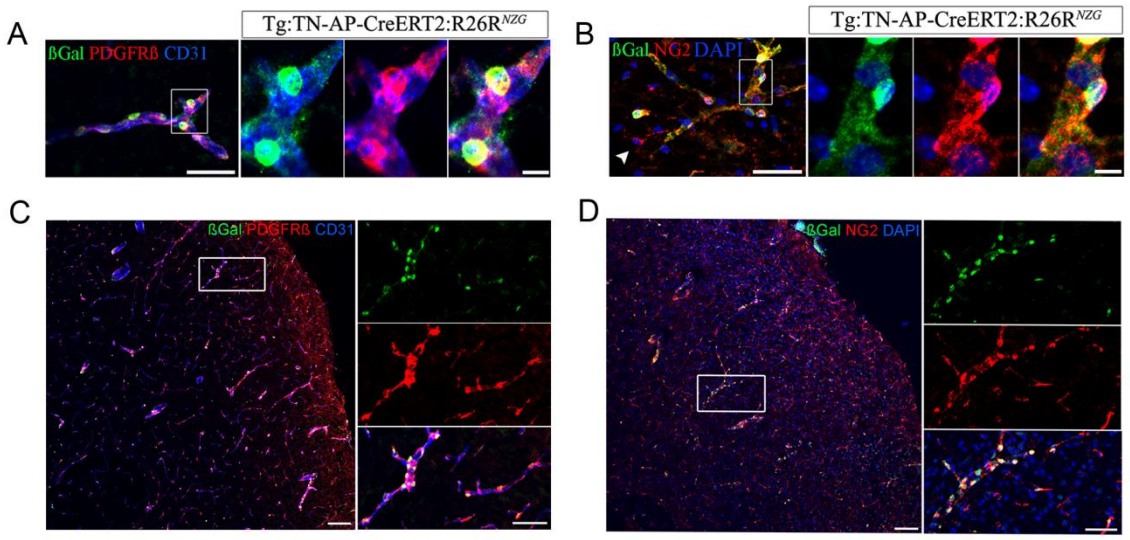

Figure 2.32: Specific expression of β-galactosidase in microvessel-associated pericytes in the cortex of Tg:TN-AP-CreERT2:R26R^{NZG} mice. Specific β-galactosidase expression associated with CD31-positive blood vessels in the cerebral cortex of Tg:TN-AP-CreERT2:R26R^{NZG} mice. **A,** ß-Galactosidase-positive cells express the pericyte marker PDGFRß. Note the restricted expression around microvessels. β-galactosidase (green), PDGFRß (red), CD31 (blue). Scale bars: left panel 50 µm, right panels 10 µm**. B,** β-Galactosidase-positive cells lining microvessels express NG2. Note a NG2-positive, β-galactosidase-negative cell that is not associated with a microvessel (white arrowhead). β-galactosidase (green), NG2 (red), DAPI (blue). Scale bars: left panel 50 µm, right panels 10 µm. Sagittal sections of cortical tissue (postnatal day 30) were analyzed for the expression of β-galactosidase together with PDGFRß or NG2. **C,** Overview showing β-galactosidase (green), PDGFRß (red) and CD31 (blue) expression. Note the restricted expression of β-galactosidase and PDGFRß (red) associated to blood vessels. **D,** Overview showing β-galactosidase (green) and NG2 (red) expression. Note co-expression of β-galactosidase and NG2 in cells associated with blood vessels. DAPI (blue). Scale bars: left panels 100µm, right panels 50µm.

Originally, the TN-AP:CreERT2 mouse line has been used to label pericytes in skeletal muscle since alkaline phosphatase (AP) expression can be detected in vessel-associated cells at juvenile and adult stages in this tissue [233]. AP expression is not restricted to skeletal muscle and can be found widespread in intestine, bone and liver [234]. Three

isoforms of AP have been identified in mouse: placental, intestinal and tissue-nonspecific AP, with only the latter being exclusively expressed in skeletal muscle [233]; however, no information regarding the specific labeling of pericytes in the brain by AP was available. TN-AP-CreERT2 mice were crossed to R26R reporter lines to identify cells by expression of a nuclear form of ß-Galactosidase (ß-Gal) for *in vivo* analysis (TN-AP-CreERT2:R26^{NZG}) or enhanced yellow fluorescent protein (EYFP) for *in vitro* reprogramming experiments (TN-AP-CreERT2:R26^{EYFP}) following postnatal tamoxifen-induced Cre-mediated excision of the stop cassette allowing expression of the reporter gene. I first examined the specificity of recombination in the cerebral cortex of these mice at late postnatal stages (P25) by immunofluorescence and confocal microscopy (**Figure 2.32**). As pericytes are vessel-associated cells, I used antibodies against CD31 [235] to label endothelial cells forming the blood vessels for anatomical localization of perivascular cells. The TN-AP-CreERT2:R26^{NZG} mice were analyzed for the expression of ß-Galactosidase, readily and exclusively detectable along blood vessels throughout the cerebral cortex (**Figure 2.32**). As expected, the signal corresponding to ß-Galactosidase (ß-Gal) was confined to the soma of the reporter positive cells (**Figure 2.32**), adding further evidence for a specific expression profile. Confocal analysis of the brain sections showed that these ß-Gal positive cells were lining CD31-positive vessels, being negative for CD31 expression and therefore excluding that they were endothelial cells (**Figure 2.32**). To further demonstrate that these reporter-positive cells were indeed pericytes, I performed co-localization analyses using markers of pericytes such as PDGFRß and NG2. As expected, ß-Galactosidase expression co-localized with both PDGFRß, which is exclusively expressed by pericytes in the brain, and NG2 confirming that TN-AP promoter activity allows for reliable genetic fate mapping of pericytes in the cerebral cortex of mice TN-AP-CreERT2 (**Figure 2.32**). Of note, NG2 cells not located at perivascular positions (presumably OPCs) were negative for the expression of ß-Gal, and so excluding labeling of cells of non pericytic origin (**Figure 2.32**).

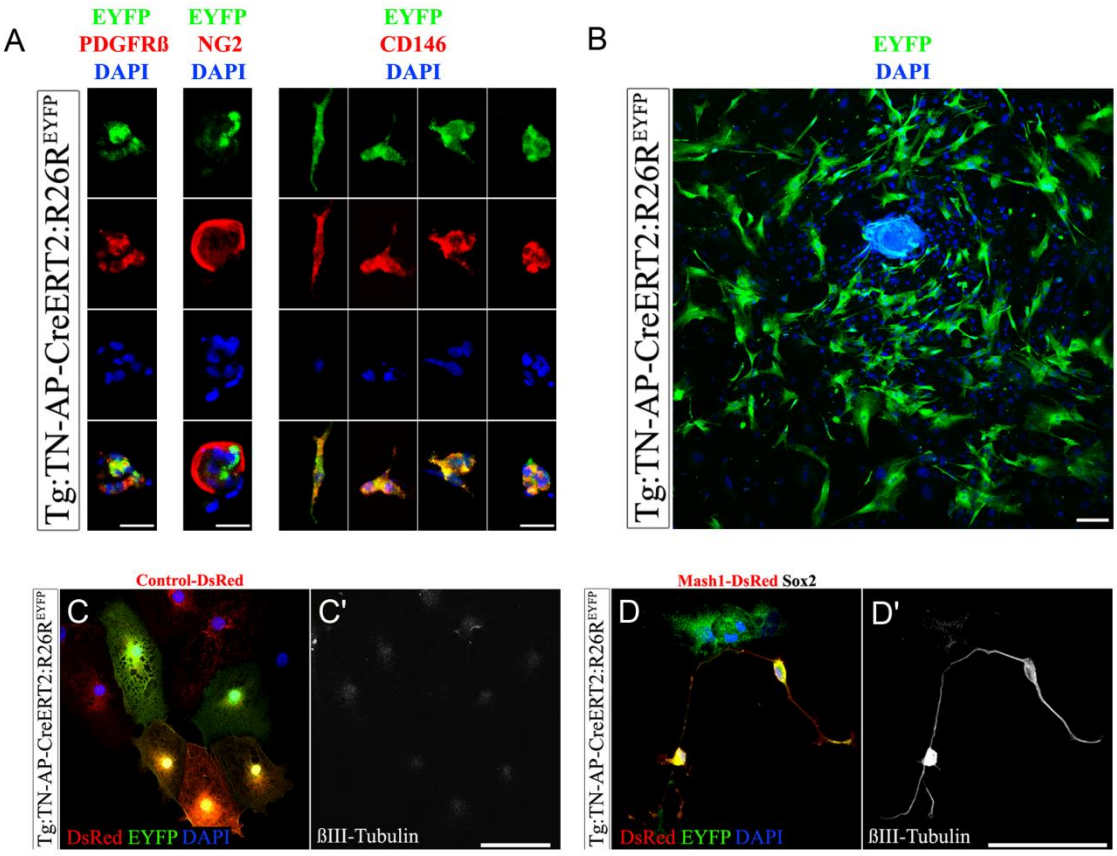

Figure 2.33: In vitro conversion of fate-mapped adult mouse brain pericyte-derived cells into neurons. A, B, Fate-mapped pericyte-derived cells isolated from mice Tg:TN-AP-CreERT2:R26R^{EYFP} can be expanded in vitro. **A,** Upon tissue dissociation, cells were directly plated on PDL-coated coverslips and analyzed 5 days later for the expression of EYFP (green), PDGFRß (red), NG2 (red) and CD146 (red). Single cells or small clones of EYFP (green) positive cells co-express pericyte markers. **B,** Large clone of EYFP-positive (green) fate-mapped cells following direct plating at low density demonstrating substantial clonal expansion in vitro; 20DIV. DAPI (blue). Scale bars: **C**, 50 µm, **D**,100 µm. **C-C',** EYFP-positive cells (green) isolated from the cerebral cortex of adult Tg:TN-AP-CreERT2:R26R^{EYFP} mice transduced with a control vector (red). Note the lack of ß-tubulin immunoreactivity (white); 14DPI. Scale bar: 100 µm. **d-d',** Reprogramming of EYFP-positive cells isolated from the cerebral cortex of adult Tg:TN-AP-CreERT2:R26R^{EYFP} mice into neurons. EYFP-positive cells (green) transduced with Mash1 (red) and Sox2 (without reporter) display a neuronal morphology and express ßIII-tubulin; 14 DPI. Scale bar: 100 µm.

Next, I prepared cultures from the adult cerebral cortex of TN-AP-CreERT2:R26^{EYFP} mice under the same conditions as used with wild type mice samples. I plated the cells at low density to observe the formation of clones and performed immunocytochemical analyses at different time points for the expression of EYFP. After 5 days in culture, reporter positive cells could be found as single cell or in small clones, positive for the expression of the pericyte markers PDGFRß, NG2 and CD146 (**Figure 2.33**). After 20 days, clones containing large number of reporter-positive protoplasmic cells could be easily detected, demonstrating that pericyte-derived cells could be expanded *in vitro* (**Figure 2.33**). In order to confirm their ability to proliferate, I infected EYFP-positive cells with retrovirus encoding for DsRed (control), with a majority of the pericyte-

derived cells being positive for the retroviral reporter gene expression and thus demonstrating that pericytes can be expanded and targeted with retroviral constructs *in vitro* (**Figure 2.33**). To investigate whether these EYFP-positive pericyte-derived cells can be reprogrammed to neurons, I used retroviral constructs encoding for Mash1 together with Dsred and Sox2 without reporter to allow visualization of potentially generated EYFP-positive neurons, indicating a pericyte origin. While no changes occurred upon control vector transduction, the generation of ßIII-tubulin positive pericyte-derived neurons in Mash1 and Sox2 transduced cultures could be observed (**Figure 2.33**), corroborating that cells of pericytic origin can undergo neuronal conversion by the combined activity of Mash1 and Sox2.

3. DISCUSSION

3.1. Summary

In this study I provide compelling evidence for the feasibility of a direct conversion approach to reprogram somatic cells from the adult human cerebral cortex into functional neurons *in vitro* by forced expression of neurogenic transcription factors.
Somatic cells could be isolated from adult human brain tissue and subsequently cultured and expanded in adherent conditions. Characterization of these cell cultures by immunocytochemistry, qRT-PCR and FACsorting revealed the enrichment of a cell type which shares marker expression with perivascular cells *in vivo.* Although the expression levels vary upon culturing and the presence of other cell types such as fibroblasts, endothelial cells, etc. cannot be excluded, the vast majority of the proliferative cells resemble perivascular cells based on their molecular expression profile. Notably, gene expression analysis excluded the presence of neural progenitor and stem cells. Under standard culturing methods, barely any astroglial cells were observed in culture. In contrast, applying milder dissociation conditions allows the isolation of astroglial cells, which *in vitro* did not have the ability to proliferate and die upon passaging. Retroviral vectors are limited in their use as they only target dividing cells. However most of the cells in culture were mitotically active and, therefore, a high proportion of them were transduced with retroviruses encoding neurogenic transcription factors. Among all tested factors, only the combination of Mash1 and Sox2 resulted in the direct conversion of adult human perivascular cells isolated from the cerebral cortex into functional neurons. The identity of the pericyte-derived cells was assessed by immunocytochemistry, showing expression of markers of mature neurons (MAP2 and NeuN), as well as neuronal subtype specific molecules (GABA and Calretinin). Importantly, the electrical properties of the neuron-like cells were assessed by patch-clamp recordings, revealing the ability of these cells to fire action potentials and receive synaptic inputs from embryonic mouse neurons. In order to exclude the presence of pre-existing neurons and to monitor the neuronal conversion, cultured human perivascular cells were sorted based on the surface expression of PDGFRß, typically labeling brain perivascular cells *in vivo,* and subsequently transduced with Mash1 and Sox2. Double-positive cells were followed by means of time-lapse video microscopy for a period of 14 days demonstrating the transition from protoplasmic to neuronal cell. To corroborate the feasibility of a direct pericyte-to-neuron conversion, a transgenic mouse line was used in which brain

pericytes could be labeled *in vivo* prior to culturing. Following the same procedure as with human brain material, fate-mapped pericytes could be expanded and reprogrammed to a neuronal phenotype by combination of Mash1 and Sox2, thus confirming the neurogenic potential of perivascular cells isolated from the cerebral cortex of adult mammals.

3.2. Are pericytes stem cells?

When aiming at the development of cell-based replacement strategies, it is worthwhile targeting a cell type which displays a high degree of plasticity (differentiation into other cell types) as well as the potential to resume proliferation upon tissue damage (to replace lost cells). The adult mammalian brain contains two regions of neurogenesis which could serve as a source of new neurons [236]. However, great number of replacing neurons would be necessary as well as approaches to induce targeted migration to the spot of injury or disease [237]. Alternatively, cell types found at the site of neurodegeneration (e.g. astrocytes, microglia, OPCs, endothelial and perivascular cells) could be amenable for direct conversion. First, some of them such as astrocytes and perivascular cells are developmentally related to neurons, as they share an ectodermal origin [84,217]. In addition, stem cell properties have been reported regarding astrocytes and perivascular cells, indicating their potential to differentiate into other cell types [84,214]. One advantage of this approach is that there is no need for migration since they are located at the site of disease. In particular, brain perivascular cells are excellent candidates for a direct conversion approach as their counterparts in other organs display stem cell potential, which is discussed below.

The hematopoietic stem cell (HSC) system is so far the best characterized tissue-specific stem cell population with all blood cell components being derived from a subset of bone marrow (BM) residing stem cells [238]. The HSC system importantly contributed to the definition of the term “stem cell”, a cell type which is characterized by their ability to differentiate into different mature cell lineages (multipotency) and to self-renew in order to replenish the stem cell pool [239]. The finding that bone marrow stromal cells can generate bone, cartilage, fat and reticular cells suggested the presence of BM multipotent precursor cells with broad differentiation potential [240,241]. Further experiments showed that these precursor cells were fibroblast-like cells selected by adherence to plastic surfaces and with the ability to proliferate *in vitro* and, therefore, termed colony-forming unit fibroblasts (CFU-Fs) [240]. *In vitro*, cells derived from single CFU-Fs retain their

ability to differentiate into osteoblasts, chondrocytes and adipocytes and became designated as "mesenchymal stem cells" (MSCs) [242] referring to *in vivo* precursors and their *in vitro*-expanded progeny. Latest attempts to redefine the nomenclature have led to the use of "mesenchymal stromal cell" for the *in vitro* cultured cells [243,244]. Beyond their *in vitro* properties [245], mesenchymal stromal cells have the ability to differentiate *in vivo* into cartilage and bone when transplanted in mice [246,247]. Moreover, the differentiation of diverse cell types of mesodermal and non-mesodermal origin such as endothelial cells [248], cardiomyocytes [249], and hepatocytes [250] has been reported from mesenchymal stromal cells, however, accompanied by controversy due to a lack of standard methods for isolation, expansion and identification [206]. Indeed, heterogeneity can be observed in mesenchymal stromal cell cultures as assessed by differences in morphology, proliferative capacity and *in vitro* and *in vivo* differentiation potential [251-254]. Additional studies have shown that stromal cells derived from postnatal and embryonic tissues give rise to cultures with diverse morphologies, differentiation potential and gene expression profiles, suggesting the absence of a biological equivalent among mesenchymal stromal cells from different anatomical locations [255-257].

Immunophenotype analyses of mesenchymal stromal cell cultures have revealed a panel of human cell surface markers expressed such as CD73, CD90 and CD105, with endothelial and hematopoietic cell markers being absent [238]; however, their expression varies depending on the isolation methods and passage [244]. The identification of CD146 as a marker for perivascular self-renewing progenitors located surrounding microvessels in the bone marrow has contributed to the *in vivo* characterization of MSCs [258]. Due to their *in vivo* perivascular location, morphology and similar cell surface antigen profile when cultured, an association has been proposed for pericytes and MSCs [259,260]. In addition, pericyte-derived cultures have been shown to differentiate into chondrocytes, adipocytes, osteoblasts as well as smooth muscle cells and myocytes [261-263]. Furthermore, recent work has identified a combination of markers such as PDGFRß, NG2 and CD146 specifically labeling pericytes in diverse human organs of human fetal and adult origin [205]. Cultures derived from directly isolated human pericytes displayed osteogenic, chondrogenic and adipogenic potential *in vitro* as well as osteogenic potential *in vivo* [205]. Although a relationship between pericytes and MSCs has been suggested, it is worthwhile mentioning that the term pericyte refers exclusively to cells at perivascular locations around capillaries and post-capillary venules [259] and that MSC-like cells have been isolated from the walls of arteries and veins [264,265]. Thus, it can be

concluded that not all MSCs can be defined as pericytes and not all pericytes display properties of MSCs [206].

Considering the potential of perivascular cells to differentiate into other cell types and the data provided in this thesis demonstrating the feasibility of converting brain perivascular cells into induced neuron-like cells, it is likely that perivascular cells outside the CNS might respond similarly to the combined expression of Mash1 and Sox2. This is relevant when using human cells from easily accessible tissues in order to generate personalized *in vitro* disease models from patients with neurological diseases, avoiding the use of brain tissue biopsies. Recent observations from other groups support the idea that cells from organs outside the CNS (such as skin fibroblasts and hepatocytes) may serve as a substrate for direct neuronal conversions.

3.3. **Fibroblast to neuron direct conversion**

In this study I have shown data demonstrating the feasibility of the *in vitro* direct neuronal conversion of non-neural somatic cells of adult human origin following retrovirally-mediated expression of neurogenic transcription factors. Other groups have shown that cells from non-related cell lineages (such as skin fibroblasts and hepatocytes) can be directly converted into neurons by the combined activity of several reprogramming factors such as transcription factors and microRNAs, corroborating the approach of direct conversion of adult non-neural-to-neural cell through the addition of exogenous factors shown in this thesis.

In order to the test the feasibility of neuronal direct conversion from distant cell lineages, Wernig and colleagues [266] selected a pool of transcription factors involved in neural lineage specification to screen for factors which could induce neurogenesis. Alone or in random combinations, these transcription factors were over-expressed in embryonic mouse fibroblasts; Mash1 itself (also known as Ascl1) was shown to instruct an immature neuronal phenotype. The authors identified a pool of three transcription factors sufficient to instruct functional neuronal identity, namely Mash1, Brn2 and Myelin transcription factor 1-like (Myt1l), (ABM), as assessed by the ability of these induced neurons to fire repetitive action potentials and to form synaptic contacts with mouse embryonic cortical neurons [266].

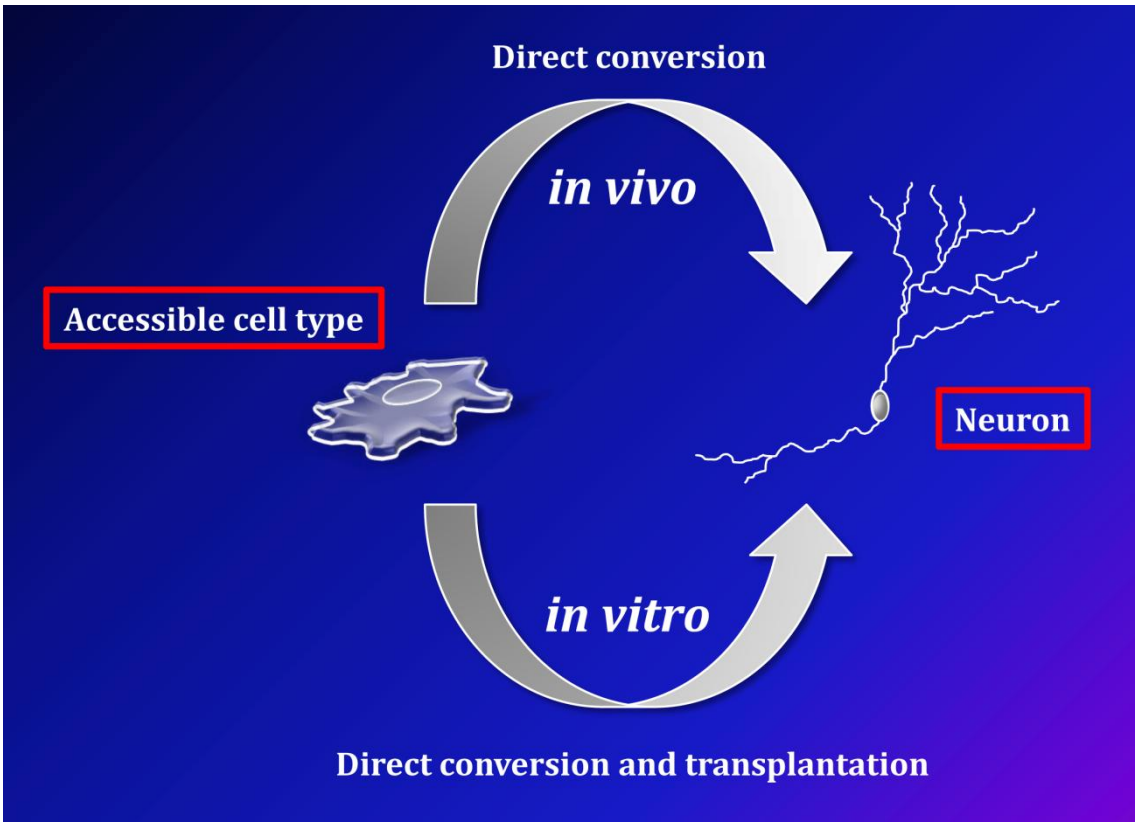

Figure 3.1: Direct conversion approaches.

Despite the fact that Mash1 specifies GABAergic interneurons during cortical development [135], when co-cultured with primary astrocytes, ABM expressing neurons adopted an excitatory glutamatergic phenotype. Brn2 is expressed in the developing mouse ventral telencephalon and spinal cord, co-localizing with the expression of Mash1 in the ventricular and subventricular regions. Together they synergistically regulate transcription of Delta1, a component of the notch signaling pathway and cooperatively regulate neuronal differentiation [153]. Brn2 is also expressed in progenitors which give rise to glutamatergic cortical neurons located in layers II/III and V [267]. Myt1l is a CCHC domain-containing zinc finger transcription factor expressed by differentiating neurons in both the central and peripheral nervous system [268,269]. In the following, various groups have shown that functional neurons can be generated from human fibroblasts. One approach takes advantage of the ABM combination to convert fetal and postnatal human fibroblasts to neurons, but requires the addition of the basic helix-loop-helix NEUROD1 to facilitate neuronal conversion[270]. Interestingly, the expression of the microRNAs miR-9* and miR124 are sufficient to generate cells with immature neuronal morphologies in human skin fibroblast cultures while in

combination with ASCl1,MYT1L and NEUROD2 induces the conversion to functional neurons [271]. The microRNAs miR-9* and miR124 instruct compositional changes of SWItch/Sucrose NonFermentable (SWI/SNF)-like BAF chromatin-remodeling complexes, a process required during neuronal differentiation [272]. In addition, other groups have focused on the generation of different types of neurons from human fibroblasts. The combination of the transcription factors Mash1, nur related protein 1 (Nurr1) and LIM homeobox transcription factor 1 alpha (Lmx1a) [273] or Mash1, Brn2, Myt1l, Lmx1a and forkhead box A2 (FoxA2) [274] induces the formation of dopamine-releasing tyrosine hydroxylase-positive neurons from mouse fibroblasts, however without the ability to form synapses. Furthermore, human neurons with a spinal motor phenotype could be generated, yet requiring the combination of 8 transcription factors [275]. Of note, skin fibroblast isolated from familial Alzheimer disease patients could be converted to neuronal cells which exhibited some hallmarks of this pathology such as increased production of Aß peptide compared to neuronal cells generated from skin fibroblasts of healthy individuals [276]. However, fibroblast cultures represent a heterogeneous mesenchymal progenitor cell population that may contain neural crest-derived cells. A recent study has reported that terminally differentiated endodermal cells (i.e. hepatocytes) can be directly converted to neurons [277].

Taken together, these reports support the feasibility of transcription factor-mediated direct neuronal conversion from different cell lineages and its potential application in human cell based-replacement strategies and disease modeling (**Figure 3.1**).

3.4. **Properties of directly converted neurons from adult brain perivascular cells**

In order to assess the extent of neuronal reprogramming from adult perivascular cells it is necessary to establish some criteria, which could be equivalent to those applied to neurons generated *in vitro* upon differentiation of neural or embryonic stem cells [278-280]. Despite a great heterogeneity among neurons present in the nervous system, some common features can be defined [281]:

1, a neuron is polarized and extends one main process (axon) and several dendrites from an elliptic/round soma; the expression of proteins such as the nuclear epitope NeuN, restricted to the nucleus of newly generated neurons, or specific cytoskeletal proteins

such as the microtubule-associated protein MAP2, in dendrites, provides information in regard to the neuronal identity (**Figure 3.2**).

2, neurons display characteristic membrane properties conferred by the presence of voltage-gated and transmitter–dependent ion channels; the ability of a neuron to fire action potentials relies on the orchestrated action of these proteins. As an immature neuron differentiates, the resting potential becomes hyperpolarized (-50mV to -70mV) (**Figure 3.2**) and the capacitance increases, proportional to the increase in cell surface area. As more membrane channel proteins are expressed during neuronal differentiation, the input resistance of a neuron´s membrane decreases (**Figure 3.2**). Also the action potential amplitudes increase as a neuron matures (**Figure 3.2**). A mature action potential is characterized by a constant amplitude, with fast depolarization and fast repolarization; the latter is responsible for the rapid regeneration of voltage-gated Na+ channels allowing the characteristic firing of trains of action potentials (**Figures 2.24, 3.2**) in mature neurons [282,283]. Experimentally, action potential firing can be evoked by injecting currents in the neuron (**Figure 3.2**).

3, neurons have the ability to form synapses, structures that neurons use to contact to each other and where neurotransmitter release occurs with high temporal and spatial precision. While almost all neurons generate synaptic outputs (except for neuromodulatory neurons), some do not receive synaptic inputs (e.g. primary sensory neurons). A fully functional neuron has the competence to establish synaptic inputs to other neurons. Synapse formation can be revealed by the presence of presynaptic vesicular structures in close proximity to MAP2 positive dendrites (**Figure 2.24**). By recording spontaneous synaptic currents, the synaptic activity can be unambiguously proved, as this technique can reveal the process of exocytosis and the postsynaptic response in form of sharp rise and slow decay phases (**Figure 2.24**). When neurons are exposed to specific neurotransmitter blockers, the synaptic activity can be definitively demonstrated; it also allows the distinction between excitatory and inhibitory responses (**Figure 2.24**). Furthermore, the presence of soluble glial factors and input from neighboring neurons is required for maturation and formation of functional synapses (**Figure 2.24**) [284,285].

	Human cells (no co-culture)	Human cells (co-culture)	Mouse cells
Resting potential V_R (mV)	-54 ± 13	-66 ± 11	-73 ± 10
Input resistance (MΩ)	2510 ± 919	2075 ± 940	811 ± 577
Number of cells exhibiting action potentials	12 /17	12 /12	6 /6
Number of action potentials / 1000 ms	1.3 ± 1.1	3.8 ± 6.8	5.0 ± 3.2
Action potential amplitude (mV)	56 ± 18	71 ± 30	77 ± 16
Peak Na^+ current (pA)	318 ± 268	912 ± 534	n.d .
Average age (days post infection)	35 ± 6	41 ± 5	32 ± 7

Figure 3.2: Comparison of electrophysiological properties of neurons following co-expression of Mash1-Sox2 in human and mouse perivascular cells culture.

3.5. **Synergism between Mash1 and Sox2**

I have shown that the expression of Mash1 or Sox2 alone does not result in the formation of neuron-like cells when expressed in perivascular cells from the adult human brain (**Figure 2.21**). In sharp contrast, the co-expression of Mash1 and Sox2 leads to the generation of functional neuron-like cells, suggesting a synergism between these transcription factors (**Figure 2.19, 2.24**).

The bHLH transcription factor Mash1 (and neurogenins) promotes cell cycle exit, inhibit differentiation of neighboring progenitors through Notch signaling-mediated lateral inhibition and drives both neuronal differentiation and subtype specification [137]. bHLH transcription factors form heterodimers with bHLH proteins encoded by the E2A gene, and bind to subtype- and tissue-specific hexa-nucleotide motifs (E-box) present in the promoter of target genes [137,286]. Additional interactions between DNA-binding proteins are required for specificity of target gene recognition. One example of cooperative interaction during vertebrate neurogenesis involves the synergistic activation of the motor neuron determination gene Hb9 by interaction of the bHLH protein NeuroM and the LIM-homeodomain transcription factors Islet1 and Lhx3 [287]. Interestingly, a mechanism of synergistic cooperation for Mash1 has been proposed [153]. Mash1 regulates the expression of the Notch ligand Delta1 in differentiating neurons, resulting in the activation of Notch signaling in a subset of neural progenitors and thereby promoting maintenance of an undifferentiated state [153]. This study revealed the synergistic activity through cooperative binding to a conserved motif of the Delta1 gene by Mash1 and

POU3F2, a member of the class III POU family of homeodomain proteins (also Brn2). Further analysis demonstrated the role of Brn proteins in cell cycle exit, initiation of neuronal differentiation and radial migration of neurons [153] highlighting the critical roles of DNA-binding cofactors during neural vertebrate development.

During *Drosophila* embryogenesis, CNS midline neurons and glia provide signals for differentiation of neighboring neuroectodermal and mesodermal cells [288]. The epidermal growth factor (EGF)-repeat protein Slit is highly expressed in midline glial cells and prevents commissural axons from re-crossing the midline [289]. The bHLH transcription factor *single minded* (Sim), the Sox HMG domain protein *Fish-hook* (Fish) and the POU protein *drifter* (Dfr) regulate Slit transcription by directly interacting to each other on the promoter of the Slit gene and so regulating CNS midline development and gene expression [290]. This study demonstrates the physical interaction of bHLH proteins together with HMG-Sox domain proteins and identifies a synergistic cooperative mechanism of gene expression involving these families of transcription factors.

All together, these findings support the idea of synergistic control of gene expression by the bHLH protein Mash1 and the HMG domain-containing protein Sox2, and offers a likely explanation for the generation of neurons following forced expression of Mash1 and Sox2 in adult human perivascular cells.

3.6. **The role of Sox2 in neuronal differentiation and GABAergic specification**

I have shown that forced co-expression of the neurogenic transcription factors Mash1 and Sox2 in perivascular cultures from adult human cortex results in the formation of neurons immunoreactive for GABA and, to a lower extent, Calretinin (**Figure 2.24**).

Over-expression experiments in chick embryo neural tube have shown that increased Sox2 levels prevents neuronal differentiation of neural progenitors into ßIII-tubulin positive neurons, reinforcing their self-renewal [116]. Additional experiments in embryonic neural precursors *in vitro* led to similar results indicating a direct correlation between Sox2 expression and inhibition of neurogenesis [212].

The *in vivo* expression of Sox2 in subsets of differentiated cortical neurons at early postnatal stages has been reported [121], suggesting a role for Sox2 beyond neural stem cell/precursor cells maintenance [115]. By means of a Sox2 enhancer deletion, *Cavallaro et al.* [291] have suggested a novel function for Sox2 in neuronal differentiation and

specification. Heterozygous Sox2-deficient mice display a reduction in Sox2 expression by about 70% and exhibit neural stem/precursor cell proliferative defects in the hippocampus and periventricular zone [121]. *In vitro*, embryonic Sox2-deficient neural stem cells display differentiation defects, assessed by the abnormal morphology and reduced expression of mature neuronal markers, suggesting a role of Sox2 in neuronal differentiation. Rescue experiments in which Sox2 lentiviral delivery was performed at the onset of neuronal differentiation resulted in normal arborized MAP2-positive phenotype in mutant cells [291]. Interestingly, late expression of Sox2 did not rescue the mutant phenotype, indicating an early role of Sox2 in neuronal differentiation. Additionally, mutant cells showed expression of ßIII-tubulin and GFAP simultaneously. By co-transfection of a GFAP promoter-driven reporter transgene, a direct repressor activity of Sox2 could be demonstrated since following Sox2 over-expression reporter activity was inhibited [291]. *In vivo* analysis revealed abnormalities in subset of neurons. *Cavallaro et al*. reported a decrease by 40-60% in the number of GABAergic cells in the cortex and the olfactory bulb of Sox2-deficient mice at P0. The authors found migration defects in GABAergic neurons from the ganglionic eminences during embryonic stages to the cortex as well as abnormalities in neuronal morphology in the early postnatal cortex; also the olfactory bulb displayed a slight reduction in the number in Calretinin-positive neurons at early postnatal stages [291]. In summary, the authors concluded that *in vivo* only a subpopulation of GABAergic neurons in the Sox2-deficient mice is affected by the reduction in the levels of Sox2.

Together with the role of Mash1 in GABAergic neuronal specification, the data of *Cavallaro et al.* [291] supports the finding of GABA- and Calretinin-positive neuronal cell generation following forced co-expression of Sox2 and Mash1 in perivascular cells from the adult cerebral cortex (**Figure 2.21**).

A precise quantitative expression profile plays a major role in the activity of Sox2 and other transcription factors [127]. Moreover, as Sox2 plays a role in early differentiation, it is possible that constitutive expression of Sox2 may inhibit neuronal maturation. For this reason, an approach to time-dependently reduce the levels of exogenous Sox2 by generation of microRNAs against the Sox2 cDNA encoded in a lentiviral construct was designed (**Figure 3.3**).

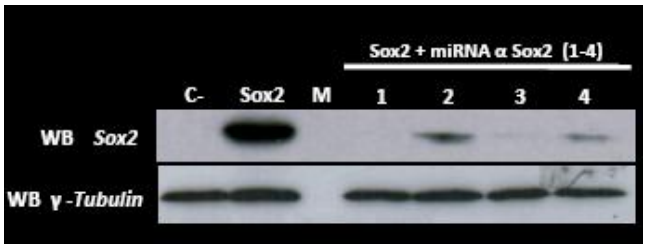

Figure 3.3: MicroRNA-mediated Sox2 down-regulation in HEK cells. Western blot analysis shows 4 different microRNAs agains Sox2 (1-4). As loading control, gamma-tubulin was analyzed; C-: negative control.

It remains open whether a Sox2 down-regulation approach results in further maturation of Mash1/Sox2-induced neurons from adult perivascular brain cells.

3.7. **Astroglia and pericytes in cell-based replacement strategies**

Both astroglia and pericytes have been shown to resume proliferation upon acute CNS injury [5,203]. After acute brain lesion, adult astroglia express markers only found in subventricular and hippocampal astroglia-like stem cells in the healthy brain [5,84]. The acquisition of stem cell properties are revealed by the ability of astrocytes to resume proliferation *in vivo* and to form self-renewing and multipotent neurospheres *in vitro* e.g. after stab wound injury or stroke [5,84]. Following acute stab wound injury, the astrocyte cortical population doubles in number within the first 2 weeks, with a peak of proliferation three to seven days after injury, and returns to baseline levels two weeks after injury [213]. Some of these newly generated astrocytes also take part in the formation of the glial scar following CNS injury. Over-expression of neurogenic factors or blockage of gliogenic cues in astroglia, resulted in the appearance of neuroblasts in nearby locations at the lesion, suggesting a role for astrocytes as a candidate cell type for cell-based repair purposes after brain injury[292].

Interestingly, also pericytes have been shown to react and resume proliferation in response to CNS lesion. After contusive spinal cord injury, pericyte reaction follows a similar time line as shown for astrocytes. At day one and two after injury, the core lesion area is largely devoid of blood vessels. Within three and five days after injury, blood vessel sprout paralleled by an increased density of associated pericytes, which appear at the lesion site [203]. *Göritz et al.* demonstrated that the increase in pericyte number is indeed due to a reactivation of proliferation following spinal cord injury and not due to migration from unaffected spinal cord regions [203]. The number of pericyte-derived cells reached a peak two weeks after spinal cord injury. Notably, two weeks

after a lesion, there are about two times more pericyte-derived cells as newly generated astrocytes in an injured spinal cord segment [203].

Therefore, the ability of astroglia and pericytes to resume proliferation following CNS acute injury supports the development of *in situ* reprogramming approaches; considering the increase in cell number, potential direct conversion strategies may rely on proliferating astroglia and/or pericytes to replace neuronal cells which are permanently lost upon injury or disease.

Epilepsy is one neurological disorder which could be treated by a cell-based replacement strategy. The most common form of human epilepsy is the mesial temporal lobe epilepsy (MTLE) which is characterized by epileptogenic abnormalities in mesial temporal structures where neural loss and reorganization takes places [293]. This type of epilepsy is associated with cognitive impairment and pharmacoresistance; it is not known what precise cell type causes the network imbalance or generates seizure discharges [293]. Surgical selective resection of medial temporal structures, including the amygdala and the hippocampus, results in effective relief of the symptoms, indicating that these are brain regions are involved in most cases of MTLE [293]. The onset of epilepsy is preceded by a phase of epileptogenesis, causing alterations in neuronal structure and function; the disease proceeds with the spontaneous generation of seizures in the affected regions [293]. Some hypothesis have been proposed to explain the initiation of focal seizures; in the hippocampus, mossy fibers redirect their axonal output to each other, creating a recurrent excitatory network; alternatively, it has been observed that hippocampal hyperinhibition collapses before a seizure, allowing the generation of granule cell discharges through hyperexcitablity [293]. Therapeutical strategies might focus on modifying the neuronal circuitry to inhibit the hyperexcitable neurons. Electrical activity remains abnormal within the epileptic focus by afterpolarization, a process which in normal conditions is dependent on feedback inhibition by inhibitory interneurons [293]. Distortion of this network impairs neuronal membrane repolarization and causes the generation of synchronous high-frequency action potentials [293]. By formation of new inhibitory synaptic contacts, hyperexcitation-driven discharges could be abolished.

One transplantation approach has shown functional integration of medial ganglionic eminence (MGE)-derived GABAergic interneurons in the cortex and hippocampus of juvenile mouse; by electrophysiological recordings it was shown that the MGE-derived grafted cells adopted mature neuronal phenotypes as well as modified the activity of the

host brain [293]. In order to compensate the hyper-excitatory neuronal activity, one possible strategy would be the generation of inhibitory GABA-ergic neurons by expression of Mash1 and Sox2 in adjacent glial or perivascular cells, thereby creating a balanced electrical network. An emerging concern of this strategy is the low efficiency of survival and integration of newly generated neurons in adult diseased tissue. Additional studies regarding the requirement of soluble factors (i.e. neurotrophins) to modulate the environment are essential to advance in the development of cell-based strategies in adult CNS tissue.

3.8. **Induced pluripotency *versus* direct conversion strategies**

Both approaches represent complementary methods to better understand pathologies and to design strategies for regenerative medicine; in particular, the lack of human neurons for experimental purposes accounts for one of the reasons of the limited available knowledge about most of human brain disorders.

Reprogramming of somatic cells to an induced pluripotent state has the advantage of unlimited growth, allowing the performance of high throughput assays (e.g. multiple drug testing assays) but the process is long and laborious [30]; in addition, generating patient-specific induced pluripotent cells (iPS) from numerous individuals is an arduous challenge. Furthermore, the differentiation of iPS cell lines it has been shown to be highly variable and, in the case of generation of neuronal cells, commonly displaying neuronal subtype heterogeneity and functional immature phenotypes [275]. Last, transplantation of iPS-derived cells may lead to teratoma (tumor) formation when differentiation protocols are inefficient and part of the transplanted cells remains undifferentiated [30]. On the other hand, direct conversion approaches are faster than the iPS generation methods and, when reprogramming efficiencies are improved, high number of patient-derived cells can be generated. Direct conversion is, in part, faster than the iPS strategy due to the fact that the latter requires a two-step process (reprogramming and differentiation), while the first is achieved in one single step; however, scale-up from patient´s somatic cells is not possible as they have limited proliferation capacity, representing a limitation when millions of cells must be replaced. Additionally, transcription factor-based direct conversion allows a higher degree of reproducibility regarding e.g. neuronal subtype specification [275]. For human therapy development, both approaches require the application of integration-free gene delivery methods to avoid mutagenesis. Potentially, *in vivo* direct conversion of endogenously

present cells in the organ to be repaired would eliminate the process of *in vitro* culturing and, more importantly, the problems associated with transplantation (**Figure 3.1, 3.4**).

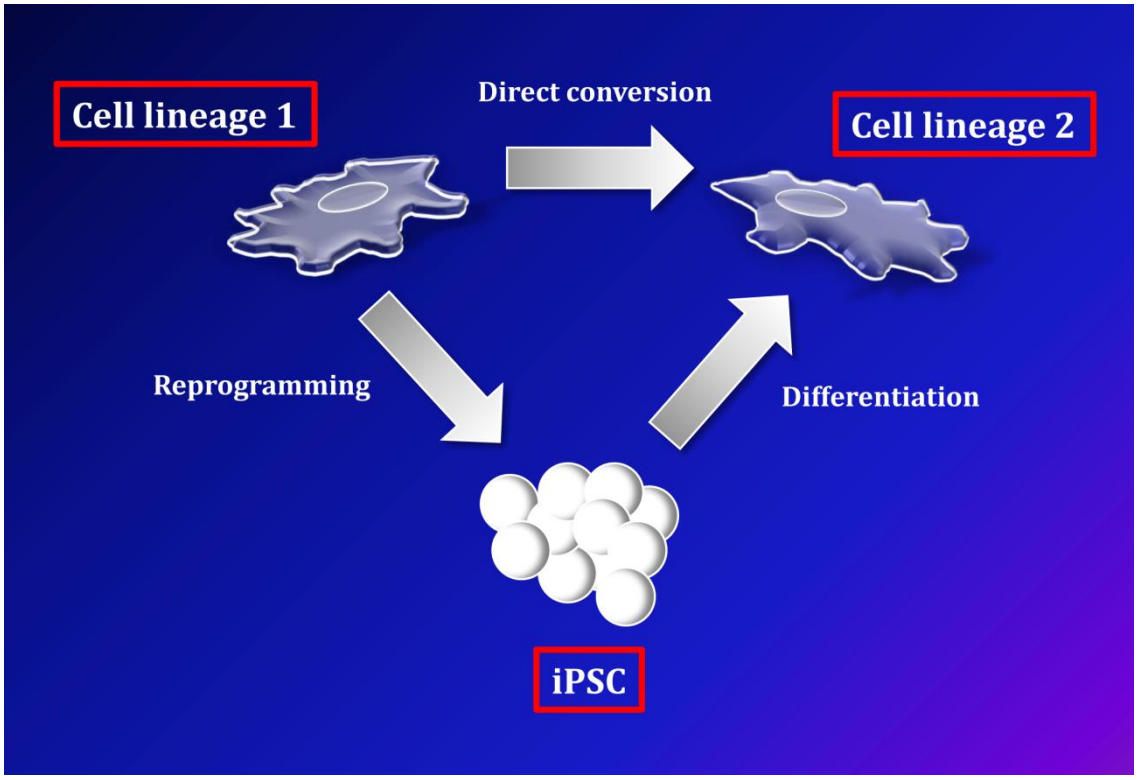

Figure 3.4: Cell reprogramming approaches.

3.9. **Non-retroviral methods for cellular reprogramming**

Retroviral constructs are excellent tools to force expression of reprogramming molecules by incorporation of DNA sequences into the host cell´s genome [294]. However, DNA integration of both i.e. transcription factors and retroviral sequences can lead to undesired side effects such as insertional mutagenesis and thereby tumor formation [295]. In addition, retroviral integration can promote expression of unwanted genes if certain loci are targeted [295]. Also it might be necessary to silence the expression of exogenous genes which are required at early stages to promote differentiation but impair functional maturation [295]. Therefore, an approach relying on classical retroviral transduction cannot be used for potential cell-based replacement therapies. Some alternatives have been proposed and are listed below:

1, Excision: the principle of this approach is to allow transgene integration, followed by their excision from the host genome once reprogramming has occurred. One approach relies on the activitiy of the Cre recombinase at the *loxP* site, which has been successfully tested on the generation of patient-derived iPSC [296]. However, a *loxP* site, as well as some residual viral DNA, remains in the iPSC´s genome and therefore potential insertional mutagenesis cannot be excluded [296]. An alternative method is the use of a tranposon/tranposase approach, the so called *PiggyBac* system [297]**.** The *PiggyBac* construct is capable of excising itself completely without leaving any remnants of exogenous DNA in the iPSC´s genome. The *PiggyBac* transposon/transposase system requires only the inverted terminal repeats flanking a transgene and transient expression of the transposase enzyme to catalyse insertion or excision events. The *PiggyBac* system shows comparable efficiency to retroviral methods with the benefit of increased safety [297] .

2, Adenoviral methods: unlike retroviruses, adenoviruses do not incorporate their genome into the host DNA [295]; therefore, there is no need for excision and represents a method which substantially reduces the risk of tumor formation. Despite the low reprogramming efficiencies using this method, it proves to be a viable and safer alternative to retroviral-integration strategies [295].

3, Protein transduction: a DNA independent method which replaces gene delivery by direct protein activity. A fusion protein consisting of a reprogramming factor and a cell-penetrating peptide (CPP), which facilitates cellular uptake of various molecular cargo, can be generated and applied directly to the target cell (both *in vivo* and *in vitro*) [298]. The incorporation of the fusion protein into the cell occurs commonly through endocytosis. The first described CPP was the trans-activating transcriptional activator (Tat) from the Human Immunodeficiency Virus 1 (HIV-1) [299]. CPPs typically have an amino acid composition that contains a high relative abundance of positively charged amino acids such as lysine or arginine. The absence of DNA intermediates would eliminate aberrant gene expression by transgene reactivation as well as any tumor formation risk; however, the use of this system is limited by the lack of cell specificity, insufficient understanding of the uptake mechanism and a very low reprogramming efficiency [298].

4, RNA-mediated reprogramming: Transcriptome Induced Phenotype Remodelling (TIPeR) is a method based on the ability of transfected RNA (mRNA, miRNA, etc.) to produce cell-to-cell phenotypic conversion [300]**.** This approach displays a number of advantages in comparison with DNA-based reprogramming methods. There is no

requirement for a vector or promoter-driven regulation, and mRNA does not need to be directed to the nucleus reducing approach complexity [300]. While precise control of expression cannot be achieved in DNA-based strategies, known and specific amounts of synthesized mRNA can be applied; also several RNAs can be added in multiple ratios [300]. This approach may allow the use of RNA populations with edited and spliced forms of RNAs with specific reprogramming potential. As RNA is transiently present in the cell cytoplasm, exogenous influence can be efficiently removed. Importantly, no integration to the genome or DNA damage occurs, minimizing the risk of malignancy. This reprogramming strategy carries, however, some disadvantages such as a, the requirement of increased RNA stability (i.e. poly-adenylation) for intracellular translational stability; b, RNA addition may need to be repeated multiple times; and c, transient inhibition of the host transcriptional machinery may be required to facilitate TIPeR [300].

3.10. **Perspectives for direct lineage conversion strategies**

The results shown in this thesis and the work of others in regard to the ability of somatic cell types to be converted into other cell types by the presence of exogenous transcription factors raise important questions which have to be addressed in order to design safe clinically applicable strategies. Considering that different somatic cells display different patterns of chromatin modifications, it is not yet clear how transcription factors find their binding sites and exert their activities; it is likely that these proteins have the ability to modify chromatin, thereby facilitating their access to certain loci; this hypothesis might partially explain the ability of the reprogramming factors to also down-regulate the expression of the transcriptional program of the starting cell. It is essential to determine whether the reprogramming process faithfully mimics terminal differentiation of the cell type to be generated; detailed gene expression profiles must be performed in order to ensure that reprogrammed cells are identical to their native counterparts; in line with this aspect of reprogramming, also epigenetic patterning must be taken in consideration when using different starting cell types, which might have an influence in the phenotype of the reprogrammed cell. It is also important to determine whether some cells are more susceptible to lineage conversion approaches and how important cell division is for an efficient reprogramming process. Last, in all examples of iPS reprogramming and lineage conversion approaches, human cells seem to be more refractory to reprogramming than cells isolated from other species [301] ; since

the goal of these experiments is to develop therapies to treat human diseases, it is critical to understand the molecular barriers to make human cells more amenable to lineage conversion, differentiation and maturation.

4. Materials and methods

4.1. Standard Solutions

Phosphate buffered Saline (PBS):

400 g NaCl (1.37 mol/l), 10g KCl (0.02 mol/l), 10 g K_2HPO_4 (0.015 mol/l), 58.75 g Na_2HPO_4 x $2H_2O$ (0.066 mol/l) were dissolved in 5 liter millipore water and autoclaved in 1l-bottles. This 10x PBS stock was diluted 1:10 with autoclaved Millipore water to around 0.15 M 1x PBS.

Lysis buffer for tail biopsies (10 ml):

1 ml 1 M Tris HCL pH 8.5, 100 µl 0.5 M EDTA, 200µl 10% SDS, 2 ml 1 M NaCl, 6.6ml H2O (autoclaved) are stored together at RT in one solution. Before lysis 100 µl Proteinase K (10 mg/ml) was added freshly.

Tris 10 mM for DNA (1 l):

1,211 g Trisbase (M=121.1 g/mol) dissolved in 1 liter Millipore water. pH was adjusted to 8.0 with HCl.

Electrophoresis buffer (1 l) for Western Blot:

30.3 g Trizma, 144 g Glycine, and 10 g SDS are dissolved in 1 liter of water. pH was adjusted to 8.45.

Sample buffer for Western Blot:

2 ml 1 M Tris-HCl pH 8.5, 8 ml 20% SDS, 5 ml Glycerol, 1.6 ml ß-Mercaptoethanol, 3.4 ml H2O, 50 mg Bromphenolblue. Store aliquots at -20°C.

TBST for Western Blot:

100 ml TBS 10x [1 l: 12.1 g TRIS-Base and 87.8 g NaCl are dissolved in 900 ml autoclaved water and pH is adjusted with 5 M HCl to pH 8.0. Autoclave.], 10 ml 20% Tween [200 ml H2O and 50 ml Tween 20], and 900 ml H2O are mixed.

Para-Formaldehyde (PFA) 4% (1 l):

PFA was diluted with autoclaved Millipore water from a frozen (-20°C) 20% PFA stock in 50 ml aliquots prepared according to the following protocol: 67 g Na2HPO4 x 2H2O were dissolved in 800 ml water thereby heated up to 60°C (temperature control!). 200 g PFA (Sigma) was added and stirred for around 5 minutes, until the cloudy solution was homogenous. Around 18 g of NaOH pellets were added until complete dissolvent of PFA. The pH was adjusted to 7.4 with 37% HCl.

4.2. **Surgery**

Brain tissue was acquired directly from the operating room. Specimens of cerebral cortex (frontal and temporal lobe) of 30 patients aged between 19 and 70 years of both sexes were obtained from standard neurosurgical approaches to deep-seated, non-traumatic, non-malignant lesions or epilepsy surgical procedures. The study was approved by the ethical committee of the Medical Faculty of the LMU Munich and written informed consent was obtained from all patients.

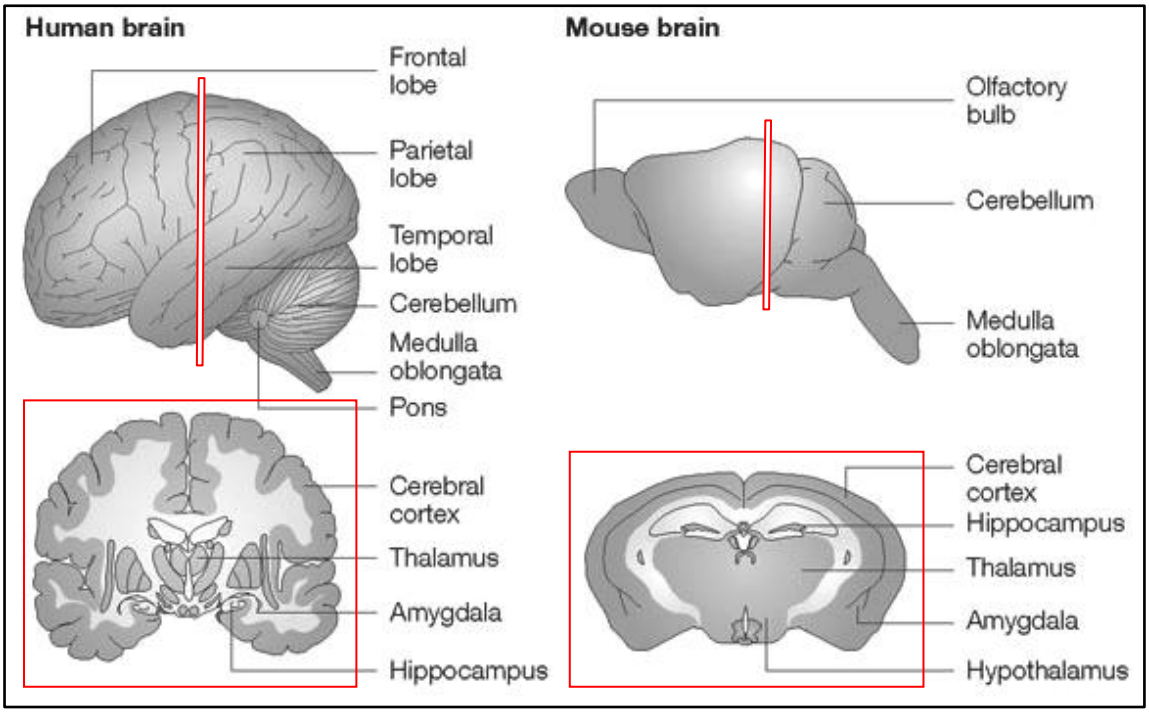

Figure 4.1: The human brain and the mouse brain: lateral and sagital views (Modified from *John F. Cryan & Andrew Holmes, Nature reviews/Drug discovery 2005).*

4.3. **Cell cultures from adult human, rat and mouse cerebral cortex**

After removal of the meninges, tissue was dissected and dissociated mechanically. Subsequently, cells were centrifuged for 5 min at 1000 rpm, re-suspended, and plated in a medium consisting of DMEM high glucose with GlutaMAX (Gibco), 20% fetal calf serum (Gibco), penicillin/streptomycin (Gibco). Originally, we also added 10 ng/ml epidermal growth factor (EGF, Roche) and fibroblast growth factor 2 (FGF2, Roche) to the medium to enhance the cell proliferation during expansion. However, we noted that

pericyte-derived cells could be expanded without treatment with these factors with similar reprogramming efficiencies and thus both factors were omitted from the medium. After expansion for 2-3 weeks as adherent culture under normoxygenated conditions, cells were harvested using trypsin/EDTA (Gibco) and either plated onto poly-D-lysine (Sigma-Aldrich) coated glass coverslips at a density of 50,000 cells per coverslip (in 24-well plates; BD Biosciences) in the same medium as above for reprogramming experiments or passaged for further expansion (up to five times in this study). As for the human specimens, gray matter of the mouse (BL6) or rat (Wistar) cerebral cortex was dissociated mechanically. The subsequent steps of culturing were identical.

4.4. **Co-culture with E14 mouse cortical neurons**

For co-culture experiments, E14 mouse cerebral cortices were dissected and dissociated mechanically with a fire-polished glass Pasteur pipette. Mouse cells were added to the human cultures 20 days after retroviral transduction at a density of 10.000-50.000 cells per coverslip. Electrophysiological recordings and/or immunocytochemistry were performed 39-47 days post retroviral infection. Experiments were repeated with 3 independent patients.

4.5. **DNA preparations**

Plasmid preparations

Plasmid preparations were carried out using the QIAGEN Mini Kit. The DNA pellet was resuspended in 30-50µl dist. H_2O or TE buffer. For larger amounts of DNA the QIAGEN Maxi Kit was used and the DNA resuspended in 300-500µl TE buffer.

Transformation of bacteria using heat shock

For the transformation of competent bacteria (TOP10, Invitrogene), one frozen aliquot (50µl) of bacteria was thawed on ice. 10 minutes later, 1-50ng of plasmid DNA was added to the bacteria and incubated on ice for 30min. For heat shock, the mixture was put on 42°C in a water bath for 90s. Immediately after, the bacteria were placed on ice, diluted with 1ml LB medium and incubated while shaking at room temperature for 30-60min.

Agarose gel electrophoresis

Agarose gels were prepared according to the expected fragment size with 0.8-2.0% agarose in TAE buffer (50X Stock: 2M Tris, 50mM Glacial acetic acid, 50mM EDTA). Heating in the microwave dissolved the agarose. Once the solution cooled down, 5µl ethidiumbromide (EtBr)-solution (EtBr=1mg/µl, final concentration: 0.005%) were added, mixed by swirling and poured into a prepared gel chamber avoiding bubbling. Loading of the samples on the gel was carried out by mixing the DNA solution with loading buffer (60% Glycerol, 2% SDS, 0.2% bromine phenol blue, 100mM EDTA). Separation of the DNA samples was carried out at a voltage of 100V for ca. 30-45min. Under UV light, fluorescent DNA fragments were documented with a BioRad Gel documentation system and, if necessary, removed from the gel under low intensity- UV light to avoid UV-induced mutations.

4.6. **Retroviral particle preparation**

The VSV-G (vesicular stomatitis virus glycoprotein)-pseudotyped retrovirus preparation with GPG293 cells only requires the addition of the retroviral expression plasmid vector. Additional viral genes are integrated in the genome of this cell line [294,302]. Cells were cultured in DMEM/high glucose/Glutamax (Gibco) containing 10% FCS (Invitrogen, heat inactivated at 56°C for 30 min), 1X Non-Essential Amino Acids (NEAA, 100 X, Gibco), 1X Sodium-Pyruvate (100 X, Gibco). In addition, cells were submitted to a triple selection of antibiotics: 1 mg/ml penicillin/streptomycin (Gibco), 1 mg/ml tetracycline (for repression of the VSVG production, Sigma) 2 mg/ml puromycin (for selection of the integrated VSVG gene and Tet-repressor which regulates VSVG expression, Sigma) and 0.3 mg/ml G418 (=Geneticin, for selection of the integrated MMLV genome -gagpol-, Gibco). Retroviral constructs were transfected with Lipofectamine 2000 (Invitrogene) into the GPG293 cell line and 48hours later supernatant harvested. After filtration through a 0,45 µm low protein-binding PVDF filter (Millipore), the supernatant was subsequently ultracentrifuged a 50000 x g for 90min at 4°C (Beckmann, SW40Ti rotor). Pellet containing retroviral particles was resuspended in TBS, aliquoted and stored at -80°C.

4.7. **Retroviral transduction**

The transcription factors Mash1 or Sox2 were expressed under control of an internal chicken β-actin promoter with cytomegalovirus enhancer (pCAG) together with DsRed located behind an internal ribosomal entry site (IRES) [110]. The Mash1 coding cDNA was subcloned from the pCLIG-Mash1 construct into the EcoRI site of the pSKSP shuttle vector, from where it was then subcloned between the 5′SfiI and 3′PmeI restriction sites of the pCAG retroviral vector to generate pCAG-Neurog2-IRES-DsRed. The Sox2 coding cDNA was subcloned from the pLIB-Sox2 construct[303], also used in fate-mapping experiments, and inserted into the pCAG retroviral vector following the same cloning strategy to generate pCAG-Mash1-IRES-DsRed. The coding region of the human Neurog2 was subcloned into pMX-IRES-GFP retroviral vector between BamHI and EcoRI restriction sites. The coding sequence of mouse E47 was subcloned into pMX-IRES-GFP between BamHI and EcoRI sites. The fusion construct corresponding to the REST coding sequence lacking its repressor domain and VP16 located at REST´s 3´end was subcloned into the pMX-IRES-GFP retroviral vector between XhoI and SacII sites. For control, cultures were transduced with a virus encoding only DsRed behind an IRES (pCAG-IRES-DsRed).

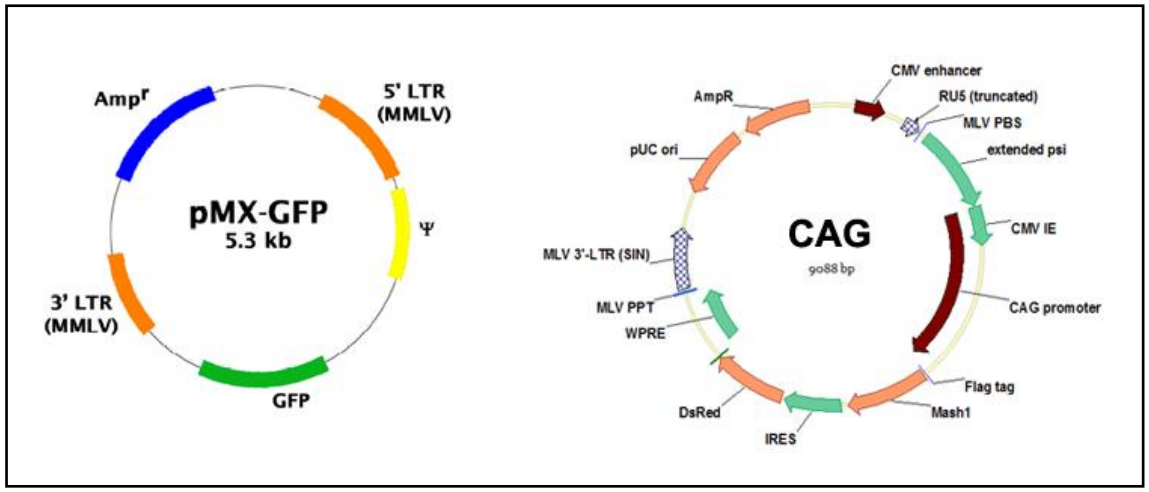

Figure 4.2: **Retroviruses are efficient tools for delivering heritable genes into the genome of dividing cells**. (Left) The pMX-GFP retroviral vector is based on Moloney murine leukemia virus (MMLV). The vector provides the viral package signal, transcription and processing elements. The viral *env* gene, produced by the package cell line, encodes the envelop protein, which determines the viral infectivity range. Transfection into a package cell line produces high-titer, replication-incompetent viruses. MCS (multiple cloning site). *Cell Biolabs, INC.* (Right) CAG-Mash1-IRES-DsRed retroviral vector.

Retroviral transduction of cultures was performed 2-3 h after plating on glass coverslips. Expression of the transcription factors was confirmed by immunocytochemistry. Twenty four hours after transduction, the medium was replaced by a differentiation medium consisting of DMEM high glucose with GlutaMAX, penicillin/streptomycin and B27 supplement (Gibco). Cells were allowed to differentiate under low oxygen conditions (5% O_2, 5% CO_2) (Galaxy 170R, New Brunswick).

4.8. **Immunocytochemistry**

Cell cultures were fixed in 4 % paraformaldehyde (PFA) in phosphate buffered saline (PBS) for 15 min at room temperature. Cells were first pre-treated in 0.5% Triton X-100 in PBS for 30 min, followed by incubation in 10% goat serum and 0.5% Triton X-100 in PBS for 30 min. Primary antibodies were incubated on specimen for 1 h at room temperature or overnight at 4°C in 10% goat serum, 0.5% Triton X-100 in PBS. After extensive washing in PBS, cells were incubated with appropriate species- or subclass-specific secondary antibodies conjugated to fluorophores. Coverslips were finally mounted onto a glass slide with an anti-fading mounting medium (Aqua Poly/Mount; Polysciences, Warrington, PA).

4.9. **Immunohistochemistry**

Human brain tissue specimens were transferred into 4% paraformaldehyde and incubated for 48 h at 4° C. Thereafter, specimens were embedded in Tissue-tek (OCT compound, Sakura) and 20µm thick cryostat sections were cut. Mice were anesthetized and transcardially perfused with 4% paraformaldehyde (PFA). Brains were collected, shortly post-fixed in 4% PFA and 20µm thick cryostat sections were cut. Sections were incubated with primary antibodies over night at 4ºC. After washing, secondary staining was performed using appropriate secondary antibodies. The following primary antibodies were used: chicken anti-Green Fluorescent Protein (Aves Labs, 1:1000), rabbit anti-Red Fluorescent Protein (Chemicon, 1:500), rabbit monoclonal anti-PDGFRβ (Cell Signalling, 1:200), mouse anti-Vimentin (Dako, 1:600), mouse anti-αSMA (Sigma-Aldrich, 1:400,), rabbit anti-NG2 (Millipore, 1:400), rabbit anti-hGFAP (Sigma-Aldrich, 1:600), rabbit anti-Sox2 (Chemicon, 1:1000), mouse anti-βIII-tubulin (Sigma-Aldrich, 1:400), mouse anti-Mash1 (Jackson-Price, 1:200), rabbit anti-CD146 (Abcam, 1:400), mouse anti-CD31 (Dako, 1:100), rat anti-CD31 (BD Pharmingen, 1:400), mouse

anti-MAP2 (Millipore, 1:200), mouse anti-NeuN (Millipore, 1:200), rabbit anti-GABA (Sigma, 1:500), rabbit anti-Calretinin (Millipore,1:500), rabbit anti- vGluT1 (Synaptic Systems, 1:1000), and chicken anti-β-galactosidase (Abcam, 1:1000). Secondary antibodies conjugated to: Alexa Fluor 488 (Invitrogen, 1:500), Cy3, Cy5, FITC, TRITC (Jackson ImmunoResearch, 1:500), or biotin (1:500, Jackson ImmunoResearch or Vector Laboratories) for 1h in the dark at room temperature, followed by extensive washing in PBS. Following treatment with secondary antibodies conjugated to biotin, cells were subsequently incubated for 2h at room temperature with AMCA streptavidin (1:200, Vector Laboratories). Nuclei were stained with 4′,6-Diamidino-2-phenylindole (DAPI) (Sigma Aldrich, 1:10000).

4.10. **Preparation of genomic DNA from tissue**

The preparation of genomic DNA requires the lysis of the cells composing the tissue, precipitation of the DNA and its subsequent purification. The lysis step is carried out using SDS-containing buffers, supplemented with proteinase K to remove DNA-associated and other proteins. The incubation is performed at 55°C, the optimal temperature for the proteinase activity. Following, DNA is precipitated by addition of salt and ethanol. Afterwards, the DNA is washed with ethanol and dissolved in water or buffer and can be frozen a -20°C.

4.11. **Transgenic animals and tamoxifen induction**

- **NG2-EYFP:** Gray matter of the cerebral cortex of adult heterozygous NG2-EYFP knock-in mice was dissected and subsequently cultured as described above.

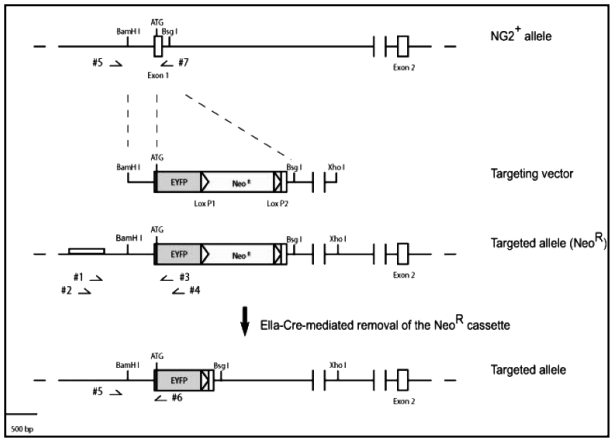

Figure 4.3: Homologous recombination of the murine NG2 gene [232].

- **TNAP-CreERT2:** Postnatal Tg:TN-AP-CreERT2:R26R^{NZG} and Tg:TN-AP-CreERT2:R26R^{EYFP} mice [233] were injected subcutaneously with 0.25mg of tamoxifen, diluted in corn oil for 3 consecutive days at 6, 7 and 8 days after birth to induce Cre-mediated recombination. At postnatal stage P25, Tg:TN-AP-CreERT2:R26R^{NZG} were sacrificed and the expression of nuclear ß-Galactosidase analyzed *in vivo*. Gray matter of the cerebral cortex of adult Tg:TN-AP-CreERT2:R26R^{EYFP} animals was dissected and cultured as decribed above.

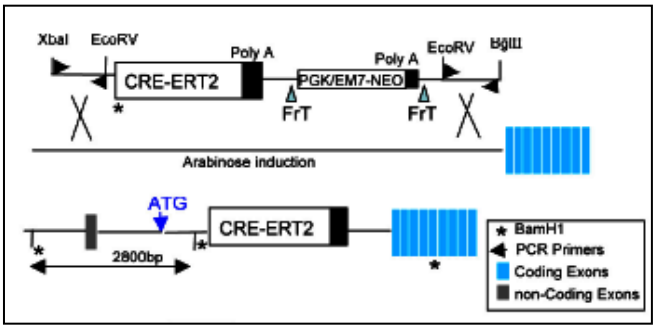

Figure 4.4: Scheme of the cloning strategy used to obtain mice *Tg:TN-AP-CreERT2* [233].

4.12. **Microscopy**

Immunocytochemical and immunohistochemical stainings were first examined with an epifluorescence microscope (BX61, Olympus) equipped with the appropriate filter sets. Stainings were further analyzed with a LSM710 laser-scanning confocal microscope (Carl Zeiss,). Digital images were captured using the ZEN software (Carl Zeiss). Cell counts were performed using a 40X objective in at least five fields of view randomly selected from each coverslip. At least 3 independent experiments were counted.

4.13. **Flow cytometry and FACS sorting**

Human brain-derived cells were detached from the culture dish using 0.25% trypsin for 4-6 minutes and subsequently 1-3 x 10^5 cells were resuspended in 100 µl staining solution (PBS plus 0.5% BSA). For surface marker analysis, primary antibodies (PE-conjugated CD140b (PDGFR-β) (1:100, BD Biosciences) and APC-conjugated CD34 (1:100, BD Biosciences) were added individually and cells were incubated for 20 min at 4°C. After washing three times in staining solution, cells were resuspended in 500 µl staining solution and subjected to surface marker analysis using a FACS Aria (BD). The

same setup was used to sort cells after co-staining with conjugated antibodies against CD34 and CD140b. APC-conjugated and PE-conjugated isotype control antibodies (1:100, AbD Serotec) were used to gate the proper populations. CD34-negative/CD140b-positive as well as double negative cells (CD34-negative/CD140b-negative) were sorted. Following sorting, cells were plated on PDL-coated glass cover slips on 24-well plates.

4.14. **Reverse Transcription (RT)-PCR Assay**

Total RNA was extracted with RNeasy MicroKit (Qiagen), according to the manufacturer's instructions. Total RNA was retro-transcribed as follows: 1-1,5 µg was adjusted to a final volume of 10µl with DEPC water and incubate at 65°C for 15 minutes, then transferred to ice; in a separate tube, 4µl of 5X First strand Buffer (Invitrogen), 2µl DTT 0,1M, 2µl dNTPs (10mM), 0,8µl Random Primers (500µM, Roche), 0,2µl RNasiOut (Invitrogen) and 1µl of cDNA MMLV-Retrotranscriptase (Invitrogen) were combined. This mixture was added to the RNA-water mixture and incubated at 37°C for 1 hour. The reaction was stopped by incubating the sample at 70°C for 10 minutes. The obtained cDNA was diluted one to ten, and 2µl was used in each PCR sample. Retrotranscribed cDNA was used as template, and the PCR reaction was performed as following:

Mix	**Amount**
DNA	2µl
10X Buffer	2µl
Primer Forward (10µM)	1µl
Primer Forward (10µM)	1µl
dNTPs (2µM)	1µl
*Taq*Polymerase	0,2µl
H2O	12,8µl
Total	20µl

Gene	Forward	Reverse
GAPDH	CGCATCTTCTTGTGCAGTG	GTTCAGCTCTGGGATGAC
Sox-2	ACCTACAGCATGTCCTACTCG	GGGCAGTGTGCCGTTAATGG
RGS5	ATGTGTAAGGGACTGGCAGC	TACTTGATTAGCTCCTTAT
Acta2	GATCCTGACGCTGAAGTATCCG	TACCCCCTGACAGGACGTTGT
Csrp2	CCTCGGTCAGACCTCGTTAGC	CACAGTAGTGAGCGCCATAAACG
Axl	GGTCGCTGTGAAGACCATGA	CTCAGGTACTCCATACCACT
Annexin5	GAAGCAATGCTCAGCGCCAGG	TATCCCCCACCACATCATCTTC
PdgfRBeta	AGCTACATGGCCCCTTATGA	GGATCCCAAAAGACCAGACA

Table 4.1: Mouse oligonucleotide primers for RT-PCR assay.

4.15. **Quantitative RT-PCR assay**

Total RNA was extracted with RNeasy Plus MicroKit (Qiagen), according to the manufacturer's instructions. One µg of total RNA was retro-transcribed using Super-ScriptIII Reverse Transcriptase (Invitrogen) and random primers. Each cDNA was diluted one to ten, and 1µl was used for each real-time reaction. Messenger RNA quantitation was performed on a LightCycler480 (Roche) using the Light Cycler TaqMan Master kit (Roche) according to the manufacturer's instructions. The amount of each gene was analyzed in triplicate. Data analysis was performed with the ΔΔCt method.

Gene	Accession number	Forward primer	Reverse primer	Amplicon
GAPDH	NM_002046	agccacatcgctcagacac	gcccaatacgaccaaatcc	66
PDGFRβ	NM_002609	cccttatcatcctcatcatgc	ccttccatcggatctcgtaa	60
VIM (Vimentin)	NM_003380	gtttcccctaaaccgctagg	agcgagagtggcagagga	68
SOX2	NM_003106	atgggttcggtggtcaagt	ggaggaagaggtaaccacagg	60
SOX9	NM_000346	aacgccttcatggtgtgg	tctcgctctcgttcagaagtc	124
ASCL1 (Mash1)	NM_004316	cgacttcaccaactggttctg	atgcaggttgtgcgatca	89
MECAM (CD146)	NM_006500	gggtaccccattcctcaagt	cagtctgggacgactgaatg	91
GFAP	NM_002055	ccaacctgcagattcgaga	tcttgaggtggccttctgac	63
P75	NM_002507.2	tcatccctgtctattgctcca	tgttctgcttgcagctgttc	93
SOX1	NM_005986.2	tcttttgggttggtttgttaattt	aatataactccgccgtctgaag	76
PROM1 (CD133)	NM_006017	tccacagaaatttacctacattgg	cagcagagagcagatgacca	77

CSPG4 (NG2)	NM_001897	gagaggcagctgagatcagaa	tgagaatacgatgtctgcaggt	77
ACTA2 (αSMA)	NM_001141945.1	ctgttccagccatccttcat	tcatgatgctgttgtaggtggt	70
CD34	NM_001773.2	tggctatttcctgatgaatcg	aagagtggtcagggttccag	75
S100B	NM_006272.2	ggaaggggtgagacaagga	ggtggaaaacgtcgatgag	73
NES (Nestin)	NM_006617.1	tgcgggctactgaaaagttc	tgtaggccctgtttctcctg	64
PAX6	NM_000280.3	ggcacacacacattaacacactt	ggtgtgtgagagcaattctcag	71
OLIG2	NM_005806	agctcctcaaatcgcatcc	atagtcgtcgcagctttcg	70
SOX10	NM_006941.3	ggctcccccatgtcagat	ctgtcttcggggtggttg	85

Table 4.2: Human oligonucleotide primers used in qRT-PCR analysis.

4.16. **Electrophysiology**

Electrophysiological properties of neurons derived from reprogrammed pericyte-like cells were analyzed following retroviral transduction. The electrode is composed of a glass micropipette whose tip is sealed onto the surface of the cell membrane rather inserted through it. The interior of the pipette is filled with a solution matching the ionic composition of the neuron´s cytoplasm, with a silver wire placed in contact with the solution which conducts the electric current to the amplifier. Measurement of changes in voltage or in current can be carried out by current-clamp or voltage-clamp mode, respectively. In current-clamp mode, the membrane potential is free to vary and the amplifier records voltage (mV) changes generated spontaneously or as a result of current injection (pA) in the cell. In voltage clamp, in contrast, the membrane potential is fixed at a certain value (mV) allowing the measurement of ionic current flow (pA) through the cell membrane at any given voltage. Single perforated patch-clamp recordings were performed at room temperature with amphotericin-B (Calbiochem) for perforation. Micropipettes were made from borosilicate glass capillaries (Garner, Claremont, CA, USA). Pipettes were tip-filled with internal solution and back-filled with internal solution containing 200 mg/mL amphotericin-B. The electrodes had resistances of 2–2.5 MV. The internal solution contained 136.5 mM K-gluconate, 17.5 mM KCl, 9 mM NaCl, 1 mM MgCl2, 10 mM HEPES, and 0.2 mM EGTA (pH 7.4) at an osmolarity of 300 mOsm. The external solution contained 150 mM NaCl, 3 mM KCl, 3 mM CaCl2, 2 mM MgCl2, 10 mM HEPES, and 5 mM glucose (pH 7.4) at an osmolarity of 310 mOsm. The recording chamber was continuously perfused with external solution at a rate of 0.5 mL/min. Cells were visualized with an epifluorescence microscope (Axioskop2, Carl Zeiss) equipped with the appropriate filter sets. For patch

clamp recordings, virally transduced cells were selected on the basis of their DsRed and/or GFP immunoreactivity. Digital pictures of the recorded cells were acquired using a digital camera (AxioCam, Carl Zeiss). Signals were sampled at 10 kHz with Axopatch 200B patchclamp amplifiers (Axon Instruments, Foster City, CA, USA), filtered at 5 kHz and analyzed with Clampfit 9.2 software (Axon Instruments). For assessing a cell's ability to fire APs, cells received depolarizing step-current injections and were treated with the sodium channel antagonist TTX (Tetrodotoxin), revealing the neuronal sodium channel component responsible for the generation of action potentials. AP amplitudes were measured by subtracting the threshold voltage of the AP from the AP maximum amplitude. For determining input resistance, hyperpolarizing currents of small amplitudes were injected into the cells under current clamp condition at a holding potential of 270 mV and input resistances were calculated from the corresponding voltage deviation. To examine spontaneous synaptic input into a given neuron, cells were kept in voltage clamp at a holding potential of 270 mV and synaptic events were recorded throughout a period of 1 to 5 min. To determine the nature of the synaptic responses, neurons were step-depolarized as described above and we assessed whether responses could be abolished in the presence of the AMPA/kainate receptor antagonist CNQX (5 mM). Finally, the recovery of the synaptic response was assessed following washout of the pharmacological drugs.

4.17. **Time-lapse video microscopy**

Time-lapse video microscopy of sorted PDGFRß-positive human cells was performed with a cell observer (Zeiss) at a constant temperature of 37^{o}C and 8 % CO_2. Phase contrast images were acquired every 5 minutes, and fluorescence pictures every 7.5 hours for 14 days using a 10x phase contrast objective (Zeiss), and an AxioCamHRm camera with a self-written VBA module remote controlling Zeiss AxioVision 4.7 software [305]. Movies were assembled using Image J 1.42q (National Institute of Health, USA) software and are played at speed of 3 frames per second.

4.18. **Western Blot**

Samples were loaded on SDS-PAGE gels.

Collecting Gel 4 % (7.5 ml): 4.575 ml clean H_2O, 0.975 ml acryl amide (Bio-Rad), 1.875 ml gel buffer pH 6.8 (0.5 M Tris pH 6.8), 37.5 µl 20 % SDS, 37.5 µl APS, 7.5 µl TEMED (Biorad).

Separation Gel 12 % (15 ml): 5.1 ml clean H_2O, 6 ml 30 % acryl amide, 3.75 ml gel buffer pH 8.8 (1.5 M Tris pH 8.8), 75 µl 20% SDS, 75 µl 10 % APS, 7.5 µl TEMED.

Western Blot Gels run under the following conditions: 1.5h, 120V. Gels were equilibrated in Transfer buffer (200 ml MetOH, 100 ml electrophoresis buffer and 700 ml H20) for 30 minutes.

Blotting: Membranes (PVDF, Biorad) were first incubated in MetOH; 30 minutes later, replaced by transfer buffer. Blot was performed in semi-dry conditions (Bio-Rad): 320 mA per gel / 15 V limited, 45 minutes. Immediately after the end of the blot PVDF membranes were washed three times for 5 minutes in 1 x TBST.

Detection: Membranes were prepared for antibody staining by blocking in 1 x TBST containing 5 % milk powder (Bio-Rad) for 1 hour at room temperature. The primary antibody rabbit against Sox2 (1:1000 in TBST containing 5 % milk powder) was incubated overnight at 4°C; washed out the next day for three times 15 minutes in 1x TBST. The secondary HRP-labelled antibody (anti-rabbit 1:10.000 in TBST containing 5 % milk powder) was applied for one hour at room temperature. Membranes were washed again three times in 1x TBST for one hour minutes. Detection of proteins bound onto the membrane was performed in a dark chamber using an ECL-Plus detection Kit (Amersham) (2 ml Solution A; 50 µl Solution B) and the x-ray film (Amersham photo paper) developed at different exposure time points.

4.19. **Lentiviral construct containing microRNAs against Sox2 cDNA**

Four different microRNAs against the coding sequence of Sox2 were designed using the software BLOCK-iT™ RNAi Designer (Invitrogene ^{TM}) and the corresponding oligonucleotide sequences chemically generated. Every oligonucleotide sequence was cloned into pcDNA™6.2 (Invitrogene ^{TM}) and transfected into HEK cells, together with a plamid over-expressing Sox2 to assess microRNA-induced Sox2 down-regulation. Next, all four sequences were subcloned in tandem into the lentiviral vector pLENTI7.3 (Invitrogene ^{TM}).

Sox2 cDNA target sequences (green):

miRNA 230:	TGGGCGCGGAGTGGAAACTTT
miRNA 313:	AAGGAGCACCCGGATTATAAA
miRNA 357:	GACGCTCATGAAGAAGGATAA
miRNA 477:	GGACAGCTACGCGCACATGAA

Example strategy miRNA 230 (reverse sequences in red):

Top Strand
5'- TGCTGAAAGTTTCCACTCCGCGCCCAGTTTTGGCCACTGACTGACTGGGCGCGGTGGAAACTTT -3'

Bottom Strand
5'- CCTGAAAGTTTCCACCGCGCCCAGTCAGTCAGTGGCCAAAACTGGGCGCGGAGTGGAAACTTTC -3'

ds Oligo
5'- TGCTGAAAGTTTCCACTCCGCGCCCAGTTTTGGCCACTGACTGACTGGGCGCGGTGGAAACTTT -3'
3'- CTTTCAAAGGTGAGGCGCGGGTCAAAACCGGTGACTGACTGACCCGCGCCACCTTTGAAAGTCC -5'

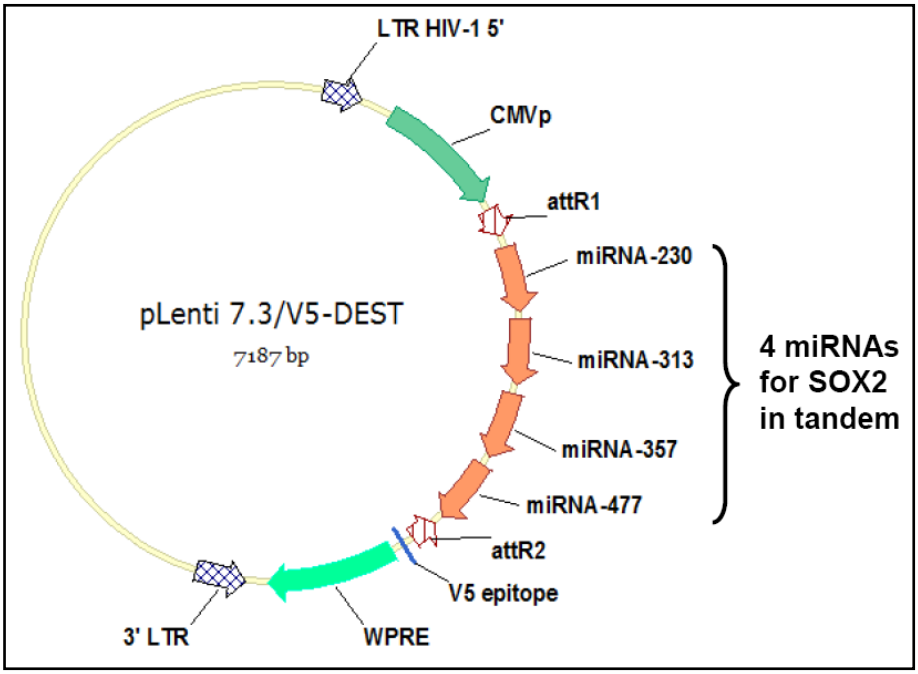

Figure 4.3: Cloning of four microRNAs in tandem into a lentiviral vector.

4.20. **Data analysis**

Virally transduced cells were identified by reporter–immunoreactivity (GFP or DsRed) and co-localization with cell type specific antigens and subsequently quantified. The total number of cells counted in all experiments is indicated in the text or figure legends. For each analysis at least 3 independent experiments were performed. Statistical analyses were performed by Student's two-tailed paired t-test using GraphPrism 4 software. P-values smaller than 0.05 were considered significant; P-values smaller than 0.001 were considered highly significant. Significant changes are indicated with the symbol ***** on top of the corresponding diagram bars. Error bars represent the standard error of the mean.

BIBLIOGRAPHY

1 Doetsch, F., Caille, I., Lim, D. A., Garcia-Verdugo, J. M. & Alvarez-Buylla, A. Subventricular zone astrocytes are neural stem cells in the adult mammalian brain. *Cell* **97**, 703-716 (1999).

2 Seri, B., Garcia-Verdugo, J. M., McEwen, B. S. & Alvarez-Buylla, A. Astrocytes give rise to new neurons in the adult mammalian hippocampus. *The Journal of neuroscience : the official journal of the Society for Neuroscience* **21**, 7153-7160 (2001).

3 Kriegstein, A. & Alvarez-Buylla, A. The glial nature of embryonic and adult neural stem cells. *Annual review of neuroscience* **32**, 149-184, doi:10.1146/annurev.neuro.051508.135600 (2009).

4 Ninkovic, J. & Gotz, M. Signaling in adult neurogenesis: from stem cell niche to neuronal networks. *Current opinion in neurobiology* **17**, 338-344, doi:10.1016/j.conb.2007.04.006 (2007).

5 Buffo, A. *et al.* Origin and progeny of reactive gliosis: A source of multipotent cells in the injured brain. *Proceedings of the National Academy of Sciences of the United States of America* **105**, 3581-3586, doi:10.1073/pnas.0709002105 (2008).

6 Khanna, A., Swistowska, A. M., Rao, M. S. & Zeng, X. Generation and transplantation of dopaminergic neurons derived from embryonic stem cells. *Current stem cell research & therapy* **2**, 139-147 (2007).

7 Lee, H. *et al.* Directed differentiation and transplantation of human embryonic stem cell-derived motoneurons. *Stem Cells* **25**, 1931-1939, doi:10.1634/stemcells.2007-0097 (2007).

8 Takahashi, K. & Yamanaka, S. Induction of pluripotent stem cells from mouse embryonic and adult fibroblast cultures by defined factors. *Cell* **126**, 663-676, doi:10.1016/j.cell.2006.07.024 (2006).

9 Brill, M. S. *et al.* A dlx2- and pax6-dependent transcriptional code for periglomerular neuron specification in the adult olfactory bulb. *The Journal of neuroscience : the official journal of the Society for Neuroscience* **28**, 6439-6452, doi:10.1523/JNEUROSCI.0700-08.2008 (2008).

10 Colak, D. *et al.* Adult neurogenesis requires Smad4-mediated bone morphogenic protein signaling in stem cells. *The Journal of neuroscience : the official journal of the Society for Neuroscience* **28**, 434-446, doi:10.1523/JNEUROSCI.4374-07.2008 (2008).

11 Hack, M. A. *et al.* Neuronal fate determinants of adult olfactory bulb neurogenesis. *Nature neuroscience* **8**, 865-872, doi:10.1038/nn1479 (2005).

12 Jessberger, S., Toni, N., Clemenson, G. D., Jr., Ray, J. & Gage, F. H. Directed differentiation of hippocampal stem/progenitor cells in the adult brain. *Nature neuroscience* **11**, 888-893, doi:10.1038/nn.2148 (2008).

13 Berninger, B., Guillemot, F. & Gotz, M. Directing neurotransmitter identity of neurones derived from expanded adult neural stem cells. *The European journal of neuroscience* **25**, 2581-2590, doi:10.1111/j.1460-9568.2007.05509.x (2007).

14 Saghatelyan, A., de Chevigny, A., Schachner, M. & Lledo, P. M. Tenascin-R mediates activity-dependent recruitment of neuroblasts in the adult mouse forebrain. *Nature neuroscience* **7**, 347-356, doi:10.1038/nn1211 (2004).

15 Nakatomi, H. *et al.* Regeneration of hippocampal pyramidal neurons after ischemic brain injury by recruitment of endogenous neural progenitors. *Cell* **110**, 429-441 (2002).

16 Aboody, K., Capela, A., Niazi, N., Stern, J. H. & Temple, S. Translating stem cell studies to the clinic for CNS repair: current state of the art and the need for a Rosetta Stone. *Neuron* **70**, 597-613, doi:10.1016/j.neuron.2011.05.007 (2011).

17 Ormerod, B. K., Palmer, T. D. & Caldwell, M. A. Neurodegeneration and cell replacement. *Philosophical transactions of the Royal Society of London. Series B, Biological sciences* **363**, 153-170, doi:10.1098/rstb.2006.2018 (2008).

18 Reubinoff, B. E. *et al.* Neural progenitors from human embryonic stem cells. *Nature biotechnology* **19**, 1134-1140, doi:10.1038/nbt1201-1134 (2001).

19 Keirstead, H. S. *et al.* Human embryonic stem cell-derived oligodendrocyte progenitor cell transplants remyelinate and restore locomotion after spinal cord injury. *The Journal of neuroscience : the official journal of the Society for Neuroscience* **25**, 4694-4705, doi:10.1523/JNEUROSCI.0311-05.2005 (2005).

20 Blum, B. & Benvenisty, N. The tumorigenicity of diploid and aneuploid human pluripotent stem cells. *Cell Cycle* **8**, 3822-3830 (2009).

21 Svendsen, C. N., Clarke, D. J., Rosser, A. E. & Dunnett, S. B. Survival and differentiation of rat and human epidermal growth factor-responsive precursor cells following grafting into the lesioned adult central nervous system. *Experimental neurology* **137**, 376-388, doi:10.1006/exnr.1996.0039 (1996).

22 Cummings, B. J. *et al.* Human neural stem cells differentiate and promote locomotor recovery in spinal cord-injured mice. *Proceedings of the National Academy of Sciences of the United States of America* **102**, 14069-14074, doi:10.1073/pnas.0507063102 (2005).

23 Seidenfaden, R., Desoeuvre, A., Bosio, A., Virard, I. & Cremer, H. Glial conversion of SVZ-derived committed neuronal precursors after ectopic grafting into the adult brain. *Molecular and cellular neurosciences* **32**, 187-198, doi:10.1016/j.mcn.2006.04.003 (2006).

24 Gupta, P. *et al.* Disruption of PPT1 or PPT2 causes neuronal ceroid lipofuscinosis in knockout mice. *Proceedings of the National Academy of Sciences of the United States of America* **98**, 13566-13571, doi:10.1073/pnas.251485198 (2001).

25 Tamaki, S. J. *et al.* Neuroprotection of host cells by human central nervous system stem cells in a mouse model of infantile neuronal ceroid lipofuscinosis. *Cell stem cell* **5**, 310-319, doi:10.1016/j.stem.2009.05.022 (2009).

26 Hagell, P. *et al.* Dyskinesias following neural transplantation in Parkinson's disease. *Nature neuroscience* **5**, 627-628, doi:10.1038/nn863 (2002).

27 Grealish, S. *et al.* The A9 dopamine neuron component in grafts of ventral mesencephalon is an important determinant for recovery of motor function in a rat model of Parkinson's disease. *Brain : a journal of neurology* **133**, 482-495, doi:10.1093/brain/awp328 (2010).

28 Isacson, O. & Mendez, I. Being too inclusive about synuclein inclusions. *Nature medicine* **16**, 960-961; author reply 961, doi:10.1038/nm0910-960b (2010).

29 Gurdon, J. B. From nuclear transfer to nuclear reprogramming: the reversal of cell differentiation. *Annual review of cell and developmental biology* **22**, 1-22, doi:10.1146/annurev.cellbio.22.090805.140144 (2006).

30 Hochedlinger, K. & Jaenisch, R. Nuclear reprogramming and pluripotency. *Nature* **441**, 1061-1067, doi:10.1038/nature04955 (2006).

31 Sridharan, R. *et al.* Role of the murine reprogramming factors in the induction of pluripotency. *Cell* **136**, 364-377, doi:10.1016/j.cell.2009.01.001 (2009).

32 Kim, J. B. *et al.* Oct4-induced pluripotency in adult neural stem cells. *Cell* **136**, 411-419, doi:10.1016/j.cell.2009.01.023 (2009).

33 Kim, J. B. *et al.* Direct reprogramming of human neural stem cells by OCT4. *Nature* **461**, 649-643, doi:10.1038/nature08436 (2009).
34 Masui, S. *et al.* Pluripotency governed by Sox2 via regulation of Oct3/4 expression in mouse embryonic stem cells. *Nature cell biology* **9**, 625-635, doi:10.1038/ncb1589 (2007).
35 Jaenisch, R. & Young, R. Stem cells, the molecular circuitry of pluripotency and nuclear reprogramming. *Cell* **132**, 567-582, doi:10.1016/j.cell.2008.01.015 (2008).
36 Park, I. H. *et al.* Reprogramming of human somatic cells to pluripotency with defined factors. *Nature* **451**, 141-146, doi:10.1038/nature06534 (2008).
37 Ebert, A. D. *et al.* Induced pluripotent stem cells from a spinal muscular atrophy patient. *Nature* **457**, 277-280, doi:10.1038/nature07677 (2009).
38 Dimos, J. T. *et al.* Induced pluripotent stem cells generated from patients with ALS can be differentiated into motor neurons. *Science* **321**, 1218-1221, doi:10.1126/science.1158799 (2008).
39 Soldner, F. *et al.* Parkinson's disease patient-derived induced pluripotent stem cells free of viral reprogramming factors. *Cell* **136**, 964-977, doi:10.1016/j.cell.2009.02.013 (2009).
40 Brennand, K. J. *et al.* Modelling schizophrenia using human induced pluripotent stem cells. *Nature* **473**, 221-225, doi:10.1038/nature09915 (2011).
41 Taylor, S. M. & Jones, P. A. Multiple new phenotypes induced in 10T1/2 and 3T3 cells treated with 5-azacytidine. *Cell* **17**, 771-779 (1979).
42 Davis, R. L., Weintraub, H. & Lassar, A. B. Expression of a single transfected cDNA converts fibroblasts to myoblasts. *Cell* **51**, 987-1000 (1987).
43 Choi, J. *et al.* MyoD converts primary dermal fibroblasts, chondroblasts, smooth muscle, and retinal pigmented epithelial cells into striated mononucleated myoblasts and multinucleated myotubes. *Proceedings of the National Academy of Sciences of the United States of America* **87**, 7988-7992 (1990).
44 Weintraub, H. *et al.* Activation of muscle-specific genes in pigment, nerve, fat, liver, and fibroblast cell lines by forced expression of MyoD. *Proceedings of the National Academy of Sciences of the United States of America* **86**, 5434-5438 (1989).
45 Schafer, B. W., Blakely, B. T., Darlington, G. J. & Blau, H. M. Effect of cell history on response to helix-loop-helix family of myogenic regulators. *Nature* **344**, 454-458, doi:10.1038/344454a0 (1990).
46 Albini, S. & Puri, P. L. SWI/SNF complexes, chromatin remodeling and skeletal myogenesis: it's time to exchange! *Experimental cell research* **316**, 3073-3080, doi:10.1016/j.yexcr.2010.05.023 (2010).
47 Gerber, A. N., Klesert, T. R., Bergstrom, D. A. & Tapscott, S. J. Two domains of MyoD mediate transcriptional activation of genes in repressive chromatin: a mechanism for lineage determination in myogenesis. *Genes & development* **11**, 436-450 (1997).
48 Xie, H., Ye, M., Feng, R. & Graf, T. Stepwise reprogramming of B cells into macrophages. *Cell* **117**, 663-676 (2004).
49 Bussmann, L. H. *et al.* A robust and highly efficient immune cell reprogramming system. *Cell stem cell* **5**, 554-566, doi:10.1016/j.stem.2009.10.004 (2009).
50 Zhou, Q. *et al.* A multipotent progenitor domain guides pancreatic organogenesis. *Developmental cell* **13**, 103-114, doi:10.1016/j.devcel.2007.06.001 (2007).

51 Zhou, Q., Brown, J., Kanarek, A., Rajagopal, J. & Melton, D. A. In vivo reprogramming of adult pancreatic exocrine cells to beta-cells. *Nature* **455**, 627-632, doi:10.1038/nature07314 (2008).

52 Gu, G., Dubauskaite, J. & Melton, D. A. Direct evidence for the pancreatic lineage: NGN3+ cells are islet progenitors and are distinct from duct progenitors. *Development* **129**, 2447-2457 (2002).

53 Kaneto, H. *et al.* PDX-1/VP16 fusion protein, together with NeuroD or Ngn3, markedly induces insulin gene transcription and ameliorates glucose tolerance. *Diabetes* **54**, 1009-1022 (2005).

54 Jonsson, J., Carlsson, L., Edlund, T. & Edlund, H. Insulin-promoter-factor 1 is required for pancreas development in mice. *Nature* **371**, 606-609, doi:10.1038/371606a0 (1994).

55 Gradwohl, G., Dierich, A., LeMeur, M. & Guillemot, F. neurogenin3 is required for the development of the four endocrine cell lineages of the pancreas. *Proceedings of the National Academy of Sciences of the United States of America* **97**, 1607-1611 (2000).

56 Yechoor, V. *et al.* Neurogenin3 is sufficient for transdetermination of hepatic progenitor cells into neo-islets in vivo but not transdifferentiation of hepatocytes. *Developmental cell* **16**, 358-373, doi:10.1016/j.devcel.2009.01.012 (2009).

57 Matsuoka, T. A. *et al.* Members of the large Maf transcription family regulate insulin gene transcription in islet beta cells. *Molecular and cellular biology* **23**, 6049-6062 (2003).

58 Zhang, C. *et al.* MafA is a key regulator of glucose-stimulated insulin secretion. *Molecular and cellular biology* **25**, 4969-4976, doi:10.1128/MCB.25.12.4969-4976.2005 (2005).

59 Dallos, P. & Harris, D. Properties of auditory nerve responses in absence of outer hair cells. *Journal of neurophysiology* **41**, 365-383 (1978).

60 Bermingham-McDonogh, O. & Reh, T. A. Regulated reprogramming in the regeneration of sensory receptor cells. *Neuron* **71**, 389-405, doi:10.1016/j.neuron.2011.07.015 (2011).

61 Corwin, J. T. Postembryonic production and aging in inner ear hair cells in sharks. *The Journal of comparative neurology* **201**, 541-553, doi:10.1002/cne.902010406 (1981).

62 Jorgensen, J. M. & Mathiesen, C. The avian inner ear. Continuous production of hair cells in vestibular sensory organs, but not in the auditory papilla. *Die Naturwissenschaften* **75**, 319-320 (1988).

63 Corwin, J. T. Auditory neurons expand their terminal arbors throughout life and orient toward the site of postembryonic hair cell production in the macula neglecta in elasmobranchs. *The Journal of comparative neurology* **239**, 445-452, doi:10.1002/cne.902390410 (1985).

64 Roberson, D. W., Alosi, J. A. & Cotanche, D. A. Direct transdifferentiation gives rise to the earliest new hair cells in regenerating avian auditory epithelium. *Journal of neuroscience research* **78**, 461-471, doi:10.1002/jnr.20271 (2004).

65 Gubbels, S. P., Woessner, D. W., Mitchell, J. C., Ricci, A. J. & Brigande, J. V. Functional auditory hair cells produced in the mammalian cochlea by in utero gene transfer. *Nature* **455**, 537-541, doi:10.1038/nature07265 (2008).

66 Bermingham, N. A. *et al.* Math1: an essential gene for the generation of inner ear hair cells. *Science* **284**, 1837-1841 (1999).

67 Haddon, C., Jiang, Y. J., Smithers, L. & Lewis, J. Delta-Notch signalling and the patterning of sensory cell differentiation in the zebrafish ear: evidence from the mind bomb mutant. *Development* **125**, 4637-4644 (1998).

68 Cotanche, D. A. & Kaiser, C. L. Hair cell fate decisions in cochlear development and regeneration. *Hearing research* **266**, 18-25, doi:10.1016/j.heares.2010.04.012 (2010).

69 Izumikawa, M. *et al.* Auditory hair cell replacement and hearing improvement by Atoh1 gene therapy in deaf mammals. *Nature medicine* **11**, 271-276, doi:10.1038/nm1193 (2005).

70 Izumikawa, M., Batts, S. A., Miyazawa, T., Swiderski, D. L. & Raphael, Y. Response of the flat cochlear epithelium to forced expression of Atoh1. *Hearing research* **240**, 52-56, doi:10.1016/j.heares.2008.02.007 (2008).

71 Parnavelas, J. G. The origin and migration of cortical neurones: new vistas. *Trends in neurosciences* **23**, 126-131 (2000).

72 Rakic, P. Specification of cerebral cortical areas. *Science* **241**, 170-176 (1988).

73 Alvarez-Buylla, A., Buskirk, D. R. & Nottebohm, F. Monoclonal antibody reveals radial glia in adult avian brain. *The Journal of comparative neurology* **264**, 159-170, doi:10.1002/cne.902640203 (1987).

74 Hartfuss, E., Galli, R., Heins, N. & Gotz, M. Characterization of CNS precursor subtypes and radial glia. *Developmental biology* **229**, 15-30, doi:10.1006/dbio.2000.9962 (2001).

75 Campbell, K. Signaling to and from radial glia. *Glia* **43**, 44-46, doi:10.1002/glia.10247 (2003).

76 Anthony, T. E., Klein, C., Fishell, G. & Heintz, N. Radial glia serve as neuronal progenitors in all regions of the central nervous system. *Neuron* **41**, 881-890 (2004).

77 Kriegstein, A. R. & Gotz, M. Radial glia diversity: a matter of cell fate. *Glia* **43**, 37-43, doi:10.1002/glia.10250 (2003).

78 Malatesta, P. *et al.* Neuronal or glial progeny: regional differences in radial glia fate. *Neuron* **37**, 751-764 (2003).

79 Costa, M. R., Bucholz, O., Schroeder, T. & Gotz, M. Late origin of glia-restricted progenitors in the developing mouse cerebral cortex. *Cereb Cortex* **19 Suppl 1**, i135-143, doi:10.1093/cercor/bhp046 (2009).

80 Miyata, T., Kawaguchi, A., Okano, H. & Ogawa, M. Asymmetric inheritance of radial glial fibers by cortical neurons. *Neuron* **31**, 727-741 (2001).

81 Noctor, S. C., Martinez-Cerdeno, V., Ivic, L. & Kriegstein, A. R. Cortical neurons arise in symmetric and asymmetric division zones and migrate through specific phases. *Nature neuroscience* **7**, 136-144, doi:10.1038/nn1172 (2004).

82 Zhou, Q., Choi, G. & Anderson, D. J. The bHLH transcription factor Olig2 promotes oligodendrocyte differentiation in collaboration with Nkx2.2. *Neuron* **31**, 791-807 (2001).

83 Park, J. K., Williams, B. P., Alberta, J. A. & Stiles, C. D. Bipotent cortical progenitor cells process conflicting cues for neurons and glia in a hierarchical manner. *The Journal of neuroscience : the official journal of the Society for Neuroscience* **19**, 10383-10389 (1999).

84 Robel, S., Berninger, B. & Gotz, M. The stem cell potential of glia: lessons from reactive gliosis. *Nature reviews. Neuroscience* **12**, 88-104, doi:10.1038/nrn2978 (2011).

85 Chojnacki, A. & Weiss, S. Pigment epithelium-derived growth factor: modulating adult neural stem cell self-renewal. *Nature neuroscience* **12**, 1481-1483, doi:10.1038/nn1209-1481 (2009).

86 Merkle, F. T., Tramontin, A. D., Garcia-Verdugo, J. M. & Alvarez-Buylla, A. Radial glia give rise to adult neural stem cells in the subventricular zone. *Proceedings of the National Academy of Sciences of the United States of America* **101**, 17528-17532, doi:10.1073/pnas.0407893101 (2004).

87 Brill, M. S. *et al.* Adult generation of glutamatergic olfactory bulb interneurons. *Nature neuroscience* **12**, 1524-1533, doi:10.1038/nn.2416 (2009).

88 Petryniak, M. A., Potter, G. B., Rowitch, D. H. & Rubenstein, J. L. Dlx1 and Dlx2 control neuronal versus oligodendroglial cell fate acquisition in the developing forebrain. *Neuron* **55**, 417-433, doi:10.1016/j.neuron.2007.06.036 (2007).

89 Costa, M. R., Gotz, M. & Berninger, B. What determines neurogenic competence in glia? *Brain research reviews* **63**, 47-59, doi:10.1016/j.brainresrev.2010.01.002 (2010).

90 Ables, J. L., Breunig, J. J., Eisch, A. J. & Rakic, P. Not(ch) just development: Notch signalling in the adult brain. *Nature reviews. Neuroscience* **12**, 269-283, doi:10.1038/nrn3024 (2011).

91 Dang, L., Yoon, K., Wang, M. & Gaiano, N. Notch3 signaling promotes radial glial/progenitor character in the mammalian telencephalon. *Developmental neuroscience* **28**, 58-69, doi:10.1159/000090753 (2006).

92 Yoon, K. *et al.* Fibroblast growth factor receptor signaling promotes radial glial identity and interacts with Notch1 signaling in telencephalic progenitors. *The Journal of neuroscience : the official journal of the Society for Neuroscience* **24**, 9497-9506, doi:10.1523/JNEUROSCI.0993-04.2004 (2004).

93 Ishibashi, M. *et al.* Persistent expression of helix-loop-helix factor HES-1 prevents mammalian neural differentiation in the central nervous system. *The EMBO journal* **13**, 1799-1805 (1994).

94 Hatakeyama, J. *et al.* Hes genes regulate size, shape and histogenesis of the nervous system by control of the timing of neural stem cell differentiation. *Development* **131**, 5539-5550, doi:10.1242/dev.01436 (2004).

95 Gaiano, N., Nye, J. S. & Fishell, G. Radial glial identity is promoted by Notch1 signaling in the murine forebrain. *Neuron* **26**, 395-404 (2000).

96 Alexson, T. O., Hitoshi, S., Coles, B. L., Bernstein, A. & van der Kooy, D. Notch signaling is required to maintain all neural stem cell populations--irrespective of spatial or temporal niche. *Developmental neuroscience* **28**, 34-48, doi:10.1159/000090751 (2006).

97 Androutsellis-Theotokis, A. *et al.* Notch signalling regulates stem cell numbers in vitro and in vivo. *Nature* **442**, 823-826, doi:10.1038/nature04940 (2006).

98 Han, Y. G. *et al.* Hedgehog signaling and primary cilia are required for the formation of adult neural stem cells. *Nature neuroscience* **11**, 277-284, doi:10.1038/nn2059 (2008).

99 Ahn, S. & Joyner, A. L. In vivo analysis of quiescent adult neural stem cells responding to Sonic hedgehog. *Nature* **437**, 894-897, doi:10.1038/nature03994 (2005).

100 Lai, K., Kaspar, B. K., Gage, F. H. & Schaffer, D. V. Sonic hedgehog regulates adult neural progenitor proliferation in vitro and in vivo. *Nature neuroscience* **6**, 21-27, doi:10.1038/nn983 (2003).

101 Balordi, F. & Fishell, G. Hedgehog signaling in the subventricular zone is required for both the maintenance of stem cells and the migration of newborn neurons. *The Journal of neuroscience : the official journal of the Society for Neuroscience* **27**, 5936-5947, doi:10.1523/JNEUROSCI.1040-07.2007 (2007).

102 Kempermann, G. & Gage, F. H. Neurogenesis in the adult hippocampus. *Novartis Foundation symposium* **231**, 220-235; discussion 235-241, 302-226 (2000).
103 Han, Y. G. & Alvarez-Buylla, A. Role of primary cilia in brain development and cancer. *Current opinion in neurobiology* **20**, 58-67, doi:10.1016/j.conb.2009.12.002 (2010).
104 Abbott, N. J., Ronnback, L. & Hansson, E. Astrocyte-endothelial interactions at the blood-brain barrier. *Nature reviews. Neuroscience* **7**, 41-53, doi:10.1038/nrn1824 (2006).
105 Malatesta, P., Hartfuss, E. & Gotz, M. Isolation of radial glial cells by fluorescent-activated cell sorting reveals a neuronal lineage. *Development* **127**, 5253-5263 (2000).
106 Noctor, S. C., Flint, A. C., Weissman, T. A., Dammerman, R. S. & Kriegstein, A. R. Neurons derived from radial glial cells establish radial units in neocortex. *Nature* **409**, 714-720, doi:10.1038/35055553 (2001).
107 Duan, X., Kang, E., Liu, C. Y., Ming, G. L. & Song, H. Development of neural stem cell in the adult brain. *Current opinion in neurobiology* **18**, 108-115, doi:10.1016/j.conb.2008.04.001 (2008).
108 Heins, N. *et al.* Glial cells generate neurons: the role of the transcription factor Pax6. *Nature neuroscience* **5**, 308-315, doi:10.1038/nn828 (2002).
109 Berninger, B. *et al.* Functional properties of neurons derived from in vitro reprogrammed postnatal astroglia. *The Journal of neuroscience : the official journal of the Society for Neuroscience* **27**, 8654-8664, doi:10.1523/JNEUROSCI.1615-07.2007 (2007).
110 Heinrich, C. *et al.* Directing astroglia from the cerebral cortex into subtype specific functional neurons. *PLoS biology* **8**, e1000373, doi:10.1371/journal.pbio.1000373 (2010).
111 Blum, R. *et al.* Neuronal network formation from reprogrammed early postnatal rat cortical glial cells. *Cereb Cortex* **21**, 413-424, doi:10.1093/cercor/bhq107 (2011).
112 Mori, T. *et al.* Inducible gene deletion in astroglia and radial glia--a valuable tool for functional and lineage analysis. *Glia* **54**, 21-34, doi:10.1002/glia.20350 (2006).
113 Episkopou, V. SOX2 functions in adult neural stem cells. *Trends in neurosciences* **28**, 219-221, doi:10.1016/j.tins.2005.03.003 (2005).
114 Zhao, S., Nichols, J., Smith, A. G. & Li, M. SoxB transcription factors specify neuroectodermal lineage choice in ES cells. *Molecular and cellular neurosciences* **27**, 332-342, doi:10.1016/j.mcn.2004.08.002 (2004).
115 Bylund, M., Andersson, E., Novitch, B. G. & Muhr, J. Vertebrate neurogenesis is counteracted by Sox1-3 activity. *Nature neuroscience* **6**, 1162-1168, doi:10.1038/nn1131 (2003).
116 Graham, V., Khudyakov, J., Ellis, P. & Pevny, L. SOX2 functions to maintain neural progenitor identity. *Neuron* **39**, 749-765 (2003).
117 Avilion, A. A. *et al.* Multipotent cell lineages in early mouse development depend on SOX2 function. *Genes & development* **17**, 126-140, doi:10.1101/gad.224503 (2003).
118 Miyagi, S. *et al.* Consequence of the loss of Sox2 in the developing brain of the mouse. *FEBS letters* **582**, 2811-2815, doi:10.1016/j.febslet.2008.07.011 (2008).
119 Favaro, R. *et al.* Hippocampal development and neural stem cell maintenance require Sox2-dependent regulation of Shh. *Nature neuroscience* **12**, 1248-1256, doi:10.1038/nn.2397 (2009).

120 Takanaga, H. *et al.* Gli2 is a novel regulator of sox2 expression in telencephalic neuroepithelial cells. *Stem Cells* **27**, 165-174, doi:10.1634/stemcells.2008-0580 (2009).
121 Ferri, A. L. *et al.* Sox2 deficiency causes neurodegeneration and impaired neurogenesis in the adult mouse brain. *Development* **131**, 3805-3819, doi:10.1242/dev.01204 (2004).
122 Suh, H. *et al.* In vivo fate analysis reveals the multipotent and self-renewal capacities of Sox2+ neural stem cells in the adult hippocampus. *Cell stem cell* **1**, 515-528, doi:10.1016/j.stem.2007.09.002 (2007).
123 Merkle, F. T. & Alvarez-Buylla, A. Neural stem cells in mammalian development. *Current opinion in cell biology* **18**, 704-709, doi:10.1016/j.ceb.2006.09.008 (2006).
124 Gubbay, J. *et al.* A gene mapping to the sex-determining region of the mouse Y chromosome is a member of a novel family of embryonically expressed genes. *Nature* **346**, 245-250, doi:10.1038/346245a0 (1990).
125 Remenyi, A. *et al.* Crystal structure of a POU/HMG/DNA ternary complex suggests differential assembly of Oct4 and Sox2 on two enhancers. *Genes & development* **17**, 2048-2059, doi:10.1101/gad.269303 (2003).
126 Kamachi, Y., Uchikawa, M. & Kondoh, H. Pairing SOX off: with partners in the regulation of embryonic development. *Trends in genetics : TIG* **16**, 182-187 (2000).
127 Rizzino, A. Sox2 and Oct-3/4: a versatile pair of master regulators that orchestrate the self-renewal and pluripotency of embryonic stem cells. *Wiley interdisciplinary reviews. Systems biology and medicine* **1**, 228-236, doi:10.1002/wsbm.12 (2009).
128 Uchikawa, M., Ishida, Y., Takemoto, T., Kamachi, Y. & Kondoh, H. Functional analysis of chicken Sox2 enhancers highlights an array of diverse regulatory elements that are conserved in mammals. *Developmental cell* **4**, 509-519 (2003).
129 Tanaka, S. *et al.* Interplay of SOX and POU factors in regulation of the Nestin gene in neural primordial cells. *Molecular and cellular biology* **24**, 8834-8846, doi:10.1128/MCB.24.20.8834-8846.2004 (2004).
130 Inoue, M. *et al.* PAX6 and SOX2-dependent regulation of the Sox2 enhancer N-3 involved in embryonic visual system development. *Genes to cells : devoted to molecular & cellular mechanisms* **12**, 1049-1061, doi:10.1111/j.1365-2443.2007.01114.x (2007).
131 Lin, Y. P., Ouchi, Y., Satoh, S. & Watanabe, S. Sox2 plays a role in the induction of amacrine and Muller glial cells in mouse retinal progenitor cells. *Investigative ophthalmology & visual science* **50**, 68-74, doi:10.1167/iovs.07-1619 (2009).
132 Kamachi, Y., Uchikawa, M., Tanouchi, A., Sekido, R. & Kondoh, H. Pax6 and SOX2 form a co-DNA-binding partner complex that regulates initiation of lens development. *Genes & development* **15**, 1272-1286, doi:10.1101/gad.887101 (2001).
133 Yasuhara, N. *et al.* Triggering neural differentiation of ES cells by subtype switching of importin-alpha. *Nature cell biology* **9**, 72-79, doi:10.1038/ncb1521 (2007).
134 Kondoh, H. & Kamachi, Y. SOX-partner code for cell specification: Regulatory target selection and underlying molecular mechanisms. *The international journal of biochemistry & cell biology* **42**, 391-399, doi:10.1016/j.biocel.2009.09.003 (2010).

135 Castro, D. S. *et al.* A novel function of the proneural factor Ascl1 in progenitor proliferation identified by genome-wide characterization of its targets. *Genes & development* **25**, 930-945, doi:10.1101/gad.627811 (2011).
136 Ross, S. E., Greenberg, M. E. & Stiles, C. D. Basic helix-loop-helix factors in cortical development. *Neuron* **39**, 13-25 (2003).
137 Bertrand, N., Castro, D. S. & Guillemot, F. Proneural genes and the specification of neural cell types. *Nature reviews. Neuroscience* **3**, 517-530, doi:10.1038/nrn874 (2002).
138 Roth, S. Y., Denu, J. M. & Allis, C. D. Histone acetyltransferases. *Annual review of biochemistry* **70**, 81-120, doi:10.1146/annurev.biochem.70.1.81 (2001).
139 Nieto, M., Schuurmans, C., Britz, O. & Guillemot, F. Neural bHLH genes control the neuronal versus glial fate decision in cortical progenitors. *Neuron* **29**, 401-413 (2001).
140 Nakada, Y., Hunsaker, T. L., Henke, R. M. & Johnson, J. E. Distinct domains within Mash1 and Math1 are required for function in neuronal differentiation versus neuronal cell-type specification. *Development* **131**, 1319-1330, doi:10.1242/dev.01008 (2004).
141 Hand, R. *et al.* Phosphorylation of Neurogenin2 specifies the migration properties and the dendritic morphology of pyramidal neurons in the neocortex. *Neuron* **48**, 45-62, doi:10.1016/j.neuron.2005.08.032 (2005).
142 Ge, W. *et al.* Coupling of cell migration with neurogenesis by proneural bHLH factors. *Proceedings of the National Academy of Sciences of the United States of America* **103**, 1319-1324, doi:10.1073/pnas.0510419103 (2006).
143 Corbin, J. G., Nery, S. & Fishell, G. Telencephalic cells take a tangent: non-radial migration in the mammalian forebrain. *Nature neuroscience* **4 Suppl**, 1177-1182, doi:10.1038/nn749 (2001).
144 Tekki-Kessaris, N. *et al.* Hedgehog-dependent oligodendrocyte lineage specification in the telencephalon. *Development* **128**, 2545-2554 (2001).
145 Schuurmans, C. *et al.* Sequential phases of cortical specification involve Neurogenin-dependent and -independent pathways. *The EMBO journal* **23**, 2892-2902, doi:10.1038/sj.emboj.7600278 (2004).
146 Poitras, L., Ghanem, N., Hatch, G. & Ekker, M. The proneural determinant MASH1 regulates forebrain Dlx1/2 expression through the I12b intergenic enhancer. *Development* **134**, 1755-1765, doi:10.1242/dev.02845 (2007).
147 Fode, C. *et al.* A role for neural determination genes in specifying the dorsoventral identity of telencephalic neurons. *Genes & development* **14**, 67-80 (2000).
148 Chapouton, P., Schuurmans, C., Guillemot, F. & Gotz, M. The transcription factor neurogenin 2 restricts cell migration from the cortex to the striatum. *Development* **128**, 5149-5159 (2001).
149 Casarosa, S., Fode, C. & Guillemot, F. Mash1 regulates neurogenesis in the ventral telencephalon. *Development* **126**, 525-534 (1999).
150 Parras, C. M. *et al.* Divergent functions of the proneural genes Mash1 and Ngn2 in the specification of neuronal subtype identity. *Genes & development* **16**, 324-338, doi:10.1101/gad.940902 (2002).
151 Sun, Y. *et al.* Neurogenin promotes neurogenesis and inhibits glial differentiation by independent mechanisms. *Cell* **104**, 365-376 (2001).
152 Farah, M. H. *et al.* Generation of neurons by transient expression of neural bHLH proteins in mammalian cells. *Development* **127**, 693-702 (2000).

153 Castro, D. S. *et al.* Proneural bHLH and Brn proteins coregulate a neurogenic program through cooperative binding to a conserved DNA motif. *Developmental cell* **11**, 831-844, doi:10.1016/j.devcel.2006.10.006 (2006).

154 Henke, R. M., Meredith, D. M., Borromeo, M. D., Savage, T. K. & Johnson, J. E. Ascl1 and Neurog2 form novel complexes and regulate Delta-like3 (Dll3) expression in the neural tube. *Developmental biology* **328**, 529-540, doi:10.1016/j.ydbio.2009.01.007 (2009).

155 Kageyama, R. & Nakanishi, S. Helix-loop-helix factors in growth and differentiation of the vertebrate nervous system. *Current opinion in genetics & development* **7**, 659-665 (1997).

156 Schwab, M. H. *et al.* Neuronal basic helix-loop-helix proteins (NEX, neuroD, NDRF): spatiotemporal expression and targeted disruption of the NEX gene in transgenic mice. *The Journal of neuroscience : the official journal of the Society for Neuroscience* **18**, 1408-1418 (1998).

157 Miyata, T., Maeda, T. & Lee, J. E. NeuroD is required for differentiation of the granule cells in the cerebellum and hippocampus. *Genes & development* **13**, 1647-1652 (1999).

158 Olson, J. M. *et al.* NeuroD2 is necessary for development and survival of central nervous system neurons. *Developmental biology* **234**, 174-187, doi:10.1006/dbio.2001.0245 (2001).

159 Schwab, M. H. *et al.* Neuronal basic helix-loop-helix proteins (NEX and BETA2/Neuro D) regulate terminal granule cell differentiation in the hippocampus. *The Journal of neuroscience : the official journal of the Society for Neuroscience* **20**, 3714-3724 (2000).

160 Hirabayashi, Y. *et al.* Polycomb limits the neurogenic competence of neural precursor cells to promote astrogenic fate transition. *Neuron* **63**, 600-613, doi:10.1016/j.neuron.2009.08.021 (2009).

161 Ballas, N., Grunseich, C., Lu, D. D., Speh, J. C. & Mandel, G. REST and its corepressors mediate plasticity of neuronal gene chromatin throughout neurogenesis. *Cell* **121**, 645-657, doi:10.1016/j.cell.2005.03.013 (2005).

162 Immaneni, A. *et al.* REST-VP16 activates multiple neuronal differentiation genes in human NT2 cells. *Nucleic acids research* **28**, 3403-3410 (2000).

163 Su, X., Kameoka, S., Lentz, S. & Majumder, S. Activation of REST/NRSF target genes in neural stem cells is sufficient to cause neuronal differentiation. *Molecular and cellular biology* **24**, 8018-8025, doi:10.1128/MCB.24.18.8018-8025.2004 (2004).

164 Allt, G. & Lawrenson, J. G. Pericytes: cell biology and pathology. *Cells, tissues, organs* **169**, 1-11 (2001).

165 Sims, D. E. The pericyte--a review. *Tissue & cell* **18**, 153-174 (1986).

166 Mandarino, L. J., Sundarraj, N., Finlayson, J. & Hassell, H. R. Regulation of fibronectin and laminin synthesis by retinal capillary endothelial cells and pericytes in vitro. *Experimental eye research* **57**, 609-621 (1993).

167 Diaz-Flores, L. *et al.* Pericytes. Morphofunction, interactions and pathology in a quiescent and activated mesenchymal cell niche. *Histology and histopathology* **24**, 909-969 (2009).

168 Cuevas, P. *et al.* Pericyte endothelial gap junctions in human cerebral capillaries. *Anatomy and embryology* **170**, 155-159 (1984).

169 Courtoy, P. J. & Boyles, J. Fibronectin in the microvasculature: localization in the pericyte-endothelial interstitium. *Journal of ultrastructure research* **83**, 258-273 (1983).

170 Gerhardt, H., Wolburg, H. & Redies, C. N-cadherin mediates pericytic-endothelial interaction during brain angiogenesis in the chicken. *Developmental dynamics : an official publication of the American Association of Anatomists* **218**, 472-479, doi:10.1002/1097-0177(200007)218:3<472::AID-DVDY1008>3.0.CO;2-# (2000).

171 Mathiisen, T. M., Lehre, K. P., Danbolt, N. C. & Ottersen, O. P. The perivascular astroglial sheath provides a complete covering of the brain microvessels: an electron microscopic 3D reconstruction. *Glia* **58**, 1094-1103, doi:10.1002/glia.20990 (2010).

172 Winkler, E. A., Bell, R. D. & Zlokovic, B. V. Pericyte-specific expression of PDGF beta receptor in mouse models with normal and deficient PDGF beta receptor signaling. *Molecular neurodegeneration* **5**, 32, doi:10.1186/1750-1326-5-32 (2010).

173 Lindahl, P., Johansson, B. R., Leveen, P. & Betsholtz, C. Pericyte loss and microaneurysm formation in PDGF-B-deficient mice. *Science* **277**, 242-245 (1997).

174 Huang, F. J. *et al.* Pericyte deficiencies lead to aberrant tumor vascularizaton in the brain of the NG2 null mouse. *Developmental biology* **344**, 1035-1046, doi:10.1016/j.ydbio.2010.06.023 (2010).

175 Ruiter, D. J. *et al.* Angiogenesis in wound healing and tumor metastasis. *Behring Institute Mitteilungen*, 258-272 (1993).

176 Kunz, J., Krause, D., Kremer, M. & Dermietzel, R. The 140-kDa protein of blood-brain barrier-associated pericytes is identical to aminopeptidase N. *Journal of neurochemistry* **62**, 2375-2386 (1994).

177 Nehls, V., Denzer, K. & Drenckhahn, D. Pericyte involvement in capillary sprouting during angiogenesis in situ. *Cell and tissue research* **270**, 469-474 (1992).

178 Crisan, M. *et al.* Perivascular multipotent progenitor cells in human organs. *Annals of the New York Academy of Sciences* **1176**, 118-123, doi:10.1111/j.1749-6632.2009.04967.x (2009).

179 Nehls, V. & Drenckhahn, D. The versatility of microvascular pericytes: from mesenchyme to smooth muscle? *Histochemistry* **99**, 1-12 (1993).

180 Murfee, W. L., Skalak, T. C. & Peirce, S. M. Differential arterial/venous expression of NG2 proteoglycan in perivascular cells along microvessels: identifying a venule-specific phenotype. *Microcirculation* **12**, 151-160, doi:10.1080/10739680590904955 (2005).

181 Hellstrom, M. *et al.* Lack of pericytes leads to endothelial hyperplasia and abnormal vascular morphogenesis. *The Journal of cell biology* **153**, 543-553 (2001).

182 Speyer, C. L., Steffes, C. P. & Ram, J. L. Effects of vasoactive mediators on the rat lung pericyte: quantitative analysis of contraction on collagen lattice matrices. *Microvascular research* **57**, 134-143, doi:10.1006/mvre.1998.2134 (1999).

183 Hamilton, N. B., Attwell, D. & Hall, C. N. Pericyte-mediated regulation of capillary diameter: a component of neurovascular coupling in health and disease. *Frontiers in neuroenergetics* **2**, doi:10.3389/fnene.2010.00005 (2010).

184 Majesky, M. W. Developmental basis of vascular smooth muscle diversity. *Arteriosclerosis, thrombosis, and vascular biology* **27**, 1248-1258, doi:10.1161/ATVBAHA.107.141069 (2007).

185 Etchevers, H. C., Vincent, C., Le Douarin, N. M. & Couly, G. F. The cephalic neural crest provides pericytes and smooth muscle cells to all blood vessels of the face and forebrain. *Development* **128**, 1059-1068 (2001).

186 Korn, J., Christ, B. & Kurz, H. Neuroectodermal origin of brain pericytes and vascular smooth muscle cells. *The Journal of comparative neurology* **442**, 78-88 (2002).

187 Heglind, M. *et al.* Lack of the central nervous system- and neural crest-expressed forkhead gene Foxs1 affects motor function and body weight. *Molecular and cellular biology* **25**, 5616-5625, doi:10.1128/MCB.25.13.5616-5625.2005 (2005).

188 Wilm, B., Ipenberg, A., Hastie, N. D., Burch, J. B. & Bader, D. M. The serosal mesothelium is a major source of smooth muscle cells of the gut vasculature. *Development* **132**, 5317-5328, doi:10.1242/dev.02141 (2005).

189 Que, J. *et al.* Mesothelium contributes to vascular smooth muscle and mesenchyme during lung development. *Proceedings of the National Academy of Sciences of the United States of America* **105**, 16626-16630, doi:10.1073/pnas.0808649105 (2008).

190 Asahina, K., Zhou, B., Pu, W. T. & Tsukamoto, H. Septum transversum-derived mesothelium gives rise to hepatic stellate cells and perivascular mesenchymal cells in developing mouse liver. *Hepatology* **53**, 983-995, doi:10.1002/hep.24119 (2011).

191 Zhou, B. *et al.* Epicardial progenitors contribute to the cardiomyocyte lineage in the developing heart. *Nature* **454**, 109-113, doi:10.1038/nature07060 (2008).

192 Abbott, N. J., Patabendige, A. A., Dolman, D. E., Yusof, S. R. & Begley, D. J. Structure and function of the blood-brain barrier. *Neurobiology of disease* **37**, 13-25, doi:10.1016/j.nbd.2009.07.030 (2010).

193 Bondjers, C. *et al.* Microarray analysis of blood microvessels from PDGF-B and PDGF-Rbeta mutant mice identifies novel markers for brain pericytes. *The FASEB journal : official publication of the Federation of American Societies for Experimental Biology* **20**, 1703-1705, doi:10.1096/fj.05-4944fje (2006).

194 Daneman, R., Zhou, L., Kebede, A. A. & Barres, B. A. Pericytes are required for blood-brain barrier integrity during embryogenesis. *Nature* **468**, 562-566, doi:10.1038/nature09513 (2010).

195 Armulik, A. *et al.* Pericytes regulate the blood-brain barrier. *Nature* **468**, 557-561, doi:10.1038/nature09522 (2010).

196 Bell, R. D. *et al.* Pericytes control key neurovascular functions and neuronal phenotype in the adult brain and during brain aging. *Neuron* **68**, 409-427, doi:10.1016/j.neuron.2010.09.043 (2010).

197 Attwell, D. *et al.* Glial and neuronal control of brain blood flow. *Nature* **468**, 232-243, doi:10.1038/nature09613 (2010).

198 Peppiatt, C. M., Howarth, C., Mobbs, P. & Attwell, D. Bidirectional control of CNS capillary diameter by pericytes. *Nature* **443**, 700-704, doi:10.1038/nature05193 (2006).

199 Yemisci, M. *et al.* Pericyte contraction induced by oxidative-nitrative stress impairs capillary reflow despite successful opening of an occluded cerebral artery. *Nature medicine* **15**, 1031-1037, doi:10.1038/nm.2022 (2009).

200 Kisseleva, T. & Brenner, D. A. Mechanisms of fibrogenesis. *Exp Biol Med (Maywood)* **233**, 109-122, doi:10.3181/0707-MR-190 (2008).

201 Schrimpf, C. & Duffield, J. S. Mechanisms of fibrosis: the role of the pericyte. *Current opinion in nephrology and hypertension* **20**, 297-305, doi:10.1097/MNH.0b013e328344c3d4 (2011).

202 Fabris, L. & Strazzabosco, M. Epithelial-mesenchymal interactions in biliary diseases. *Seminars in liver disease* **31**, 11-32, doi:10.1055/s-0031-1272832 (2011).
203 Goritz, C. *et al.* A pericyte origin of spinal cord scar tissue. *Science* **333**, 238-242, doi:10.1126/science.1203165 (2011).
204 Olson, L. E. & Soriano, P. PDGFRbeta signaling regulates mural cell plasticity and inhibits fat development. *Developmental cell* **20**, 815-826, doi:10.1016/j.devcel.2011.04.019 (2011).
205 Crisan, M. *et al.* A perivascular origin for mesenchymal stem cells in multiple human organs. *Cell stem cell* **3**, 301-313, doi:10.1016/j.stem.2008.07.003 (2008).
206 Nombela-Arrieta, C., Ritz, J. & Silberstein, L. E. The elusive nature and function of mesenchymal stem cells. *Nature reviews. Molecular cell biology* **12**, 126-131, doi:10.1038/nrm3049 (2011).
207 Nunes, M. C. *et al.* Identification and isolation of multipotential neural progenitor cells from the subcortical white matter of the adult human brain. *Nature medicine* **9**, 439-447, doi:10.1038/nm837 (2003).
208 Gibbons, H. M. *et al.* Cellular composition of human glial cultures from adult biopsy brain tissue. *Journal of neuroscience methods* **166**, 89-98, doi:10.1016/j.jneumeth.2007.07.005 (2007).
209 Verbeek, M. M., Otte-Holler, I., Wesseling, P., Ruiter, D. J. & de Waal, R. M. Induction of alpha-smooth muscle actin expression in cultured human brain pericytes by transforming growth factor-beta 1. *The American journal of pathology* **144**, 372-382 (1994).
210 Oberheim, N. A., Wang, X., Goldman, S. & Nedergaard, M. Astrocytic complexity distinguishes the human brain. *Trends in neurosciences* **29**, 547-553, doi:10.1016/j.tins.2006.08.004 (2006).
211 Rudge, J. S. *et al.* Neurotrophic factor receptors and their signal transduction capabilities in rat astrocytes. *The European journal of neuroscience* **6**, 693-705 (1994).
212 Bani-Yaghoub, M. *et al.* Role of Sox2 in the development of the mouse neocortex. *Developmental biology* **295**, 52-66, doi:10.1016/j.ydbio.2006.03.007 (2006).
213 Simon, C., Gotz, M. & Dimou, L. Progenitors in the adult cerebral cortex: cell cycle properties and regulation by physiological stimuli and injury. *Glia* **59**, 869-881, doi:10.1002/glia.21156 (2011).
214 Kondo, T. & Raff, M. Oligodendrocyte precursor cells reprogrammed to become multipotential CNS stem cells. *Science* **289**, 1754-1757 (2000).
215 Farrington-Rock, C. *et al.* Chondrogenic and adipogenic potential of microvascular pericytes. *Circulation* **110**, 2226-2232, doi:10.1161/01.CIR.0000144457.55518.E5 (2004).
216 Nagoshi, N. *et al.* Schwann cell plasticity after spinal cord injury shown by neural crest lineage tracing. *Glia* **59**, 771-784, doi:10.1002/glia.21150 (2011).
217 Armulik, A., Genove, G. & Betsholtz, C. Pericytes: developmental, physiological, and pathological perspectives, problems, and promises. *Developmental cell* **21**, 193-215, doi:10.1016/j.devcel.2011.07.001 (2011).
218 Shine, J., Czernilofsky, A. P., Friedrich, R., Bishop, J. M. & Goodman, H. M. Nucleotide sequence at the 5' terminus of the avian sarcoma virus genome. *Proceedings of the National Academy of Sciences of the United States of America* **74**, 1473-1477 (1977).

219 Okabe, M., Ikawa, M., Kominami, K., Nakanishi, T. & Nishimune, Y. 'Green mice' as a source of ubiquitous green cells. *FEBS letters* **407**, 313-319 (1997).

220 Easter, S. S., Jr., Ross, L. S. & Frankfurter, A. Initial tract formation in the mouse brain. *The Journal of neuroscience : the official journal of the Society for Neuroscience* **13**, 285-299 (1993).

221 Marusich, M. F., Furneaux, H. M., Henion, P. D. & Weston, J. A. Hu neuronal proteins are expressed in proliferating neurogenic cells. *Journal of neurobiology* **25**, 143-155, doi:10.1002/neu.480250206 (1994).

222 Narahashi, T., Moore, J. W. & Scott, W. R. Tetrodotoxin Blockage of Sodium Conductance Increase in Lobster Giant Axons. *The Journal of general physiology* **47**, 965-974 (1964).

223 Geoffroy, C. G. *et al.* Engineering of dominant active basic helix-loop-helix proteins that are resistant to negative regulation by postnatal central nervous system antineurogenic cues. *Stem Cells* **27**, 847-856, doi:10.1002/stem.17 (2009).

224 Watanabe, Y. *et al.* Conversion of myoblasts to physiologically active neuronal phenotype. *Genes & development* **18**, 889-900, doi:10.1101/gad.1179004 (2004).

225 Takahashi, K. *et al.* Induction of pluripotent stem cells from adult human fibroblasts by defined factors. *Cell* **131**, 861-872, doi:10.1016/j.cell.2007.11.019 (2007).

226 Izant, J. G. & McIntosh, J. R. Microtubule-associated proteins: a monoclonal antibody to MAP2 binds to differentiated neurons. *Proceedings of the National Academy of Sciences of the United States of America* **77**, 4741-4745 (1980).

227 Mullen, R. J., Buck, C. R. & Smith, A. M. NeuN, a neuronal specific nuclear protein in vertebrates. *Development* **116**, 201-211 (1992).

228 Enna, S. J. Regional variation and characteristics of GABA-receptors in the mammalian CNS. *Advances in experimental medicine and biology* **123**, 323-337 (1979).

229 Heizmann, C. W. Calcium-binding proteins: basic concepts and clinical implications. *General physiology and biophysics* **11**, 411-425 (1992).

230 Blake, J. F., Brown, M. W. & Collingridge, G. L. CNQX blocks acidic amino acid induced depolarizations and synaptic components mediated by non-NMDA receptors in rat hippocampal slices. *Neuroscience letters* **89**, 182-186 (1988).

231 Fremeau, R. T., Jr. *et al.* The expression of vesicular glutamate transporters defines two classes of excitatory synapse. *Neuron* **31**, 247-260 (2001).

232 Karram, K. *et al.* NG2-expressing cells in the nervous system revealed by the NG2-EYFP-knockin mouse. *Genesis* **46**, 743-757, doi:10.1002/dvg.20440 (2008).

233 Dellavalle, A. *et al.* Pericytes resident in postnatal skeletal muscle differentiate into muscle fibres and generate satellite cells. *Nature communications* **2**, 499, doi:10.1038/ncomms1508 (2011).

234 Schultz-Hector, S., Balz, K., Bohm, M., Ikehara, Y. & Rieke, L. Cellular localization of endothelial alkaline phosphatase reaction product and enzyme protein in the myocardium. *The journal of histochemistry and cytochemistry : official journal of the Histochemistry Society* **41**, 1813-1821 (1993).

235 Newman, P. J. *et al.* PECAM-1 (CD31) cloning and relation to adhesion molecules of the immunoglobulin gene superfamily. *Science* **247**, 1219-1222 (1990).

236 Gage, F. H. Mammalian neural stem cells. *Science* **287**, 1433-1438 (2000).

237 Massouh, M. & Saghatelyan, A. De-routing neuronal precursors in the adult brain to sites of injury: role of the vasculature. *Neuropharmacology* **58**, 877-883, doi:10.1016/j.neuropharm.2009.12.021 (2010).

238 Garrett, R. W. & Emerson, S. G. Bone and blood vessels: the hard and the soft of hematopoietic stem cell niches. *Cell stem cell* **4**, 503-506, doi:10.1016/j.stem.2009.05.011 (2009).

239 Weissman, I. L. Stem cells: units of development, units of regeneration, and units in evolution. *Cell* **100**, 157-168 (2000).

240 Friedenstein, A. J., Piatetzky, S., II & Petrakova, K. V. Osteogenesis in transplants of bone marrow cells. *Journal of embryology and experimental morphology* **16**, 381-390 (1966).

241 Tavassoli, M. & Crosby, W. H. Transplantation of marrow to extramedullary sites. *Science* **161**, 54-56 (1968).

242 Caplan, A. I. Mesenchymal stem cells. *Journal of orthopaedic research : official publication of the Orthopaedic Research Society* **9**, 641-650, doi:10.1002/jor.1100090504 (1991).

243 Horwitz, E. M. *et al.* Clarification of the nomenclature for MSC: The International Society for Cellular Therapy position statement. *Cytotherapy* **7**, 393-395, doi:10.1080/14653240500319234 (2005).

244 Dominici, M. *et al.* Minimal criteria for defining multipotent mesenchymal stromal cells. The International Society for Cellular Therapy position statement. *Cytotherapy* **8**, 315-317, doi:10.1080/14653240600855905 (2006).

245 Pittenger, M. F. *et al.* Multilineage potential of adult human mesenchymal stem cells. *Science* **284**, 143-147 (1999).

246 Ashton, B. A. *et al.* Formation of bone and cartilage by marrow stromal cells in diffusion chambers in vivo. *Clinical orthopaedics and related research*, 294-307 (1980).

247 Li, F., Wang, X. & Niyibizi, C. Bone marrow stromal cells contribute to bone formation following infusion into femoral cavities of a mouse model of osteogenesis imperfecta. *Bone* **47**, 546-555, doi:10.1016/j.bone.2010.05.040 (2010).

248 Oswald, J. *et al.* Mesenchymal stem cells can be differentiated into endothelial cells in vitro. *Stem Cells* **22**, 377-384, doi:10.1634/stemcells.22-3-377 (2004).

249 Makino, S. *et al.* Cardiomyocytes can be generated from marrow stromal cells in vitro. *The Journal of clinical investigation* **103**, 697-705, doi:10.1172/JCI5298 (1999).

250 Snykers, S., De Kock, J., Rogiers, V. & Vanhaecke, T. In vitro differentiation of embryonic and adult stem cells into hepatocytes: state of the art. *Stem Cells* **27**, 577-605, doi:10.1634/stemcells.2008-0963 (2009).

251 Colter, D. C., Class, R., DiGirolamo, C. M. & Prockop, D. J. Rapid expansion of recycling stem cells in cultures of plastic-adherent cells from human bone marrow. *Proceedings of the National Academy of Sciences of the United States of America* **97**, 3213-3218, doi:10.1073/pnas.070034097 (2000).

252 Kuznetsov, S. A. *et al.* Circulating skeletal stem cells. *The Journal of cell biology* **153**, 1133-1140 (2001).

253 Colter, D. C., Sekiya, I. & Prockop, D. J. Identification of a subpopulation of rapidly self-renewing and multipotential adult stem cells in colonies of human marrow stromal cells. *Proceedings of the National Academy of Sciences of the United States of America* **98**, 7841-7845, doi:10.1073/pnas.141221698 (2001).

254 Digirolamo, C. M. *et al.* Propagation and senescence of human marrow stromal cells in culture: a simple colony-forming assay identifies samples with the

greatest potential to propagate and differentiate. *British journal of haematology* **107**, 275-281 (1999).

255 Panepucci, R. A. *et al.* Comparison of gene expression of umbilical cord vein and bone marrow-derived mesenchymal stem cells. *Stem Cells* **22**, 1263-1278, doi:10.1634/stemcells.2004-0024 (2004).

256 Lee, R. H. *et al.* Characterization and expression analysis of mesenchymal stem cells from human bone marrow and adipose tissue. *Cellular physiology and biochemistry : international journal of experimental cellular physiology, biochemistry, and pharmacology* **14**, 311-324, doi:10.1159/000080341 (2004).

257 Kaltz, N. *et al.* Novel markers of mesenchymal stem cells defined by genome-wide gene expression analysis of stromal cells from different sources. *Experimental cell research* **316**, 2609-2617, doi:10.1016/j.yexcr.2010.06.002 (2010).

258 Sacchetti, B. *et al.* Self-renewing osteoprogenitors in bone marrow sinusoids can organize a hematopoietic microenvironment. *Cell* **131**, 324-336, doi:10.1016/j.cell.2007.08.025 (2007).

259 Hirschi, K. K. & D'Amore, P. A. Pericytes in the microvasculature. *Cardiovascular research* **32**, 687-698 (1996).

260 Doherty, M. J. *et al.* Vascular pericytes express osteogenic potential in vitro and in vivo. *Journal of bone and mineral research : the official journal of the American Society for Bone and Mineral Research* **13**, 828-838, doi:10.1359/jbmr.1998.13.5.828 (1998).

261 Shi, S. & Gronthos, S. Perivascular niche of postnatal mesenchymal stem cells in human bone marrow and dental pulp. *Journal of bone and mineral research : the official journal of the American Society for Bone and Mineral Research* **18**, 696-704, doi:10.1359/jbmr.2003.18.4.696 (2003).

262 Collett, G. D. & Canfield, A. E. Angiogenesis and pericytes in the initiation of ectopic calcification. *Circulation research* **96**, 930-938, doi:10.1161/01.RES.0000163634.51301.0d (2005).

263 Dellavalle, A. *et al.* Pericytes of human skeletal muscle are myogenic precursors distinct from satellite cells. *Nature cell biology* **9**, 255-267, doi:10.1038/ncb1542 (2007).

264 Tintut, Y. *et al.* Multilineage potential of cells from the artery wall. *Circulation* **108**, 2505-2510, doi:10.1161/01.CIR.0000096485.64373.C5 (2003).

265 Hoshino, A., Chiba, H., Nagai, K., Ishii, G. & Ochiai, A. Human vascular adventitial fibroblasts contain mesenchymal stem/progenitor cells. *Biochemical and biophysical research communications* **368**, 305-310, doi:10.1016/j.bbrc.2008.01.090 (2008).

266 Vierbuchen, T. *et al.* Direct conversion of fibroblasts to functional neurons by defined factors. *Nature* **463**, 1035-1041, doi:10.1038/nature08797 (2010).

267 Leone, D. P., Srinivasan, K., Chen, B., Alcamo, E. & McConnell, S. K. The determination of projection neuron identity in the developing cerebral cortex. *Current opinion in neurobiology* **18**, 28-35, doi:10.1016/j.conb.2008.05.006 (2008).

268 Cahoy, J. D. *et al.* A transcriptome database for astrocytes, neurons, and oligodendrocytes: a new resource for understanding brain development and function. *The Journal of neuroscience : the official journal of the Society for Neuroscience* **28**, 264-278, doi:10.1523/JNEUROSCI.4178-07.2008 (2008).

269 Weiner, J. A. & Chun, J. Png-1, a nervous system-specific zinc finger gene, identifies regions containing postmitotic neurons during mammalian embryonic development. *The Journal of comparative neurology* **381**, 130-142 (1997).

270 Pang, Z. P. *et al.* Induction of human neuronal cells by defined transcription factors. *Nature* **476**, 220-223, doi:10.1038/nature10202 (2011).

271 Yoo, A. S. *et al.* MicroRNA-mediated conversion of human fibroblasts to neurons. *Nature* **476**, 228-231, doi:10.1038/nature10323 (2011).

272 Yoo, A. S., Staahl, B. T., Chen, L. & Crabtree, G. R. MicroRNA-mediated switching of chromatin-remodelling complexes in neural development. *Nature* **460**, 642-646, doi:10.1038/nature08139 (2009).

273 Caiazzo, M. *et al.* Direct generation of functional dopaminergic neurons from mouse and human fibroblasts. *Nature* **476**, 224-227, doi:10.1038/nature10284 (2011).

274 Pfisterer, U. *et al.* Direct conversion of human fibroblasts to dopaminergic neurons. *Proceedings of the National Academy of Sciences of the United States of America* **108**, 10343-10348, doi:10.1073/pnas.1105135108 (2011).

275 Son, E. Y. *et al.* Conversion of mouse and human fibroblasts into functional spinal motor neurons. *Cell stem cell* **9**, 205-218, doi:10.1016/j.stem.2011.07.014 (2011).

276 Qiang, L. *et al.* Directed conversion of Alzheimer's disease patient skin fibroblasts into functional neurons. *Cell* **146**, 359-371, doi:10.1016/j.cell.2011.07.007 (2011).

277 Marro, S. *et al.* Direct lineage conversion of terminally differentiated hepatocytes to functional neurons. *Cell stem cell* **9**, 374-382, doi:10.1016/j.stem.2011.09.002 (2011).

278 Song, H., Stevens, C. F. & Gage, F. H. Astroglia induce neurogenesis from adult neural stem cells. *Nature* **417**, 39-44, doi:10.1038/417039a (2002).

279 Vicario-Abejon, C., Collin, C., Tsoulfas, P. & McKay, R. D. Hippocampal stem cells differentiate into excitatory and inhibitory neurons. *The European journal of neuroscience* **12**, 677-688 (2000).

280 Wernig, M. *et al.* Functional integration of embryonic stem cell-derived neurons in vivo. *The Journal of neuroscience : the official journal of the Society for Neuroscience* **24**, 5258-5268, doi:10.1523/JNEUROSCI.0428-04.200 (2004).

281 Yang, N., Ng, Y. H., Pang, Z. P., Sudhof, T. C. & Wernig, M. Induced neuronal cells: how to make and define a neuron. *Cell stem cell* **9**, 517-525, doi:10.1016/j.stem.2011.11.015 (2011).

282 Siegelbaum, S. A. Presynaptic facilitation by hyperpolarization-activated pacemaker channels. *Nature neuroscience* **3**, 101-102, doi:10.1038/72038 (2000).

283 Lockery, S. R., Goodman, M. B. & Faumont, S. First report of action potentials in a C. elegans neuron is premature. *Nature neuroscience* **12**, 365-366; author reply 366, doi:10.1038/nn0409-365 (2009).

284 Banker, G. A. Trophic interactions between astroglial cells and hippocampal neurons in culture. *Science* **209**, 809-810 (1980).

285 Eroglu, C. & Barres, B. A. Regulation of synaptic connectivity by glia. *Nature* **468**, 223-231, doi:10.1038/nature09612 (2010).

286 Powell, L. M., Zur Lage, P. I., Prentice, D. R., Senthinathan, B. & Jarman, A. P. The proneural proteins Atonal and Scute regulate neural target genes through different E-box binding sites. *Molecular and cellular biology* **24**, 9517-9526, doi:10.1128/MCB.24.21.9517-9526.2004 (2004).

287 Lee, S. K. & Pfaff, S. L. Synchronization of neurogenesis and motor neuron specification by direct coupling of bHLH and homeodomain transcription factors. *Neuron* **38**, 731-745 (2003).

288 Kasai, Y., Stahl, S. & Crews, S. Specification of the Drosophila CNS midline cell lineage: direct control of single-minded transcription by dorsal/ventral patterning genes. *Gene expression* **7**, 171-189 (1998).

289 Guthrie, S. Axon guidance: starting and stopping with slit. *Current biology : CB* **9**, R432-435 (1999).

290 Ma, Y. *et al.* Functional interactions between Drosophila bHLH/PAS, Sox, and POU transcription factors regulate CNS midline expression of the slit gene. *The Journal of neuroscience : the official journal of the Society for Neuroscience* **20**, 4596-4605 (2000).

291 Cavallaro, M. *et al.* Impaired generation of mature neurons by neural stem cells from hypomorphic Sox2 mutants. *Development* **135**, 541-557, doi:10.1242/dev.010801 (2008).

292 Buffo, A. *et al.* Expression pattern of the transcription factor Olig2 in response to brain injuries: implications for neuronal repair. *Proceedings of the National Academy of Sciences of the United States of America* **102**, 18183-18188, doi:10.1073/pnas.0506535102 (2005).

293 Richardson, R. M., Barbaro, N. M., Alvarez-Buylla, A. & Baraban, S. C. Developing cell transplantation for temporal lobe epilepsy. *Neurosurgical focus* **24**, E17, doi:10.3171/FOC/2008/24/3-4/E16 (2008).

294 Pear, W. S., Nolan, G. P., Scott, M. L. & Baltimore, D. Production of high-titer helper-free retroviruses by transient transfection. *Proceedings of the National Academy of Sciences of the United States of America* **90**, 8392-8396 (1993).

295 Stadtfeld, M., Nagaya, M., Utikal, J., Weir, G. & Hochedlinger, K. Induced pluripotent stem cells generated without viral integration. *Science* **322**, 945-949, doi:10.1126/science.1162494 (2008).

296 Papapetrou, E. P. & Sadelain, M. Generation of transgene-free human induced pluripotent stem cells with an excisable single polycistronic vector. *Nature protocols* **6**, 1251-1273, doi:10.1038/nprot.2011.374 (2011).

297 Woltjen, K. *et al.* piggyBac transposition reprograms fibroblasts to induced pluripotent stem cells. *Nature* **458**, 766-770, doi:10.1038/nature07863 (2009).

298 van den Berg, A. & Dowdy, S. F. Protein transduction domain delivery of therapeutic macromolecules. *Current opinion in biotechnology* **22**, 888-893, doi:10.1016/j.copbio.2011.03.008 (2011).

299 Frankel, A. D. & Pabo, C. O. Cellular uptake of the tat protein from human immunodeficiency virus. *Cell* **55**, 1189-1193 (1988).

300 Sul, J. Y., Kim, T. K., Lee, J. H. & Eberwine, J. Perspectives on cell reprogramming with RNA. *Trends in biotechnology* **30**, 243-249, doi:10.1016/j.tibtech.2012.02.004 (2012).

301 Vierbuchen, T. & Wernig, M. Direct lineage conversions: unnatural but useful? *Nature biotechnology* **29**, 892-907, doi:10.1038/nbt.1946 (2011).

302 Yee, J. K. *et al.* A general method for the generation of high-titer, pantropic retroviral vectors: highly efficient infection of primary hepatocytes. *Proceedings of the National Academy of Sciences of the United States of America* **91**, 9564-9568 (1994).

303 Wernig, M. *et al.* In vitro reprogramming of fibroblasts into a pluripotent ES-cell-like state. *Nature* **448**, 318-324, doi:10.1038/nature05944 (2007).

304 Livak, K. J. & Schmittgen, T. D. Analysis of relative gene expression data using real-time quantitative PCR and the 2(-Delta Delta C(T)) Method. *Methods* **25**, 402-408, doi:10.1006/meth.2001.1262 S1046-2023(01)91262-9 [pii] (2001).

305 Rieger, M. A., Hoppe, P. S., Smejkal, B. M., Eitelhuber, A. C. & Schroeder, T. Hematopoietic cytokines can instruct lineage choice. *Science* **325**, 217-218, doi:325/5937/217 [pii] 10.1126/science.1171461 (2009).

Acknowledgments

I would like to thank Magdalena Götz for the opportunity to carry out my PhD project at her laboratory as well as her encouraging discussions.

Many thanks for all the advice and support of my supervisor Benedikt Berninger.

I would also like to warmly thank Felipe Ortega, Sergio Gascon, Marisa Karow and Giacomo Masserdotti for great help and sharing their knowledge with me

Furthermore, I would like to thank Gabi, Tatjana, Ines and Simone for their technical expertise and Lana Polero for her indispensable organizational skills.

And, of course, thanks to the most important person in my life, Gwendolyn Behrendt who has helped me in multiples ways and collaborated in an essential manner.

Eidestattliche Erklärung

Ich erkläre hiermit, dass ich diese Dissertation selbstständig ohne Hilfe Dritter und ohne Benutzung anderer als der angegebenen Quellen und Hilfsmittel verfasst habe. Alle den benutzten Quellen wörtlich oder sinngemäß entnommenen Stellen sind als solche einzeln kenntlich gemacht.

Ich bin mir bewusst, dass eine falsche Erklärung rechtliche Folgen haben wird.

_____

Ort, Datum, Unterschrift

LEBENSLAUF

PERSÖNLICHE INFORMATIONEN

Nachname:	**Sánchez del Valle**
Vorname:	**Rodrigo**
Adresse:	**Schulstr. 15, 80634, München**
Staatangehörigkeit:	**Spanisch**
Familienstand:	**Ledig**
Geburtsdatum:	**30.10.1976**
Tel:	**+49 163 520 87 45**
Email:	**rodrigo.sanchez.delvalle@gmail.com**

BERUFSERFAHRUNG/STUDIUM

02/12 - 06/12 Fachseminar „**Life Science Management**" ATV GmbH, München (Note: 1)

- **Pharma-Management**: Pharma-Business, Regulatory Affairs, Klinische Studien, Gesundheitspolitische Grundlagen, AMG, Qualitätsmanagement
- **Wirtschaftliche Grundlagen**: Projektmanagement, Betriebswirtschaft, Marketing
- **Persönlichkeitstraining**: Kommunikations-, Team- und Führungstraining

01/07 - 07/12 **Promotion** am Institut für Physiologie (Abteilung Physiologische Genomik) der ***Ludwig-Maximilians-Universität München***

„ In vitro direct conversion of somatic cells from the adult human brain into functional neurons by defined factors"

06/01 – 08/01 Wissenschaftlicher Mitarbeiter am ***European Molecular Biology Laboratory***, Heidelberg

- Verwaltung von Datenbanken

05/01 - 12/06 Wissenschaftlicher Mitarbeiter als Diplom-Biochemiker in der Abteilung Molekulare Neurobiologie am ***Max-Planck-Institut für Neurobiologie***, München

- Produktion, Reinigung und Analyse von Fusionsproteinen und Antikörpern
- Qualifizierte Handhabung vom HPLC Äkta Explorer (GE) Chromatographie System

05/00 - 11/00 „Work and travel" Dublin (Irland)

09/99 - 04/00 **Doktorat** in der Abteilung Molekulare Medizin der ***Salamanca Universität*** (Spanien)

„ Aktualisierungen in Zell- und Molekulare Biologie" (Abschluss: Sehr gut)

09/94 - 08/99 Studium der Biochemie an der ***Salamanca Universität*** (Spanien) mit Abschluss **Diplom-Biochemiker** („Licenciado en Bioquimica")

SPRACHKENNTNISSE

Spanisch	Muttersprache
Englisch	Fließend in Wort und Schrift
Deutsch	Verhandlungssicher
Italienisch	Sehr gut
Französisch	Grundkenntnisse

VERÖFFENTLICHUNGEN (Autorenschaft/Beitrag)

- *Sanchez et al*, (accepted for publication in October 2012) „Reprogramming of pericyte-derived cells of the adult human brain into induced neuronal cells" ***Cell Stem Cell*** *2012* (Impact factor: **25.4**)
- *Heinrich C, Gascón S, Masserdotti G, Lepier A, Sanchez R, Simon-Ebert T, Schroeder T, Götz M, Berninger B*. „Generation of subtype-specific neurons from postnatal astroglia of the mouse cerebral cortex" ***Nature Protocols*** *2011* (Impact factor: **9.9**)
- *Heinrich C, Blum R, Gascón S, Masserdotti G, Tripathi P, Sánchez R, Tiedt S, Schroeder T, Götz M, Berninger B*. „Directing astroglia from the cerebral cortex into subtype specific functional neurons" ***PLoS Biology*** *2010* (Impact factor: **12.5**)
- *Blum R, Heinrich C, Sánchez R, Lepier A, Gundelfinger ED, Berninger B, Götz M*. „Neuronal network formation from reprogrammed early postnatal rat cortical glial cells" ***Cerebral Cortex*** *2010* (Impact factor: **6.5**)
- *Egea J, Erlacher C, Montanez E, Burtscher I, Yamagishi S, Hess M, Hampel F, Sanchez R, Rodriguez-Manzaneque MT, Bösl MR, Fässler R, Lickert H, Klein R*. „Genetic ablation of FLRT3 reveals a novel morphogenetic function for the anterior visceral endoderm in suppressing mesoderm differentiation" ***Genes & Development*** *2008* (Impact factor: **11.7**)
- „Regulation of EphA4 Kinase Activity is Required for a Subset of Axon Guidance Decisions Suggesting a Key Role for Receptor Clustering in Eph Function" **Neuron** 2005 (Impact factor: **14.7**)
- „Mitogen-inducible gene 6 is an endogenous inhibitor of HGF/Met-induced cell migration and neurite growth" **Journal of Cell Biology** 2005 (Impact factor: **10.3**)
- „FLRT2 and FLRT3 act as repulsive guidance cues for Unc5-positive neurons" **The EMBO Journal** 2011 (Impact factor: **9.2**)

VORTRÄGE/ KONGRESSE

09/11	***Harvard Universität***, Abt. Stammzell- und Regenerative Biologie, „Roche/Harvard University Programm", **Boston** (USA) -Vortrag-
11/09	*„Neuron-Glia Interaction"* -DFG *SPP 1172*- **Frankfurt** (D) -Vortrag-
05/09	*„EMBO Workshop bHLH transcription factors"* **London** (GB) -Poster-
07/08	*„6th FENS Forum of European Neuroscience"* **Genf** (Schweiz) -Poster-
2007 - 2010	*ForNeuroCell –BayFor*- jährlicher Bericht, **Bayern** (D) -Vorträge-

EDV KENNTNISSE

MS Office 2007
Adobe Photoshop CS
FileMaker Pro

PERSÖNLICHE INTERESSEN

Musik Komponieren (http://soundcloud.com/rodrigo-sandel)
Veröffentlichung im Magazin der Technik und Technologie *„FutureMusic"* Spanien 1997
Sport: Tennis, Jogging
1994-2000 Reittrainer "*Valverde Reitschule" Salamanca (Spanien)*

REFERENZEN

Prof. Dr. Rüdiger Klein	Max-Planck-Institut für Neurobiologie Abteilung Molekulare Neurobiologie Am Klopferspitz 18 82152 Martinsried Tel: +49 (0) 89 8578 3151 reuter@neuro.mpg.de
Prof. Dr. Benedikt Berninger	LMU Institut für Physiologie Abteilung Physiologische Genomik Schillerstr. 46 80336 München Tel. +49 (0) 89 2180 75208 benedikt.berninger@helmholtz-muenchen.de
Dr. Joaquim Egea	University of Lleida Institute of Biomedical Research Montserrat Roig 2 25198 Lleida (Spanien) Tel. +34 973 702 287 joaquim.egea@cmb.udl.cat

München, 3. September 2012